

I. A SURVEY OF STRUCTURE DETERMINATIONS OF ORGANIC
MOLECULES BY DIFFRACTION METHODS

II. AN ELECTRON DIFFRACTION INVESTIGATION
OF BIPHENYLENE

III. THE CRYSTAL STRUCTURE OF BIPHENYLENE

IV. ON ARSENOMETHANE

V. ON THE RADIAL DISTRIBUTION METHOD IN ELECTRON
DIFFRACTION

T h e s i s b y

Jürg Waser

In Partial Fulfilment of the Requirements for the Degree of
Doctor of Philosophy

California Institute of Technology

Pasadena, California
1944

TABLE OF CONTENTS

Introduction	1
A survey of structure determinations of organic molecules by diffraction methods	2
X-ray diffraction method	3
Electron diffraction method	11
An electron diffraction investigation of biphenylene	23
Electron diffraction investigation	23
Quantum mechanical calculations	26
Discussion	27
Summary	27
The crystal structure of biphenylene	28
Unit cell and space group	28
Determination of the structure	29
Discussion	44
Summary	50
On arsenomethane	52
Introduction	52
Preparation and properties of arsenomethane	55
Vapor density determinations	57
X-ray diffraction study	61
Electron diffraction investigation	62
Summary	68
On the radial distribution method in electron diffraction	70
Introduction	70
The Gibbs and related phenomena	72
The artificial temperature factor	82
Modification of the intensity function in general	83
The atomic scattering factor	95
Summary	100
Summary	103
Acknowledgement	104
Propositions	105

INTRODUCTION

The first chapter of this thesis, a survey of structure determinations of organic molecules by diffraction methods, introduces an experimental part which deals with an electron diffraction study and a crystal structure determination of biphenylene and various investigations of arsenomethane. A theoretical part of the thesis deals with the radial distribution method, which is of great importance in electron diffraction. Many of the results derived there are applicable also to the Fourier and Patterson projection methods frequently used in crystal structure analysis.

A SURVEY OF STRUCTURE DETERMINATIONS OF ORGANIC MOLECULES
BY DIFFRACTION METHODS.

The question: "What is the structure of a molecule?" may be broken up into three consecutive parts. (1) What is the topological configuration of the atoms in a given molecule (e.g. have the carbon atoms in naphthalene the configuration of two joined six-rings, of a five-ring joined to a seven-ring, or still another configuration)? (2) What is the geometrical shape and symmetry of the molecule (e.g. has naphthalene a puckered or a planar configuration)? (3) What are the exact dimensions of the molecule (e.g. what are the bond lengths and angles in naphthalene)? In the past, the first of these questions was of prime importance to the chemist, who, using his characteristic methods, succeeded in answering it for an enormous number of molecules. In more recent years the second and third questions have become of equal interest, since it has become possible to correlate important properties of molecules with their sizes and shapes. For example, planarity and interatomic distances are, for many molecules, closely related to quantum mechanical resonance between various electronic structures, which in turn determines many of their macroscopic properties. The methods of the classical chemist did not, in general, permit him to answer these questions. In the last thirty years powerful new methods have however been developed making possible complete structure determinations of molecules. These methods have confirmed most of the topological configurations assigned to molecules by the classical chemist, and in some interesting cases have complemented his methods to advantage. In addition, by leading to complete determinations of structure, they have provided much insight into the relationship between the macroscopic properties of a substance and the structure of its

molecules.

Of prime importance among these new methods is the diffraction of X-rays and electrons. Since the first crystal structure determinations by X-rays in 1913 by the Braggs, and the first structure determination of molecules by electron diffraction in 1930 by Mark and Wierl, a host of molecules have yielded their structural secrets to an attack by diffraction methods. In the following paragraphs an attempt is made to describe how diffraction methods have served in the past to answer the first and the second questions regarding structure for some molecules of organic nature.

X-ray diffraction method.

At first it was questionable whether or not elucidation of crystal structures would give information about the structure of molecules, since, in generalization of the structures of rocksalt, zinc blende and other minerals, it was contended by Groth¹ and his school that no such things as molecules in crystals existed. Others, like Tutton², went so far as to hold that even in the rocksalt crystal molecules of NaCl, although not definitely identifiable, still existed. Indication of the existence of independent groups of atoms in crystals was first obtained by Wyckoff³, who established the occurrence of carbonate groups of the same dimensions in the minerals calcite (CaCO_3), rhodochrosite (MnCO_3), and siderite (FeCO_3). Even more conclusive was the determination of the crystal structure of hexamethylene tetramine by Dickinson and Raymond⁴, which showed the existence of independent molecules in this crystal.

The fundamental problem of a structure analysis with X-rays is to determine the position of the atoms in the unit cell of the crystal, while the chemical problem is to determine the position of the atoms in the molecule. Even for the simplest case in which the unit cell of the crystal contains

only one molecule, the crystal structure problem is the more complicated one, since in addition to a determination of the relative positions of the atoms in the molecule a determination of the orientation of this molecule in the unit cell is required. In most cases there is more than one molecule in the unit cell, which further complicates the crystal structure problem. If the approximate location of the atoms in the molecule is known beforehand the two problems can often be separated by the application of the method of molecular structure factors⁵, but such knowledge is not always available, and certainly was not at hand in the early days of crystal structure investigation.

Often only a partial investigation of the crystal structure is required to give a great deal of information about the molecules involved. Information about approximate size and symmetry may sometimes be obtained from a determination of the unit cell and space group of the crystal. In any given case, however, it cannot be told beforehand whether or not X-ray methods will give any useful information, nor how much labor would be required to obtain it.

A promising start in the elucidation of the topological configuration of organic molecules was the complete determination of the crystal structure of hexamethylene tetramine by Dickinson and Raymond⁴, as early as 1923. In this investigation three out of four proposed structures were eliminated, and the fourth definitely established as the correct one. Support was given to the methods of the classical organic chemist by the determination of crystal structures of cyanuric acid⁶, cyanuric triazide⁷, cyanuric tricyanamide⁸, and melamine⁹, which contain the heterocyclic six-ring of sym. triazine. The establishment of the crystal structure of dicyandiamide¹⁰ settled the question of the structure of this molecule, for which essentially two formulae had been proposed.

Of more interest to the organic chemist were, perhaps, the results of the X-ray investigations on calciferol (Vitamin D₂) and related substances. X-ray examinations of sterols by Bernal¹¹ pointed clearly to the fact that the older formulae for these compounds could not be made to fit the crystallographic cell. This, and serious chemical defects of the old formula for the sterol skeleton, led Rosenheim and King¹² to propose a new structure (Fig.1), which showed satisfactory agreement with the X-ray data. Only a little modification of this new formula was required^{12,13,14} to make it compatible with all the chemical evidence. The general trans nature of the skeleton was made more certain by an examination of cis- and trans-hexahydrochrysenes¹⁵, while X-ray observations on oestrone¹⁶ (Fig.1) provided some useful clues in the establishment of its structure. A study by Crowfoot¹⁷ on bufagin gives support to the view that this toad poison principle contains the aetiocholane ring system (Fig.1). Further investigations by Bernal and coworkers have been recently summarized¹⁸.

X-ray investigation of ascorbic acid by Cox^{14,19} contributed substantially toward establishing the structure of this vitamin (Fig.1). Cox and Goodwin succeeded shortly thereafter in completely determining the crystal structure of ascorbic acid.

X-ray measurements on rubrene²⁰ were compatible with the formula originally developed for this dye. For chemical reasons this formula was later replaced by another (Fig.1) which could be made to agree with the X-ray data also²¹. The proposed structure seems, however, unlikely, since for it the phenyl groups appear to be too close together, even if twisted out of the molecular plane. By a partial analysis of the crystal structure of calycanine (Fig.1) Hargreaves and Taylor²² recently succeeded in ruling out twelve of thirteen proposed formulae. Whether the formula favored by the X-ray data, or still another one, compatible with these data, is the correct one, can only be established by a com-

plete crystal structure determination, or by further chemical investigation.

At this point mention should be made of the crystal structure determinations of phthalocyanine (Fig.1) and some of its metal salts by Robertson²³. The simultaneous investigation of crystals of phthalocyanine and of its nickel salt enabled him to determine the structure of both from X-ray data alone. This determination is therefore a proof of the structure of this complicated molecule which is entirely independent of the chemical methods which establish its structure.

X-ray diffraction methods have become an important tool in the determination of the structure of high polymers such as proteins, cellulose, starch, rubber and artificial polymers. Convenient summaries on this subject have recently appeared²⁴.

An early start was made on the question of the spatial arrangement of groups which may be attached to a carbon atom, by the determination of the structure of diamond, in 1913, by W.H. and W.L. Bragg²⁵. This structure revealed a tetrahedral environment of the carbon atoms and thus supported the notion of the tetrahedral carbon atom of van't Hoff and LeBel. For a time, the conviction among crystal structure investigators that the carbon atom should be tetrahedral in most substances was so strong, that the structural elements in graphite, naphthalene and anthracene, and derivatives, were believed to be puckered six-rings. This misconception was furthered by the erroneous belief, prevailing at first, that a molecule cannot have higher symmetry in a crystal than is imposed upon it by the space group elements of the crystal. Since this symmetry in naphthalene and anthracene is that of a center of inversion, the picture of puckered rings was a natural one.

The correct structure of graphite was established in 1924

by Hassel and Mark²⁶, and by Bernal²⁷, who showed independently that graphite consists of infinite planar honeycomb-like sheets of carbon atoms. The first crystal structure of an aromatic compound to be completely elucidated was that of hexamethylbenzene. Lonsdale²⁸ showed in 1929 that, within experimental error limits, the hexamethylbenzene molecule was planar and had six-fold symmetry. The structure determination of crystals of hexachlorobenzene²⁹ by the same investigator, and of anthracene, naphthalene, durene, benzoquinone, chrysene, and other molecules by Robertson³⁰ in a series of brilliant investigations soon followed. All of these aromatic molecules were found to be planar. No complete analysis on benzene has been carried out so far, but the X-ray evidence³¹ points to a planar molecule also.

Methane derivatives with four identical substituents such as tetramethylmethane³² showed tetrahedral symmetry. The generality of the notion that a carbon atom carrying four groups always has a tetrahedral configuration was for some time seriously jeopardized by an investigation, by Mark and Weissenberg³³, on crystals of pentaerythritol, which seemed to indicate that the central carbon atom in this compound had a four-fold symmetry axis. At first this claim was supported by other investigators³⁴, but later examinations showed it to be untenable. The complete structure of pentaerythritol, showing the tetrahedral configuration of the central carbon atom, was worked out by Llewellyn, Cox and Goodwin, by Hughes, and by Nitta and Watanabe.³⁵

The partial structure determination of cubic crystals of hexahydrobenzene hexachloride and hexabromide³⁶ by Hendricks and Bilicke, and by Dickinson and Bilicke, who established the positions of the halogen atoms, indicated that the saturated six-ring is puckered and has the chair rather than the tub form. Further attempts³⁷ to determine the crystal structures of cyclohexane and derivatives supported the notion of a stag-

gered six-ring built of tetrahedral carbon atoms. Complete crystal structure determinations on trithioformaldehyde³⁸ and trioxymethylene³⁹ showed that these molecules contain puckered heterocyclic six-rings of the chair form, while methaldehyde was shown to contain an eight membered, puckered heterocycle which has a four-fold symmetry axis.

X-ray diffraction data of crystals of various aliphatic compounds, particularly of nonacosane⁴¹ and pentatriacontane⁴² indicated the zig-zag nature of the hydrocarbon chain. Some doubts as to the generality of this conclusion were raised by the results of X-ray investigations on crystals of a number of alkylammonium halides⁴³, which by space group considerations seemed to show that the nitrogen and carbon atoms were collinear. It was pointed out by Pauling⁴⁴, however, that the notion of staggered chains of carbon atoms which rotate about their long axis is quite compatible with the X-ray data, and that there was therefore no need to assume linear hydrocarbon chains in these substances. This explanation was later substantiated by the observation⁴⁵ that X-ray photographs made of amylammonium chloride powder at liquid air temperatures indicated a zig-zag chain, which was no longer rotating about its axis. The staggered nature of the aliphatic chain, with all carbon atoms in a plane and bond angles approximately equal to those expected for tetrahedral carbon atoms, was recently confirmed by Bunn⁴⁶, by a three dimensional Fourier analysis of X-ray data from crystals of long chain hydrocarbons.

The spatial arrangement around a carbon atom with a double bond and two single bonds was elucidated first by the structure determination of crystals of urea⁴⁷. From space group considerations alone it was found that the molecule is planar and has a two-fold symmetry axis. Similar results were obtained for thiourea⁴⁸, but in this case a complete

structure determination was required to determine the entire symmetry of the molecule. The essential coplanarity of two single bonds and a double bond attached to a carbon atom was later found in many other compounds.

Two double bonds attached to a carbon atom have been found to be collinear in the following structure determinations. Calcium cyanamide⁴⁹ has linear groups N-C-N, sodium isocyanate⁵⁰ linear groups O-C-N, and in boron carbide⁵¹ the linear configuration C-C-C occurs. Of interest here is the linear configuration of the azide group found in cyanuric triazide⁷. A single bond and a triple bond attached to the same carbon atom are collinear also. A good example of this is tolane⁵², in which the four central carbon atoms (as well as the two end carbon atoms) are in a straight line. A structure determination on diphenyldiacetylene⁵³ indicated that an analogous configuration obtains in this molecule. Another example is the configuration found in di-n-propylcyan gold⁵⁴ which shows squares with gold atoms at the corners and CN groups along the sides.

X-ray diffraction methods have been instrumental in the recognition of cis-trans-isomerism. A good example is afforded by the case of cis- and trans-azobenzene. The crystal structures⁵⁵ of both isomers were worked out shortly after the discovery of the cis-form⁵⁶. These crystal structure determinations, as well as dipole moment measurements⁵⁷, served to identify the two isomers. In analogy to stilbene⁵⁸, trans-azobenzene is expected to be planar and was found to be so. The same might be expected for the cis-azobenzene were it not for steric hindrance of the two phenyl groups. The X-ray analysis showed that the phenyl groups are indeed twisted out of the coplanar orientation. A preliminary investigation on diflavylene²⁰ (Fig.1) proved this compound to have the trans configuration.

It was found that most conjugated systems are essentially planar. The condensed aromatic systems cited earlier are exam-

ples. Further examples are anthraquinone⁵⁹, resorcinol⁶⁰, stilbene⁵⁸, oxalic acid in the dihydrate⁶¹, acenaphthene⁶², and isatin⁶³. Diphenyl, terphenyl, and quaterphenyl⁶⁴ were reported to be planar despite possible steric hindrance, while sym. triphenylbenzene⁶⁵ was found to be non-planar, with the three phenyl groups rotated around the bonds connecting them to the central benzene ring. The cyanuric acid derivatives^{6,7,8,9} mentioned earlier were found to be planar also. A condensed aromatic system reported to be not entirely planar is fluorene⁶⁶.

The guanidinium ion is another interesting planar complex which in addition has a three-fold symmetry axis showing the equivalence of the three nitrogen atoms. This was shown by a complete structure analysis of crystals of guanidinium bromide and guanidinium iodide⁶⁷. In the latter case a three-fold axis of the space group of the crystal goes through the central carbon atom of the ion.

A partial analysis of crystals of m-dinitrobenzene⁶⁸ indicated that the two nitro groups are rotated by 90° out of the plane of the molecule, the nitrogens remaining in the plane. Since the reason for this is hard to understand, further investigation on this substance seems advisable. Other deviations from planarity of an aromatic nitro compound which remain unexplained were reported for p-dinitrobenzene⁶⁹ and for 4,4'-dinitrodiphenyl⁷⁰, for which complete structure determinations were carried out. According to these investigations the molecules are planar except for the nitro groups. In p-dinitrobenzene only the oxygen atoms lie outside the plane of the molecule, but in 4,4'-dinitrodiphenyl the whole nitro group is displaced from this plane. A determination of the crystal structure of picryl iodide⁷¹ indicated that the two ortho nitro groups are rotated out of the plane of the molecule, the nitrogens remaining in that plane. The para nitro group is coplanar with the benzene ring. A complete structure determination of m-tolidine²² shows that the phenyl groups are

twisted against each other.

A very interesting question is whether it would be possible to establish the structure of an optically active molecule from X-ray and some additional data without involving, however, a theory of optical activity. This would be of importance since doubt has been expressed⁷² as to the validity of structure assignments made on the basis of present theories. Some claims have been made by Clark and co-workers to have established, from X-ray data alone, by space group considerations, the optical asymmetry of phenylamino-acetic acid⁷³ and of derivatives of diphenyl⁷⁴. However, serious mistakes were discovered in their deductions by Pauling⁷⁵ and Huggins⁷⁶, completely invalidating their work.

If Friedel's law holds, which makes the X-ray data appear as if the crystal from which they originate had a center of symmetry, it is, of course, not possible from a consideration of X-ray reflections alone to make a decision as to which of the two enantiomorphic structures represents, say, the d-crystal. It should, however, be possible in favorable cases to make such a decision if some further information is available, as for example, if a detailed theory of development of crystal faces, of etch figures or of similar properties were available, and the habitus of the crystal under consideration has no symmetry of the second kind (mirror planes, inversion center, or inversion axes).

Electron diffraction method.

The method of electron diffraction on vapors is in general simpler and less laborious than is the X-ray method for crystals. In addition it usually can be predicted, from a consideration of the various structures proposed for a molecule, whether or not electron diffraction permits a convincing assignment. Electron diffraction patterns are essentially a representation of the distance spectrum of a molecule.

If therefore, for a given substance, two or more structures are proposed whose distance spectra are similar, a decision between them will be difficult, if at all possible. In general the larger a molecule the more structures with similar distance spectra, and the harder it will be to achieve a unique interpretation of the electron diffraction data. Fortunately, this difficulty does not appear in the crystal structure method.

Simple organic substances whose topological configurations have been cleared up by electron diffraction are diazomethane¹ and methylazide². The first of these molecules is planar, with a linear CNN group, while the second involves a linear NNN configuration. The ring structures which were proposed for these molecules are incorrect. The molecules of azomethane¹, of dimethyldisulfide³ and of carbon suboxide^{1,4} have been shown to have a chain structure. Electron diffraction on formic and acetic acid⁵ indicated these compounds to be dimers, involving hydrogen bonds.

An interesting case of structure assignment by electron diffraction is that of perylene⁶, which shows this substance to be 1-methyl-2-vinylacetylene. This conclusion was later supported by chemical evidence. Another example is provided by spiropentane⁷ (Fig.1), which was recently synthesized and whose structure was first assigned on the basis of its Raman spectrum and chemical properties. An electron diffraction investigation, undertaken shortly afterwards, proved the correctness of the structure assignment. The identification of a substance as spiropentane by electron diffraction had been claimed earlier⁷, but the basis of these claims appears doubtful in the light of newer evidence⁸.

Electron diffraction experiments on ethylene ozonide¹⁰ proved this molecule to have a five-ring structure and provided strong evidence that the sequence of atoms in this five-ring is C-O-O-C-O-. An investigation on the bicyclic hydrazine derivative 1,2-trimethylenepyrazolidine¹¹ (Fig.1) con-

firmed the assignment made previously by chemical methods.

In all cases investigated of substances involving four substituents on a carbon atom the tetrahedral arrangement was found. Fluoro-, chloro-, bromo-, iodo- and mixed halogen methanes¹³ may serve as examples.

Six-membered saturated ring systems are all found to be staggered. Examples are dioxane^{11,14}, trioxane¹¹, and cyclohexane¹⁵. It is, however, very hard to decide whether the six-rings of these molecules are of the tub- or the chair-form. 1,2,4,5-tetrabromocyclohexane¹⁶ was reported to have the chair-form and evidence for the chair-form for cyclohexane¹⁵ itself was recently claimed. Paraldehyde¹⁷ was shown to contain a six-membered staggered ring of alternate oxygen and carbon atoms, while diffraction patterns on metaldehyde seemed to be incompatible with any single configuration, which suggested that the eight-ring, found in the crystal structure investigation, is very flexible. Planar five-rings accounted for the scattering of cyclopentane¹⁸, tetrahydrofuran¹⁹, methylene ethylene dioxide¹¹, and pyrazolidine¹¹, but some tests indicated that moderately puckered rings would explain the observed scattering as well.

Aromatic alicyclic and heterocyclic systems like benzene^{20,21}, quinone²², naphthalene²³, hexamethylbenzene²⁴ and many other substituted benzenes, pyridine²¹, pyrazine²¹, furan^{21,19}, pyrrole²¹, and thiophene²¹ were found to be planar. Planar models of butadiene-1,3²¹, glyoxal²⁵, and dimethylglyoxal²⁵ (disregarding hydrogen atoms) account for their electron diffraction patterns, and planar rings were compatible with the diffraction data on cyclopentadiene²¹ and dioxadiene¹⁹.

Examples for the linear configuration of two double bonds, and a single bond and a triple bond, are provided by the following: ketene²⁶, allene²⁷, carbon dioxide²⁸, carbon disulfide²⁹, carbon suboxide^{1,4}, methylacetylene³⁰, dimethylacetylene³⁰, diacetylene^{30,31}, dimethyldiacetylene³⁰, propargyl-

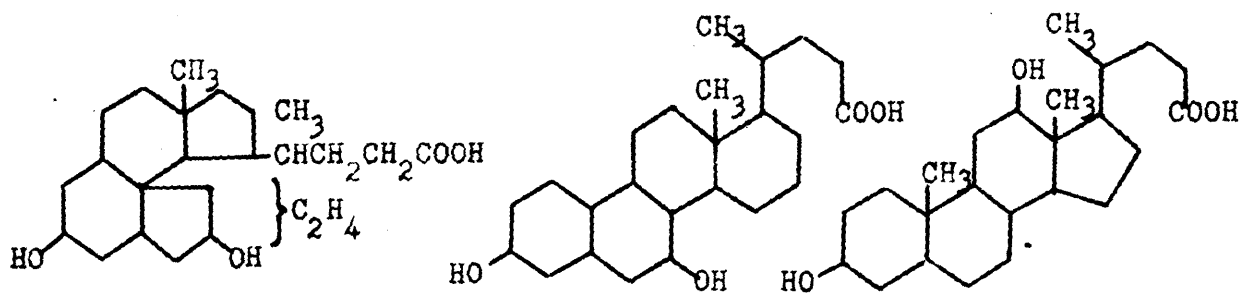
halides³², methyl cyanide^{30,33}, and cyanogen^{30,31}.

The question of cis- trans-isomerism has been attacked by electron diffraction also. It cannot always be answered satisfactorily. For example, in the case of butadiene²¹ no decision was made on the basis of electron diffraction data. An identification of cis- and trans-2-butenes³⁴ was successful while an identification of cis- and trans-2,3-epoxybutanes³⁴ was at first erroneous but was later rectified by a more complete investigation³⁵. There are no difficulties in distinguishing between cis- and trans-acetylene dihalides³⁶ because of the larger weight given the decisive distance by the heavier atoms. An electron diffraction investigation on meso and racemic 2,3-dibromobutanes³⁷, and on glyoxal and dimethylglyoxal²⁵ showed these molecules to have the trans configuration.

Electron diffraction has been applied to the question whether the eclipsed or the staggered orientation of two tetrasubstituted carbons, which are joined by a single bond, prevails. Investigations of ethylene chloride, chlorobromide, and bromide, 1,1,2-trichloroethane,³⁸ 2,3 dibromobutanes, propylenebromide,³⁹ sym. tetrachloroethane⁴⁰, and hexamethylmethane⁴¹ show that in these molecules the staggered configuration obtains. The evidence available on cyclohexane points to the staggered configuration. Of interest here is also the planar zig-zag configuration of aliphatic hydrocarbon chains in crystals.

Examples of the type mentioned in the above two sections will be found in the experimental part of this thesis. An electron diffraction investigation on the vapor of biphenylene proved the structure previously derived for this compound by Lothrop to be correct, and in particular ruled out an alternative formulation. The molecule was found to be planar. An X-ray study of crystals of biphenylene showed already in its early stages that at least one out of three

molecules must have a center of symmetry. Finally, a complete elucidation of the crystal structure confirmed the correctness of the formulation of biphenylene as dibenz-cyclobutadiene. For arsenomethane electron diffraction indicated that the molecules may be five-membered puckered rings of $(\text{AsCH}_3)_5$.

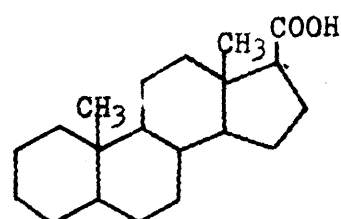
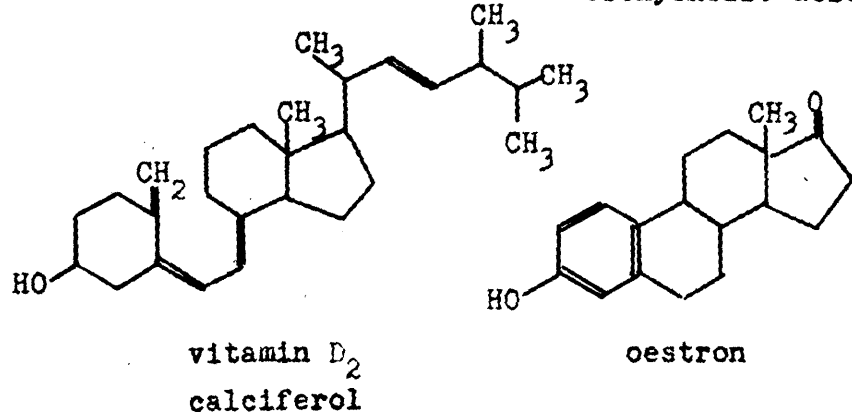


Wieland, 1928

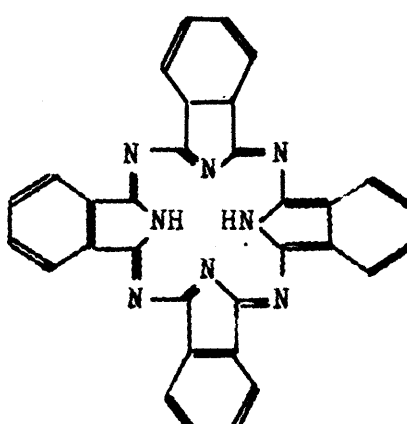
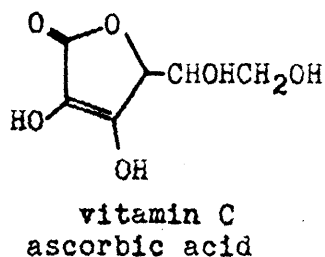
Rosenheim and King,
May 1932

Wieland and Dane, Sept. 1932
Rosenheim and King, Aug.,
Nov. 1932

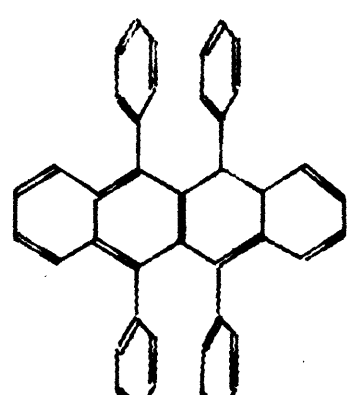
desoxycholic acid



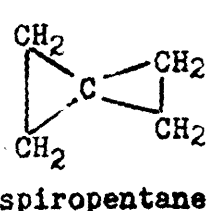
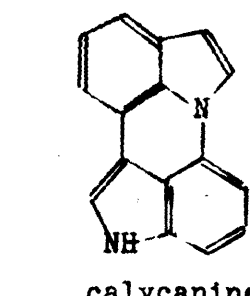
aetiocholanic acid



phthalocyanin



rubrene(?)



calycanine(?)

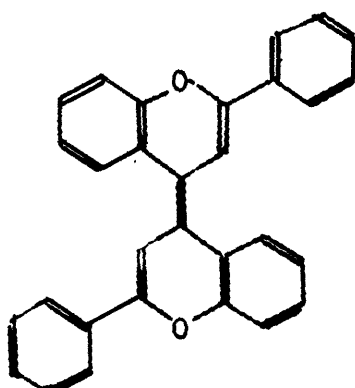
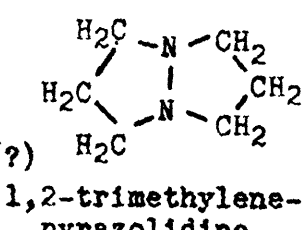


Figure 1

References cited

X-ray methods.

1. P. Groth, Z. Krist., 54, 65 (1914).
2. A.E.H. Tutton, Ann. Reports Chem. Soc., 19, 234 (1922).
3. R.W.G. Wyckoff, Amer. J. Sci., (4) 50, 317 (1920).
4. R.G. Dickinson and A.L. Raymond, J.A.C.S., 45, 22 (1923).
5. G. Knott, Proc. Phys. Soc., 52, 229 (1940).
6. E.H. Wieberger and N.F. Moerman, Z. Krist., 99, 217 (1938).
7. E.W. Hughes, J.C.P., 3, 1 (1935).
J.E. Knaggs, Proc. Roy. Soc., A150, 576 (1935); J.C.P., 3, 241 (1935).
8. J.L. Hoard, J.A.C.S., 60, 1194 (1938).
9. E.W. Hughes, J.A.C.S., 63, 1737 (1941).
10. E.W. Hughes, J.A.C.S., 62, 1258 (1940).
11. J.D. Bernal, Nature, 129, 277, 721 (1932); Chem. and Ind., 51, 466 (1932).
12. O. Rosenheim and H. King, Chem. and Ind., 51, 464, 954 (1932); 54, 699 (1935); Nature, 130, 315 (1932).
13. H. Wieland and E. Dane, Z. Physiol. Chem., 210, 268 (1932).
14. J.D. Bernal and D. Crowfoot, Ann. Reports Chem. Soc., 30, 423-424 (1934).
15. J.D. Bernal, Chem. and Ind., 52, 288 (1933).
16. J.D. Bernal, Chem. and Ind., 51, 259 (1932).
17. D. Crowfoot, Chem. and Ind., 54, 568 (1935).
18. J.D. Bernal, D. Crowfoot and I. Fankuchen, Phil. Trans. Roy. Soc., A239, 135 (1940).
19. E.G. Cox, Nature, 130, 205 (1932).
E.G. Cox and T.H. Goodwin, J. Chem. Soc., 1936, 769.
20. W.H. Taylor, Z. Krist., 93, 151 (1936).
21. E. Bergmann and E. Herlinger, J. C. P., 4, 532 (1936).
22. A. Hargreaves and W.H. Taylor, J. Sci. Instr., 18, 138 (1941).

23. J.M. Robertson, J.C.S., 1935, 615; 1936, 1195.
J.M. Robertson and I. Woodward, J.C.S., 1937, 219;
1940, 36.
24. Symposium, Chem. Rev., 26, 141-255 (1940).
D. Crowfoot, Chem. Rev., 28, 215 (1941).
25. W.H. and W.L. Bragg, Proc. Roy. Soc., A89, 277 (1913).
26. O. Hassel and H. Mark, Z. Phys., 25, 317 (1924).
27. J.D. Bernal, Proc. Roy. Soc., A106, 749 (1924).
28. K. Lonsdale, Proc. Roy. Soc., A123, 494 (1929);
Trans. Faraday Soc., 25, 352 (1929).
L.O. Brockway and J.M. Robertson, J.C.S., 1939, 1324.
29. K. Lonsdale, Proc. Roy. Soc., A133, 536 (1931).
30. J.M. Robertson, Chem. Rev., 16, 417 (1935); Rep. Prog. Physics, 6, 345 (1939).
31. E.G. Cox, Nature, 122, 401 (1928); Proc. Roy. Soc.,
A135, 491 (1932).
32. H. Mark and W. Noethling, Z. Krist., 65, 435 (1927).
33. H. Mark and K. Weissenberg, Z. Physik, 17, 301 (1923).
34. P.P. Ewald and C. Hermann, Strukturbericht I (1913-1928),
p.643-646.
35. F.I. Llewellyn, E.G. Cox and T.H. Goodwin, J.C.S., 1937, 883.
E.W. Hughes, unpublished investigation
I. Nitta and T. Watanabé, Sci. Papers Inst. Phys. Chem.
Research, Tokyo, 34, 1669 (1938).
36. S.B. Hendricks and C. Bilicke, J.A.C.S., 48, 3007 (1926).
R.G. Dickinson and C. Bilicke, J.A.C.S., 50, 764 (1928).
37. O. Hassel and H. Kringstad, Tidskr. Kemi Bergvaesen, 10,
128 (1930).
E. Halmøy and O. Hassel, Z. Phys. Chem., B16, 234 (1932).
O. Hassel and A.M. Sommerfeldt, Z. Phys. Chem., B40, 391
(1938).
E. Halmøy and O. Hassel, J.A.C.S., 61, 1601 (1939).
K. Lonsdale and H. Smith, Phil. Mag., 28, 614 (1939).
38. N.F. Moerman and E.F. Wiebenga, Z. Krist., 97, 323 (1937).
39. N.F. Moerman, Rec. Trav. Chim. Pays Bas, 56, 161 (1937).
40. L. Pauling and D.C. Carpenter, J.A.C.S., 58, 1274 (1936).

41. A. Müller, Proc. Roy. Soc., A120, 437 (1928).
42. J. Hengstenberg, Z. Krist., 67, 583 (1928).
43. S.B. Hendricks, Chem. Rev., 7, 431 (1930).
44. L. Pauling, Phys. Rev., 36, 430 (1930).
45. S.B. Hendricks, J.A.C.S., 50, 2455 (1928).
46. C.W. Bunn, Trans. Faraday Soc., 35, 482 (1939).
47. H. Mark and K. Weissenberg, Z. Physik, 16, 1 (1923).
S.B. Hendricks, J.A.C.S., 50, 2455 (1928).
R.W.G. Wyckoff, Z. Krist., 75, 529 (1930); 81, 102 (1932).
R.W.G. Wyckoff and R.B. Corey, Z. Krist., 89, 462 (1934).
48. L. Demény and I. Nitta, Bull. Chem. Soc., Japan, 3, 128 (1928).
R.W.G. Wyckoff and R.B. Corey, Z. Krist., 81, 386 (1932).
49. M.A. Bredig, J.A.C.S., 64, 1730 (1942).
50. M. Brassière, C.R., 206, 1309 (1938).
51. G.S. Zeldanov and N.G. Sevast'yanov, URSS, C.R. Acad. Sci., 32, 432 (1941).
H.K. Clark and J.L. Hoard, J.A.C.S., 65, 2115 (1943).
52. J.M. Robertson and I. Woodward, Proc. Roy. Soc., A164, 436 (1938).
53. E.H. Wiebenga, Nature, 143, 980 (1939); Z. Krist., 102, 193 (1940).
54. R.F. Phillip and H.M. Powell, Proc. Roy. Soc., A173, 147 (1939).
55. J.M. Robertson, J.C.S., 1939, 232.
J.M. Robertson, J.J. de Lange and I. Woodward, Proc. Roy. Soc., A171, 898 (1939).
56. G.S. Hartley, Nature, 140, 281 (1937); J.C.S., 1938, 633.
57. A.H. Cook, J.C.S., 1938, 876.
58. J.M. Robertson and I. Woodward, Proc. Roy. Soc., A162, 568 (1937).
59. R.C. Guha, Phil. Mag., 26, 213 (1938).
60. J.M. Robertson, Proc. Roy. Soc., A157, 79 (1936).
J.M. Robertson and A.R. Ubbelohde, Proc. Roy. Soc., A167, 122 (1928).
61. W.H. Zachariason, Z. Krist., 89, 442 (1934).
J.M. Robertson and I. Woodward, J.C.S., 1936, 1817.
R. Brill, H.G. Grimm, C. Hermann and O. Peters, Ann. Phys. (5) 42, 357 (1942).

62. K. Banerjee and K.L. Simha, Indian J. Phys., 11, 21 (1937).
63. E.G. Cox, T.H. Goodwin and A.I. Wagstaff, Proc. Roy. Soc., A157, 399 (1936).
64. J. Dhar, Indian J. Phys., 7, 43 (1932).
L.W. Picket, Proc. Roy. Soc., A142, 333 (1933); J.A.C.S., 58, 2299 (1936).
65. K. Lonsdale, Z. Krist., 97, 91 (1937).
66. J. Iball, Z. Krist., 94, 397 (1936).
67. W. Theilacker, Z. Krist., 90, 51, 256 (1935).
68. S.B. Hendricks and G.E. Hilbert, J.A.C.S., 53, 4280 (1931).
K. Banerjee and M. Ganguli, Indian J. Phys., 14, 231 (1940).
69. K. Banerjee, Phil. Mag., 18, 1004 (1935).
R.W. James, G. King and H. Horrocks, Proc. Roy. Soc., A153, 225 (1935).
70. J.N. van Niekerk, Proc. Roy. Soc., A181, 314 (1943).
71. G. Huse and H.M. Powell, J.C.S., 1940, 1398.
72. E. Hückel, Z. Elektrochemie, 50, 13 (1944).
73. G.L. Clark and G.R. Yohe, J.A.C.S., 51, 2796 (1929).
74. G.L. Clark and L.W. Pickett, J.A.C.S., 53, 167 (1931).
G.L. Clark, J.A.C.S., 53, 3826 (1931).
75. L. Pauling and R.G. Dickinson, J.A.C.S., 53, 3820 (1931).
76. M.L. Huggins, J.A.C.S., 53, 3823 (1931).

Electron diffraction method.

1. H. Boersch, Acad. Wiss. Wien IIb, 144, 1 (1935);
Monatsh., 65, 311 (1935).
2. L.O. Brockway and L. Pauling, Proc. Nat. Acad. Sci., 19, 860 (1933).
L. Pauling and L.O. Brockway, J.A.C.S., 59, 13 (1937).
3. D.P. Stevenson and J.Y. Beach, J.A.C.S., 60, 2872 (1938).
4. L.O. Brockway, Proc. Nat. Acad. Sci., 19, 860 (1933).
5. L. Pauling and L.O. Brockway, Proc. Nat. Acad. Sci., 20, 336 (1934).
J. Karle and L.O. Brockway, J.A.C.S., 66, 574 (1944).

6. R. Spurr and V. Schomaker, J.A.C.S., 64, 2693 (1942).
7. J. Donohue and G. Humphrey, J.A.C.S., 1944 (to be published shortly).
8. F. Rogowski, Ber., 72, 2021 (1939).
9. S.H. Bauer and J.Y. Beach, J.A.C.S., 64, 1142 (1942).
10. W. Shand, Jr., (unpublished investigation).
11. W. Shand, Jr., C.S. Lu, V. Schomaker and W. West (to be published).
13. cf. references given by L.R. Maxwell, J. Opt. Soc. Amer., 30, 374 (1940).
14. L.E. Sutton and L.O. Brockway, J.A.C.S., 57, 473 (1935).
15. R. Wierl, Ann. Phys. (5) 8, 521 (1931).
L. Pauling and L.O. Brockway, J.A.C.S., 59, 1223 (1937).
O. Hassel and B. Ottar, Arch. Math. Naturvidenskab., 45, 1 (1942).
O. Hassel and T. Taarland, Tids. Kemi Bergvaesen, 20, 167 (1940).
16. F. Halmøy and O. Hassel, J.A.C.S., 61, 1601 (1939).
17. C.D. Carpenter and L.O. Brockway, J.A.C.S., 58, 1270 (1936).
18. R. Wierl, Ann. Phys., (5) 8, 521 (1931); 13, 453 (1932).
L. Pauling and L.O. Brockway, J.A.C.S., 59, 1223 (1937).
19. J.Y. Beach, J.C.P., 9, 54 (1941).
20. R. Wierl, Phys. Z., 31, 366 (1930); Ann. Phys., (5) 8, 521 (1931).
L. Pauling and L.O. Brockway, J.C.P., 2, 867 (1934);
J.A.C.S., 57, 2684 (1935).
P.L.F. Jones, Trans. Faraday Soc., 31, 1036 (1935).
21. V. Schomaker and L. Pauling, J.A.C.S., 61, 1769 (1939).
22. S. Swingle, Ph.D. Thesis, California Institute of Technology, 1943.
23. H. de Laszlo, Trans. Faraday Soc., 30, 892 (1934).
O. Specchia and G. Papa, Nuovo cimento, 18, 102 (1941).
24. P.L.F. Jones, Trans. Faraday Soc., 31, 1036 (1935).
L. Pauling and L.O. Brockway, J.A.C.S., 59, 1223 (1937).
25. J.E. LuValle and V. Schomaker, J.A.C.S., 61, 3520 (1939).
26. J.Y. Beach and D.P. Stevenson, J.C.P., 6, 75 (1938).
27. R. Wierl, Ann. Phys. (5) 13, 453 (1932).
L. Pauling and L.O. Brockway, J.A.C.S., 59, 1223 (1937).

28. R. Wierl, Phys. Z., 31, 1028 (1930); Ann. Phys. (5) 8, 521 (1931).
F. Kirchner, Phys. Z., 31, 1025 (1930).
29. R. Wierl, Phys. Z., 31, 1028 (1930); Ann. Phys. (5) 8, 521 (1931).
P.C. Cross and L.O. Brockway, J.C.P., 3, 821 (1935).
P.P. Debye, Phys. Z., 40, 404 (1939).
30. L. Pauling, H.D. Springall and K.J. Palmer, J.A.C.S., 61, 927 (1939).
31. R. Wierl, Ann. Phys. (5) 13, 453 (1932).
L.O. Brockway, Proc. Nat. Acad. Sci., 19, 868 (1933).
32. L. Pauling, W. Gordy and J.H. Saylor, J.A.C.S., 64, 1753 (1942).
33. L.O. Brockway, J.A.C.S., 58, 2516 (1936).
34. L.O. Brockway and P.C. Cross, J.A.C.S., 58, 2407 (1936).
35. L.O. Brockway and P.C. Cross, J.A.C.S., 59, 1147 (1937).
36. R. Wierl, Ann. Phys. (5) 13, 453 (1932).
L.O. Brockway, J.Y. Beach and L. Pauling, J.A.C.S., 57, 2693 (1935).
H. de Laszlo, Nature, 135, 474 (1935).
A.C. Hugill, I.E. Coop and L.E. Sutton, Trans. Faraday Soc., 34, 1518 (1938).
O. Hassel and T. Taarland, Tids. Kemi Bergvaesen, 20, 152 (1940).
37. D.P. Stevenson and V. Schomaker, J.A.C.S., 61, 3173 (1939).
38. J.Y. Beach, and K.J. Palmer, J.C.P., 6, 639 (1938).
J.Y. Beach and A. Turkevich, J.A.C.S., 61, 303 (1939).
A. Turkevich and J.Y. Beach, J.A.C.S., 61, 3127 (1939).
39. D.P. Stevenson and V. Schomaker, J.A.C.S., 61, 3173 (1939)
and unpublished investigation.
40. V. Schomaker and D.P. Stevenson, J.C.P., 8, 637 (1940).
41. S. Bauer and J.Y. Beach, J.A.C.S., 64, 1142 (1942).

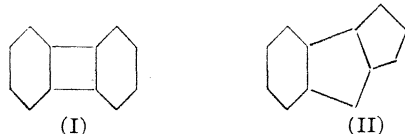
[Reprinted from the Journal of the American Chemical Society, 65, 1451 (1943).]

[CONTRIBUTION FROM THE GATES AND CRELLIN LABORATORIES OF CHEMISTRY, CALIFORNIA INSTITUTE OF TECHNOLOGY,
No. 927]

An Electron Diffraction Investigation of Biphenylene

By JURG WASER AND VERNER SCHOMAKER

W. C. Lothrop¹ has synthesized an aromatic hydrocarbon $C_{12}H_8$ to which he assigns the structure (I) and the name biphenylene. It was thought worth while to establish the structure of Lothrop's biphenylene by other than chemical means. In this we have succeeded, mainly by the electron diffraction investigation described below. Our work confirms structure (I) and in particular rules out structure (II).



which has been proposed by W. Baker² and supported by C. A. Coulson.³ Biphenylene and its derivatives synthesized by Lothrop are thus the first molecules of definitely established structure.

to contain the interesting aromatic four-ring. They should prove very valuable for studies of orientation effects due to conjugation and to strains of the bond angles (Mills-Nixon effect).

Our investigations were carried out with a 1.5-g. sample of the compound, kindly given to us by Dr. Lothrop.

Electron Diffraction Investigation

Procedure.—The electron diffraction investigation was feasible because of the relatively high vapor pressure of biphenylene. It was carried out with the use of the high temperature nozzle, which had to be heated to around 200° . The wave length of the electrons used, $\lambda = 0.0615 \text{ \AA.}$ was determined by transmission pictures of gold foil ($a_0 = 4.070 \text{ \AA.}$). Of the sixty pictures which were taken at nozzle-film distances of about 10 or 20 cm., about a fifth showed satisfactory rings, some out to about $s = 25 \text{ \AA.}^{-1}$.

In principle, the problem of an electron diffrac-

tion investigation by the visual method is the correlation of the observed features of the diffraction pattern with the corresponding features of an appropriate theoretical intensity function. In this study we have used functions of the form^{4,5}

$$I'(s) = C \sum_{ij} \frac{Z_i Z_j}{r_{ij}} \sin(sr_{ij})$$

in which $s = (4\pi/\lambda) \sin(\varphi/2)$, φ is the angle between direct and scattered beam, the r_{ij} are the interatomic distances and the Z_i are constants representing the scattering powers of the atoms.

From the appearance of the rings and their measured positions the visual curve (solid Z, Fig. 2) was drawn in accordance with our experience with the visual method to correspond to the general characteristics of curves of the type of $I'(s)$. (The position and height of the first peak were actually taken from the theoretical functions which were calculated after the rest of curve Z had been drawn.) The curve Z was used for the calculation of the radial distribution function described below and for a preliminary analysis of the theoretical scattering functions calculated for various models of the molecule. After this preliminary analysis the pictures were carefully re-examined and directly compared with the calculated scattering curves. Modifications of the original curve Z, as suggested by this reexamination, are indicated by dotted lines. For example it was found that features 6, 9 and 15 must correspond merely to small inflections of the curve.

The Radial Distribution Curve.—With the aid of the original visual curve (solid Z, Fig. 2) a radial distribution function

$$rD(r) = K \int \sin(sr) I'(s) ds$$

was obtained. This integral was approximated, with the introduction of a convergence factor $\exp(-as^2)$, by a sum⁵

$$\sum \sin(sr_i) I'(s_i) e^{-as_i^2} \Delta s$$

taken in steps of $\Delta s = \pi/10$ out to $s = 27$. The value of a was chosen so that the exponential had the value 0.10 for the last term in the sum.

This radial distribution function R (Fig. 2) confirms the general structure (I) assigned to the compound by Lothrop. E. g., the peak at 1.42 Å. corresponds to the average bonded C-C distance, while the peak at about 2.1 Å. corresponds to the diagonals of the four-ring and some C-H distances, and the peaks at 2.44 Å. (1.73×1.41) and

at 2.78 Å. (2×1.39) represent the meta and para distances of the six-ring, respectively. The distance spectrum of model D (cf. Table I) is shown below the radial distribution curve R (Fig. 2). It is seen that the agreement continues to be satisfactory out to large distances. From a more detailed examination of the curve R one would expect an average six-ring C-C bond distance of 1.41 Å. Parameters e and α (Fig. 1) are interrelated in a somewhat complicated fashion; for α equal to 120° one finds e to be about 1.46 Å. If we examine now structure (II), proposed by Baker, we find its distance spectrum to be in complete disagreement with the curve R. Let us e. g., take a model like P (Table I) as representative, consisting of a regular hexagon and two regular pentagons with a C-C bond distance of say 1.42 Å. The peak at 1.42 Å. is accounted for in this way, while the meta and para distances of the six-ring have perhaps not enough weight and the peak at 2.1 Å. is only accounted for by some C-H distances. Serious trouble however arises from the ten diagonals of the pentagons, having a length of 2.30 Å. The curve R has no peak at all near this distance. Any reasonable modification of this model would also give rise to pentagon diagonals centered around 2.30 Å. At larger distances the agreement is entirely unsatisfactory for model P and for modifications of this model. Structure (II) is therefore ruled out.

Theoretical Intensity Functions.—Theoretical scattering functions $I'(s)$ were calculated for

TABLE I
DISTANCES e AND ANGLES α FOR MODELS A TO J (ALL OTHER C-C BOND DISTANCES ARE 1.39 Å.)

e	119°	120°	121°	122°
1.39	A	C		
1.44	B	D		H
1.48			G	I
1.50		E		
1.52				J
1.54		F		

DISTANCES a TO e AND ANGLES α FOR MODELS K TO O
Model

	a	b	c	d	e	α
K	1.41	1.38	1.41	1.41	1.45	118°
L	1.41	1.38	1.41	1.41	1.45	121°
M	1.41	1.38	1.41	1.41	1.45	124°
N	1.38	1.40	1.38	1.41	1.47	122°
O	1.38	1.40	1.38	1.41	1.47	124°

Model P consists of a regular hexagon and two regular pentagons with a C-C bond distance of 1.39 Å. The bonded C-H distances in all models are 1.08 Å. These models are all about 1.5% too small and the theoretical curves are shown in Fig. 2 with the corresponding change in scale.

(4) L. O. Brockway, *Rev. Modern Phys.*, **8**, 231 (1936).

(5) R. Spurr and V. Schomaker, *This Journal*, **64**, 2693 (1942).

Aug., 1943

AN ELECTRON DIFFRACTION INVESTIGATION OF BIPHENYLENE

1453

fifteen centrosymmetric, planar models with Lothrop's structure (Table I, curves A to O, Fig. 2), and for a single model representing Baker's structure (curve P, Fig. 2). The ratio of the scattering powers of carbon and hydrogen, Z_C/Z_H , was assumed to be five. In models A to J only the distance e and the angle α (Fig. 1) were varied, while a, b, c and d were kept at 1.39 Å.

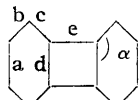


Fig. 1.

In models K to O the distances a, b, c and d were varied also; for models K to M the distances were taken from a simple valence bond treatment of the molecule,⁶ while the distances of models N and O came from a molecular orbital treatment⁷ (see below). Curve P was calculated for a regular hexagon and two regular pentagons with a C-C bond distance of 1.39 Å. The C-H bond distances were assumed for all models to be 1.08 Å. at directions bisecting the angles of the rings. (All of these distances were found to be somewhat too small and were finally increased by 1.5%; this has been accounted for in the final drawing of the intensity curves.)

The molecule was taken as rigid except for the C-H distances. For the bonded C-H terms the temperature factor $\exp(-bs^2)$, $b = 0.0022$, was used. For the non-bonded C . . . H terms the effect of the appropriate temperature factor $\exp(-b's^2)$, $b' = 0.004$, was obtained by plotting two curves for each model, the upper one out to $s = 17$ where $\exp(-b's^2) \approx 0.3$ including these terms, and the lower one beginning at $s = 8$ where $\exp(-b's^2) \approx 0.8$ omitting them. Out to about $s = 8$ the intensity function is well represented by the upper curve, from $s = 17$ on it is approximated by the lower curve, and in the intermediate region it is found by interpolation.

In the discussion of the resulting intensity curves (Fig. 2) all features except 2, 3 and 18 were helpful. Comparison between the calculated intensities and the pictures ruled out model P, as was to be expected from the disagreement of its distances with the radial distribution curve. No reasonable variation of the C-C distances of this model could possibly improve curve P, which looks so totally different from the visual curve Z.

(6) L. Pauling, "The Nature of the Chemical Bond," second edition, Cornell University Press, Ithaca, N. Y., 1940, p. 174.

(7) C. A. Coulson, *Proc. Roy. Soc. (London)*, **A169**, 413 (1939).

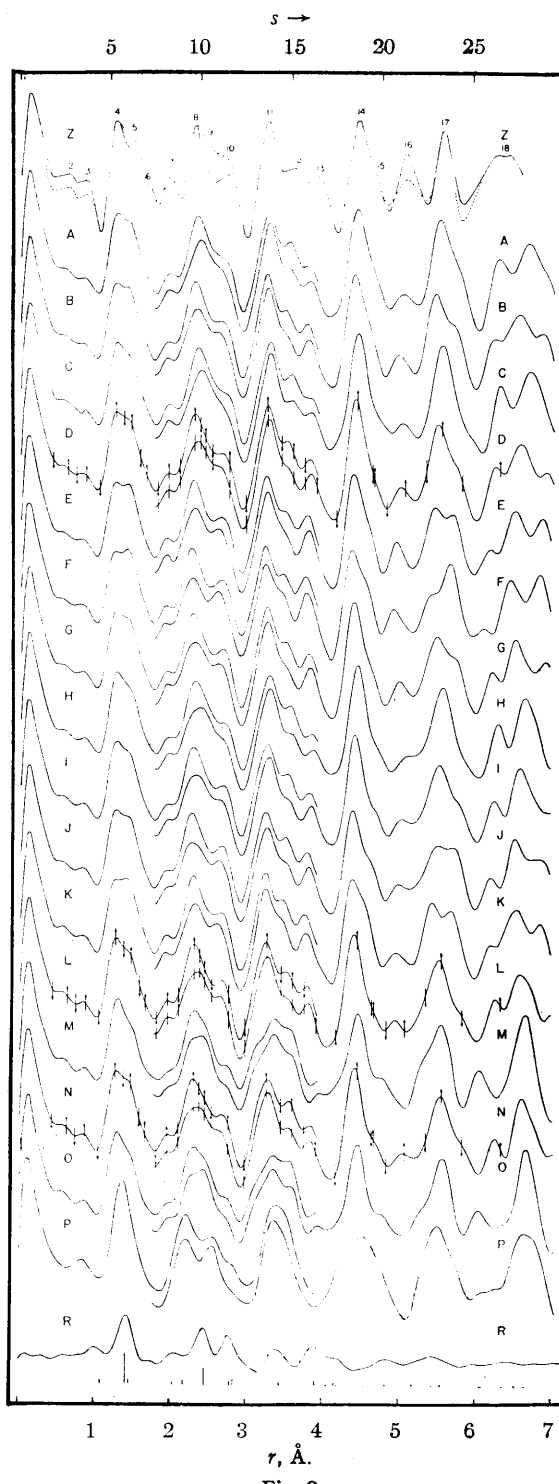


Fig. 2.

Of the models A to J, with equal ring C-C bond distances, A, C, D and I are about equally good. Models B, E, G and J are unsatisfactory and provide upper limits of the distance e for various choices of the angle α . Models M and O are

TABLE II
AGREEMENT BETWEEN OBSERVED AND CALCULATED q VALUES, ($q = 15s/\pi$)

Max.	Min.	Obs. q_0	D	q/q_0	I	q/q_0	L	q/q_0	N	q/q_0
4		25.3	25.9	1.024	26.1	1.032	25.9	1.024	25.9	1.024
	7	36.1	36.3	1.006	36.3	1.006	36.3	1.006	36.6	1.014
8		46.0	47.0	1.002	46.7	1.015	46.8	1.017	46.6	1.013
	11	59.5	59.9	1.007	59.6	1.002	59.4	0.998	59.6	1.002
11		65.1	66.8	1.026	66.9	1.028	66.5	1.022	66.9	1.028
	14	83.2	84.2	1.012	83.7	1.006	82.4	0.990	83.8	1.007
14		88.9	90.0	1.012	89.9	1.011	89.6	1.008	90.0	1.012
	16	96.5	98.4	1.020	98.9	1.025	97.9	1.015	99.0	1.026
16		101.3	102.1	1.008	102.4	1.011	100.6	0.993	102.6	1.013
Av.				1.015		1.015		1.008		1.015
a.d.				0.007		0.009		0.011		0.007

very unsatisfactory and serve to give an upper limit for α at 124° . (In these two models the ring C-C bond distances are not all alike.) Lower limits for the parameters e and α are not provided by our intensity curves, but a value for e smaller than the ring C-C bond distances can safely be ruled out on the basis of the same knowledge of molecular structure which prompted us to disregard non-planar and unsymmetrical models. Similarly a value of α smaller than say 118° is very improbable, as the strains in the molecule would tend to make α larger than 120° rather than smaller. As to models K to O, it is seen that L and N represent the scattering about equally well (N is perhaps somewhat better), although the ring C-C distances in the two models do show interesting differences. E. g., b is the smallest ring distance in model L, while b and d are the largest ring distances in model N. On the basis of the present pictures it is therefore not possible to make any exact statements as to the different ring bond distances.

Table II gives the q values ($q = 15s/\pi$) for the nine most easily measured features and the values calculated from models D, I, L and N. The ratio q/q_0 and its average for each of these four models are also given. It is seen that the respective models have to be enlarged by 0.8 to 1.5%. The best agreement with all of them and with A and C is reached with the following choice of distances: average ring C-C bond distance = 1.41 ± 0.02 Å., bridge C-C distance $e = 1.46 \pm 0.05$ Å., C-H distance = 1.10 Å. (assumed), angle $\alpha = 121^\circ \pm 3^\circ$.

Quantum Mechanical Calculations

If we assume that structure (I) is planar and centrosymmetric, we still are left with six parameters, e. g., the five distances a to e and the angle

α (Fig. 1). In order to provide a guide to the values which might be expected for these five distances, some quantum mechanical calculations were carried out.

The distances of models K, L and M were obtained by superimposing the five unexcited valence-bond structures of the molecule with equal weights.⁵ From the double-bond characters thus found the distances were obtained by interpolation between the values 1.20 Å. for acetylene, 1.33 Å.⁸ for ethylene, 1.39 Å.⁸ for benzene, and 1.54 Å. for ethane. The resonance energy of structure (I) also was calculated by the valence bond method,⁹ taking into account only the five unexcited structures with the result 2.093 α .⁹ The resonance energy of the molecule which was found by the molecular orbital method¹⁰ is 4.505 β .¹¹ The two results give a ratio of $\alpha/\beta = 2.22$, which agrees with the same ratio for benzene, provided the resonance energy between unexcited structures only is taken in the valence bond method. On the basis of the molecular orbital treatment the "bond order" p of the various bonds was calculated with the result $p_a = 0.691$, $p_b = 0.621$, $p_c = 0.683$, $p_d = 0.565$, $p_e = 0.263$ (the ethylene double bond has $p = 1$, the single bond, $p = 0$). From these values the distances for models N and O were obtained by interpolation between the values for various C-C distances given above. In all these calculations no account was taken

(8) W. S. Gallaway and E. F. Barker (*J. Chem. Phys.*, **10**, 88 (1942)) recently found the higher value of 1.35 Å. for the ethylene C-C bond. The correct value of the benzene C-C bond distance also may be somewhat higher than the one chosen here. For models K to O this may possibly account for the increase in size which was finally required.

(9) L. Pauling, *J. Chem. Phys.*, **1**, 280 (1933).

(10) L. Pauling and E. B. Wilson, "Introduction to Quantum Mechanics," McGraw-Hill Book Co., Inc., New York, N. Y., 1935, p. 381.

(11) The same value for the resonance energy was found by C. A. Coulson.¹

Aug., 1943

AN ELECTRON DIFFRACTION INVESTIGATION OF BIPHENYLENE

1455

of the strain of the four-membered ring (*cf.* however Coulson, ref. 3).

Both sets of distances had to be increased somewhat to make the corresponding intensity curves agree more closely with the observed scattering. It is interesting to note that the two methods give even qualitatively different results for the various distances. If, however, we were to replace our somewhat coarse valence bond treatment by the more refined method of Penney¹² we would probably obtain the same results as we did using Coulson's method. The results of these two methods agree in all cases which have been carried through so far.

Discussion

As pointed out above, our investigations give conclusive evidence that biphenylene has the structure (I) proposed by Lothrop. It is, however, not possible at this stage to give precise values for all of the structural parameters. Average values only have been found for the ring distances, and the distance e between the two rings and the angle α (Fig. 1) have been fixed only within wide limits. It is therefore impossible to draw any very definite conclusions about such details of the electronic structure of the molecule as the double bond character of the bond e or the distribution of the strains of the bond angles.

In collaboration with Dr. Chia-Si Lu a crystal structure investigation of biphenylene is being carried out, and will be described in a later paper. The following preliminary results have been obtained. The monoclinic unit cell contains six molecules of biphenylene and the space group is very probably $C_{2h}^5 \cdot P2_1/a$. The general position in this space group is fourfold; in addition there are four twofold positions with the point symmetry C_i . Therefore, if we assume the above space group assignment to be correct, at least two of the molecules must have a center of symmetry. This makes highly improbable any structure of biphenylene which has no center of symmetry.

Because structure (II) is definitely eliminated by our investigations of both the vapor and the crystal, it seems worth while to discuss briefly the arguments given by Baker in favor of structure (II) and against structure (I). It is no doubt true that structure (I) is considerably more

(12) W. G. Penney, *Proc. Roy. Soc. (London)*, **A158**, 306 (1937).

strained than structure (II) and probably less stable, as pointed out by Baker² and Coulson,³ but it must be remembered that a reaction does not necessarily lead to the most stable of all possible products. Although cyclobutadiene has never been prepared, cyclobutane, cyclobutenes, cyclopropane and cyclopropene¹³ have been prepared, showing that strain is no unsurmountable difficulty for the existence even of unsaturated four-rings or three-rings. Baker's catalytic reduction experiments resulted in the absorption of about three molecules of hydrogen per molecule of biphenylene. Since he expects a molecule of structure (I) to yield biphenyl upon catalytic hydrogenation, Baker used the above result as an argument for structure (II). But this result is as easily explained on the basis of structure (I) by the assumption that one of the six-rings becomes completely saturated without damage to the four-ring. Although a reliable prediction of the course of hydrogenation of biphenylene (structure (I)) could hardly have been made, the observed reduction of one of the six-rings in preference to a splitting of the four-ring is at least not surprising, inasmuch as hydrogenation of cyclobutene can be made to give cyclobutane rather than a straight chain butylene or butane and the hydrogenation of polynuclear aromatic hydrocarbons often stops at a stage such that the resulting molecule is partly aromatic and partly alicyclic (*e. g.*, naphthalene, anthracene, phenanthrene).

We are indebted to Dr. Linus Pauling for helpful discussion and criticism, and to Dr. W. C. Lothrop for the sample of biphenylene.

Summary

1. An electron diffraction investigation of biphenylene has been carried out, substantiating the formula (I) assigned to this compound by Lothrop and leading to the following distances and angles for the molecule (Fig. 1) average of $a, b, c, d = 1.41 \pm 0.02 \text{ \AA.}$, $e = 1.46 \pm 0.05 \text{ \AA.}$, C-H = 1.10 \AA. (assumed), $\alpha = 121^\circ \pm 3^\circ$.

2. Quantum-mechanical calculations of the resonance energy and relative bond strengths in biphenylene have been made.

PASADENA, CALIFORNIA

RECEIVED MARCH 26, 1943

(13) M. J. Schlatter, *THIS JOURNAL*, **63**, 1733 (1941); Demjanow and Dojarenko, *Ber.*, **56**, 2200 (1923); *Bull. Acad. Sci. Russ.*, [6] 297 (1922).

THE CRYSTAL STRUCTURE OF BIPHENYLENE

In an earlier paper¹, which reported on the electron diffraction of biphenylene molecules, $C_{12}H_8$, the configuration of the carbon atoms in these molecules, as suggested by Lothrop's synthesis², was confirmed, and values for various interatomic distances were assigned. In addition resonance energy and bond strengths were calculated. The present investigation deals with the crystal structure of biphenylene, and provides further proof that the compound investigated is indeed dibenzcyclobutadiene.

Unit cell and space group.

It was found that sublimation of biphenylene under controlled conditions resulted in sharp needles, which were, however, much too thin for X-ray work. Recrystallization from n-propyl alcohol gave satisfactory crystals. They were prisms, $1/4$ - $1/2$ mm. thick and 2 - 3 mm. long, with side faces belonging predominantly to the forms $\{110\}$, $\{310\}$, $\{100\}$, and $\{010\}$. The straw-colored crystals had no distinct cleavage and showed no abnormal birefringence. Due to their appreciable vapor pressure at room temperature their faces disappeared within a few hours on standing in open air, and the crystals evaporated completely within a few days.

All X-ray photographs showed a rather large temperature factor. Rotation and Weissenberg photographs about the three crystallographic axes led to the following dimensions of the monoclinic unit cell: $a_0 = 19.60 \pm 0.03 \text{ \AA.}$, $b_0 = 10.50 \pm 0.02 \text{ \AA.}$, $c_0 = 5.84 \pm 0.02 \text{ \AA.}$, $\beta = 91^\circ 20' \pm 20'$. The absence of $(h0\ell)$ reflections with odd h and of $(0k0)$ reflections with

odd k indicates $C_{2h}^5 - P2_1/a$ as the probable space group. Rough density measurements by flotation in an aqueous solution of potassium iodide gave $\rho = 1.24$ g./cc. Hence there are six molecules per unit cell, the calculated density being $\rho = 1.25$ g./cc.

Intensities of $(hk0)$ and $(h0\ell)$ reflections were estimated from Weissenberg photographs taken with unfiltered Cu K radiation, using the multiple film technique.³ The specimens chosen for diffraction work were small enough to make absorption corrections unnecessary. It was very difficult to obtain satisfactory visual intensity correlations between different $(h0\ell)$ reflections due to their varying sizes, as for these reflections the axis of rotation of the crystal was perpendicular to the needle axis. It was not possible to cut a crystal sufficiently short so that its length would approximate its thickness. Since there is no similar difficulty for $(hk0)$ reflections, the intensity values obtained for them should be much more reliable than the ones for $(h0\ell)$ reflections. No quantitative intensity data for $(0k\ell)$ reflections were collected, since a Fourier projection along the a axis was not expected to show any resolution.

The relative intensities obtained were corrected for the Lorentz and polarization factors with Lu's chart⁴ and the scale of their square roots was adjusted to approximately absolute scale by comparison with the values calculated from the final structure. These experimental structure factors are recorded in the second columns of Tables I and II in the order of decreasing spacing, except that the values for $(h0\ell)$ and $(h0\bar{\ell})$ have been grouped together.

Determination of the structure.

In the space group $C_{2h}^5 - P2_1/a$ there are four sets of

Table I

(hk0)	$F_{\text{obs.}}$	$F_{\text{calc.}}^{(1)}$	(hk0)	$F_{\text{obs.}}$	$F_{\text{calc.}}^{(1)}$	(hk0)	$F_{\text{obs.}}$	$F_{\text{calc.}}^{(1)}$
301	34	40	970	0	-8	21.4.0	0	4
020	51	87	15.3.0	22	-22	0.12.0	21	29
320	62	99	680	0	-4	9.11.0	0	4
600.	37	-34	12.6.0	19	22	15.9.0	0	-2
610	38	-37	15.4.0	0	-8	3.12.0	0	2
330	50	69	390	0	5	21.5.0	0	-6
620	0	7	980	20	-21	6.12.0	0	-7
040	11	11	15.5.0	0	4	18.8.0	0	1
340	19	-23	12.7.0	0	-7	12.11.0	0	-5
630	0	-2	690	0	1	21.6.0	0	-1
910	0	4	18.0.0	35	-39	15.10.0	0	-5
640	0	-8	18.1.0	14	14	24.0.0	10	15
920	31	31	18.2.0	16	-14	24.1.0	0	-1
350	23	13	0.10.0	14	22	9.12.0	0	-1
930	35	-20	15.6.0	0	0	24.2.0	0	-2
650	32	14	18.3.0	0	4	3.13.0	0	9
060	41	40	3.10.0	33	-24	18.9.0	0	-7
360	0	1	990	0	-2	24.3.0	0	-3
940	29	27	12.8.0	0	9	21.7.0	0	-3
12.0.0	30	-25	18.4.0	0	-6			
12.1.0	0	-4	6.10.0	0	-2			
12.2.0	15	-6	15.7.0	0	2			
660	32	-32	18.5.0	9	-6			
950	15	-10	12.9.0	0	-5	F_{hk0} observed for $h \neq 3n$ *)		
12.3.0	13	9	9.10.0	12	-11			
370	0	8	3.11.0	0	-2			
12.4.0	16	16	21.1.0	21	-19			
960	0	-1	15.8.0	0	4			
670	0	-8	18.6.0	11	-12			
080	0	-8	21.2.0	18	-19			
15.1.0	0	0	6.11.0	0	-11			
12.5.0	12	8	21.3.0	8	-5			
380	0	-5	12.10.0	0	-6			
15.2.0	0	1	18.7.0	0	3			

*) cf. also Table II

Table II

$(h0\ell)$	$ F_{\text{obs.}} $	$F_{\text{calc.}}^{(1)}$	$F_{\text{calc.}}^{(2)}$	$(h0\ell)$	$ F_{\text{obs.}} $	$F_{\text{calc.}}^{(1)}$	$F_{\text{calc.}}^{(2)}$
200	5	0	3	10.0.3	0	7	7
001	26	-28	-31	10.0.3	7	13	10
201	6	2	-5	14.0.1	3	0	4
201	37	44	47	14.0.1	14	-8	-10
400	5	0	1 *)	604	23	17	22
401	18	27	19	604	18	-18	-19
401	19	15	14	14.0.2	8	-4	-6
600	37	-34	-40	14.0.2	3	-9	-7
002	0	1	0	804	9	-14	-8
601	26	29	23	804	17	-7	-12
601	32	-33	-33	12.0.3	0	2	3
202	10	13	9	12.0.3	0	3	0
202	38	-32	-34	16.0.0	0	0	0
402	42	23	32	16.0.1	13	-11	-12
402	13	18	12	16.0.1	12	-1	-8
800	0	0	0	10.0.4	0	-5	-8
801	0	0	0	10.0.4	0	-1	8
801	3	4	7	005	27	-26	-32
602	11	4	5	205	23	27	22
602	8	1	6	205	6	-6	-7
10.0.0	6	0	1 *)	14.0.3	7	6	7
003	5	8	8	14.0.3	11	15	15
203	13	12	16	405	17	15	16
203	11	15	12	405	30	-31	-32
802	5	-10	-6	16.0.2	14	16	14
802	44	42	38	16.0.2	11	-10	-9
10.0.1	5	2	-10	605	7	8	9
10.0.1	6	8	18	605	8	6	11
403	34	-25	-31	18.0.0	35	-39	-31
403	28	-20	-23	12.0.4	8	7	8
603	0	0	-2	12.0.4	4	-9	-6
603	17	-12	-14	18.0.1	13	-11	-13
12.0.0	30	-25	-27	18.0.1	32	20	25
10.0.2	43	-41	-33	805	14	10	11
10.0.2	4	2	-6 *)	805	4	-6	-5
12.0.1	7	6	2	16.0.3	9	3	6
12.0.1	6	-1	4	16.0.3	4	-8	-5
803	7	-5	-7	18.0.2	0	-4	-5
803	15	-14	-12	18.0.2	5	-3	-5
004	0	0	0	14.0.4	9	-4	-8
204	13	-7	-9	14.0.4	13	-11	-16
204	13	7	13	10.0.5	0	1	3
12.0.2	0	5	1	10.0.5	7	-9	-8
12.0.2	4	3	0	20.0.0	7	0	-5
14.0.0	0	0	-2	006	0	-8	0
404	12	7	9	206	0	1	0
404	10	12	8	206	0	-2	-2

(h0ℓ)		F _{obs.}		F _{calc.} ⁽¹⁾	F _{calc.} ⁽²⁾	(h0ℓ)		F _{obs.}		F _{calc.} ⁽¹⁾	F _{calc.} ⁽²⁾
20.0.1	3	-5	-4			22.0.2	5	-4	-5		
20.0.1	7	-12	-10			22.0.2	0	-1	3		
406	5	4	6			16.0.5	0	-4	-1		
406	5	3	7			16.0.5	4	-8	-6		
18.0.3	0	0	0			12.0.6	5	6	5		
18.0.3	0	-2	1			12.0.6	5	-1	-5		
12.0.5	0	4	3			007	3	6	-1	*)	
12.0.5	3	5	5			207	0	1	1		
16.0.4	0	2	1			207	2	-1	0	*)	
16.0.4	0	-2	1			407	3	1	-3		
606	0	1	1			407	0	0	2		
606	0	0	-1			24.0.0	10	15	14		
20.0.2	0	1	2			20.0.4	10	9	9		
20.0.2	3	1	1			20.0.4	4	2	5		
806	4	-1	-4			22.0.3	0	1	0		
806	4	-2	-3			22.0.3	3	6	5		
14.0.5	9	10	12			24.0.1	2	2	6		
14.0.5	4	-7	-5			24.0.1	5	-3	-6		
22.0.0	3	0	1			607	4	4	7		
22.0.1	0	-6	-4			607	4	9	4		
22.0.1	0	-6	-1			14.0.6	0	-1	0		
20.0.3	6	-2	-2			14.0.6	0	-1	1		
20.0.3	6	-8	-8			18.0.5	5	3	4		
18.0.4	11	-5	-11			18.0.5	3	10	6		
18.0.4	4	7	9			807	0	4	4		
10.0.6	0	2	1			807	0	-7	-6		
10.0.6	0	1	0								

*) Omitted in calculation of $\rho(x,z)$.

two-fold positions with the point symmetry C_1 : $000, \frac{1}{2}\frac{1}{2}0, \frac{1}{2}00, 0\frac{1}{2}0; 00\frac{1}{2}, \frac{1}{2}\frac{1}{2}\frac{1}{2};$ and $\frac{1}{2}0\frac{1}{2}, 0\frac{1}{2}\frac{1}{2};$ and sets of four-fold general positions: $\pm (x y z, \frac{1}{2} + x \frac{1}{2} - y z).$ As there are six molecules in the unit cell, at least two must have centers of symmetry with these centers placed in the set of two-fold special positions. The special positions $000, \frac{1}{2}\frac{1}{2}0$ may be chosen without loss of generality. The considerations of the next paragraph rule out special positions for the other four molecules, which accordingly are placed in the set of general positions. All atoms will thus in general occupy four-fold positions.

The reflections $(hk0)$ show a very distinctive feature. Except for a few, all of which are very weak, only reflections $(hk0)$ with $h=3n$ appear. The reflections $(h0\ell)$ show no similar regularity. Assuming in a first approximation that all reflections $(hk0)$ vanish unless $h=3n$ ("h=3n rule"), atoms have to be grouped in triplets, the partners in each triplet occupying the following set of positions: $xyz_1, x+\frac{1}{3}yz_2, x+\frac{2}{3}yz_3.$ The part of the structure factor due to each triplet then becomes zero unless $h=3n.$

The seventy-two carbon atoms (and the forty-eight hydrogen atoms, which, however, will be neglected) thus fall into groups of twelve atoms, the positions of which are interrelated either by space-group operations or by the requirements of the "h=3n rule". The coordinates of such a set of positions are: $x_1 y_1 z_1, \bar{x}_1 \bar{y}_1 \bar{z}_1; \frac{1}{2} + x_1 \frac{1}{2} - y_1 z_1, \frac{1}{2} - x_1 \frac{1}{2} + y_1 \bar{z}_1; \frac{1}{3} + x_1 y_1 r + z_1', \frac{1}{3} - x_1 \bar{y}_1 r - z_1'; \frac{2}{3} + x_1 y_1 \bar{r} + z_1', \frac{2}{3} - x_1 \bar{y}_1 \bar{r} - z_1'; \frac{1}{6} + x_1 \frac{1}{2} - y_1 \bar{r} + z_1', \frac{1}{6} - x_1 \frac{1}{2} + y_1 \bar{r} - z_1'; \frac{5}{6} + x_1 \frac{1}{2} - y_1 r + z_1', \frac{5}{6} - x_1 \frac{1}{2} + y_1 r - z_1',$ with $r = \frac{1}{2}(z_2 - z_3), z_1' = \frac{1}{2}(z_2 + z_3).$ These positions can be grouped, as has been done above, into pairs about six centers of symmetry with the parameters $000, \frac{1}{2}\frac{1}{2}0, \frac{1}{3}0 r, \frac{2}{3}0 \bar{r}, \frac{1}{6}\frac{1}{2}\bar{r}, \frac{5}{6}\frac{1}{2}r.$ Since the magnitudes of the x parameters and of the y parameters relative

to these centers are respectively the same, these centers must be the centers of the six molecules in the unit cell. Assuming that the molecules in the general positions have the same size and shape as the ones in the special position, there are two possibilities left to relate z_1' with z_1 : (a) the molecules at 000 and $\frac{1}{3}0r$ are parallel to each other, thus $z_1' = z_1$; (b) The orientation of the molecule at $\frac{1}{3}0r$ results from the orientation of the molecule at 000 by a mirror operation by a plane perpendicular to the c axis. Then $z_1' \approx z_1$, since the c axis is almost perpendicular to the a axis.

In the present approximation the orientations of all six molecules are interrelated. This makes possible the application of the method of the molecular structure factor.⁵ In this method, the size and the shape of the molecule are assumed and its Fourier transform is constructed. If the orientations of all molecules in the unit cell are interrelated, then the molecular structure factors, read off from a chart of the Fourier transform, are related to the structure factors of the whole unit cell. The problem is then to orient the reciprocal lattice of the crystal with respect to the system of axes of the Fourier transform in such a way as to account for the observed structure factors.

In the case of biphenylene the Fourier transform has an especially useful form. Since the molecule may be assumed to have a center of symmetry and to be planar, the transform is real and essentially two-dimensional. The model chosen for the calculation was suggested by the electron diffraction investigation¹. It consists of two regular ($\alpha = 120^\circ$) co-planar hexagons of carbon atoms with bond lengths $a = 1.40 \text{ \AA.}$, joined by two bridges, in ortho positions, of lengths $b = 1.46 \text{ \AA.}$ (Fig.1). The use of the Fourier transform reduces the original fifty-four parameter problem, involving the placement of

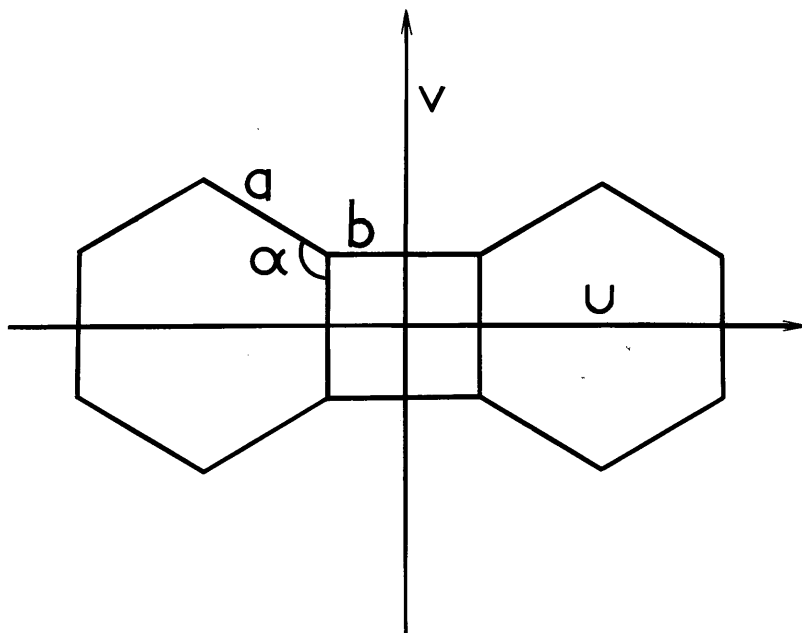


Figure 1

eighteen carbon atoms, to a four parameter problem, in which three parameters characterize the orientation of the molecule and the fourth one is the parameter r .

Reflections $(h k 0)$ are especially suited to determine the orientation of the molecules since in this case the relationship between molecular and crystal structure factors does not involve the parameter r , and does not distinguish between the possibilities (a) and (b). After a few trials, general agreement between calculated and observed structure factors was obtained, resulting in the determination of most of the phase constants. These phase constants combined with the observed structure factors were used in the calculation of the Fourier projection

$$\rho(x, y) = c \sum_h \sum_k F_{hk0} \cos 2\pi (hx + ky).$$

This calculation was carried out with use of Lipson-Beevers strips⁶ at intervals of $\frac{a_0}{180}$ and $\frac{b_0}{60}$. The plot of the final projection obtained with the signs calculated from the final choice of parameters (Table III, assignment No. 1) is shown in Fig. 2. Due to the approximation involved, the

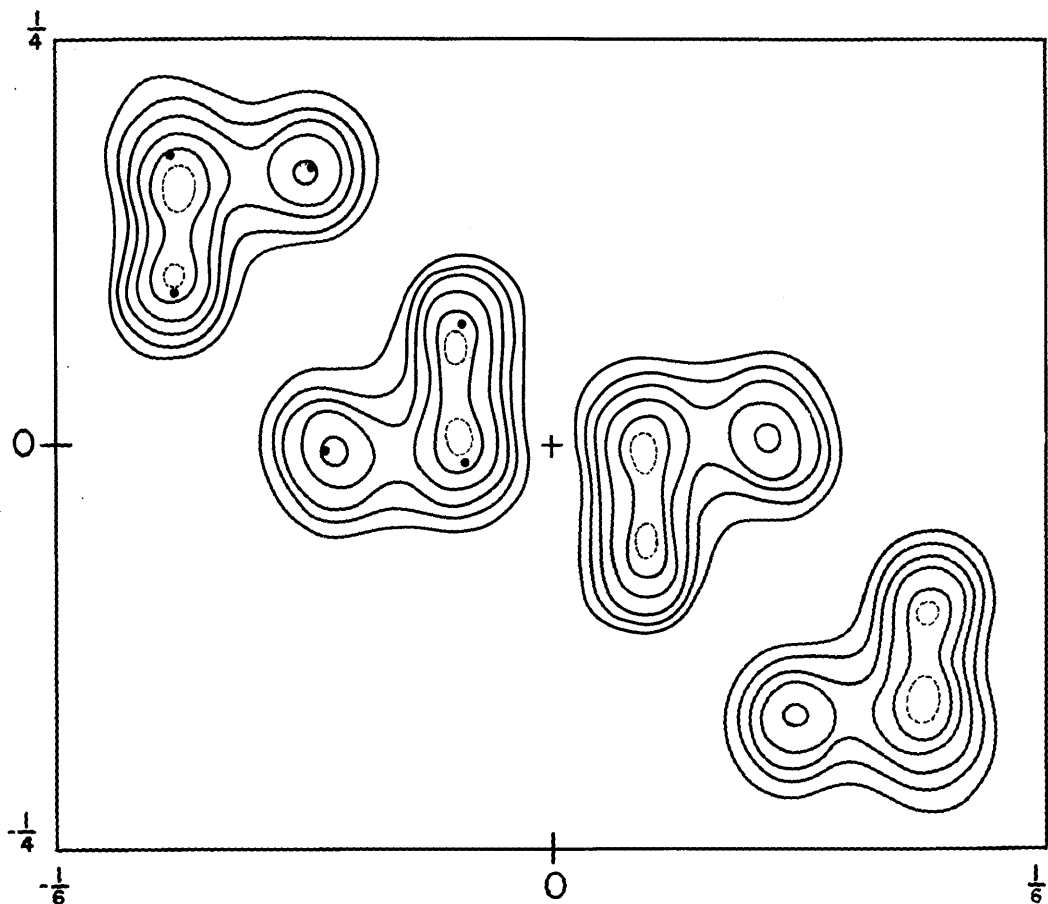


Figure 2

Fourier projection $\rho(x, y)$. Dots (●) indicate parameters of assignment No.1.

length of the a axis of the unit cell of the projection is equal to $\frac{1}{3}a_0$, and the projection shown corresponds to a superposition of the molecules at $000, \frac{1}{3}0\ r, \frac{2}{3}0\ \bar{r}$. Fig. 3

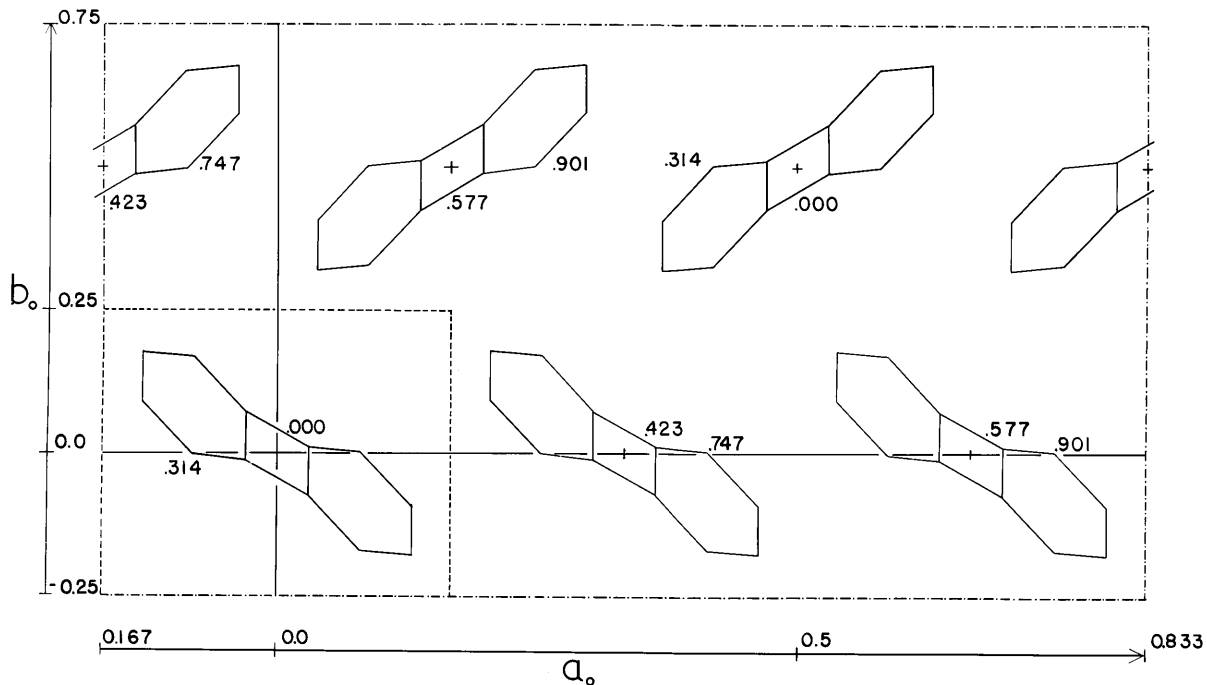


Figure 3

View of xy projection of unit cell of crystal (parameter assignment No.1). Numbers given to three decimal places are z parameters of center and of highest atom for each molecule. Section enclosed within broken lines indicates area represented in Fig. 2.

shows the actual unit cell of the crystal viewed along the c axis and its relation to Fig. 2.

The knowledge of the approximate orientations of the molecules and the observed values of $F_{h0\ell}$ were used with

the Fourier transform to decide between the alternatives (a) and (b), and to determine the parameter r . It was found that the arrangement (a) could not account for the observed $(h0\ell)$ intensities. For testing the arrangement (b) it proved helpful to determine the probable range of the parameter r in the following manner. Paper models of the xz projections of the molecules were constructed to scale and manipulated over a plot of several unit cells. The packing was tested for each value of r chosen by estimating the intramolecular distances. General agreement between observed structure factors and the values calculated from the Fourier transform was obtained for $r=0.43$, which was in the expected range. The signs of the $F_{h0\ell}$ obtained in this manner were combined with the experimental $|F_{h0\ell}|$ and a Fourier projection

$$\rho(x, z) = c \sum_h \sum_\ell F_{h0\ell} \cos 2\pi(hx + \ell z)$$

was calculated. The summations involved were evaluated with the aid of International Business Machine Corporation machines and a set of punched cards,⁷ sixty-six lines parallel to the c axis and eighty-six lines parallel to the a axis being chosen. Fig. 4 shows a plot of $\rho(x, z)$ obtained with the final choice of signs explained later. Twenty-six of the thirty-one peaks are resolved, although not all completely. The x parameters of the various resolved peaks agree well with the x parameters of the peaks in $\rho(x, y)$ (Fig. 2). Fig. 5, a diagram of two unit cells of the crystal viewed along the b axis, explains the relationship between the peaks of $\rho(x, z)$.

An interpretation of the peaks of $\rho(x, z)$ was sought in the following manner. The two crystallographically different kinds of molecules were assumed to have the dimensions suggested by the electron diffraction work¹, a coplanar molecule

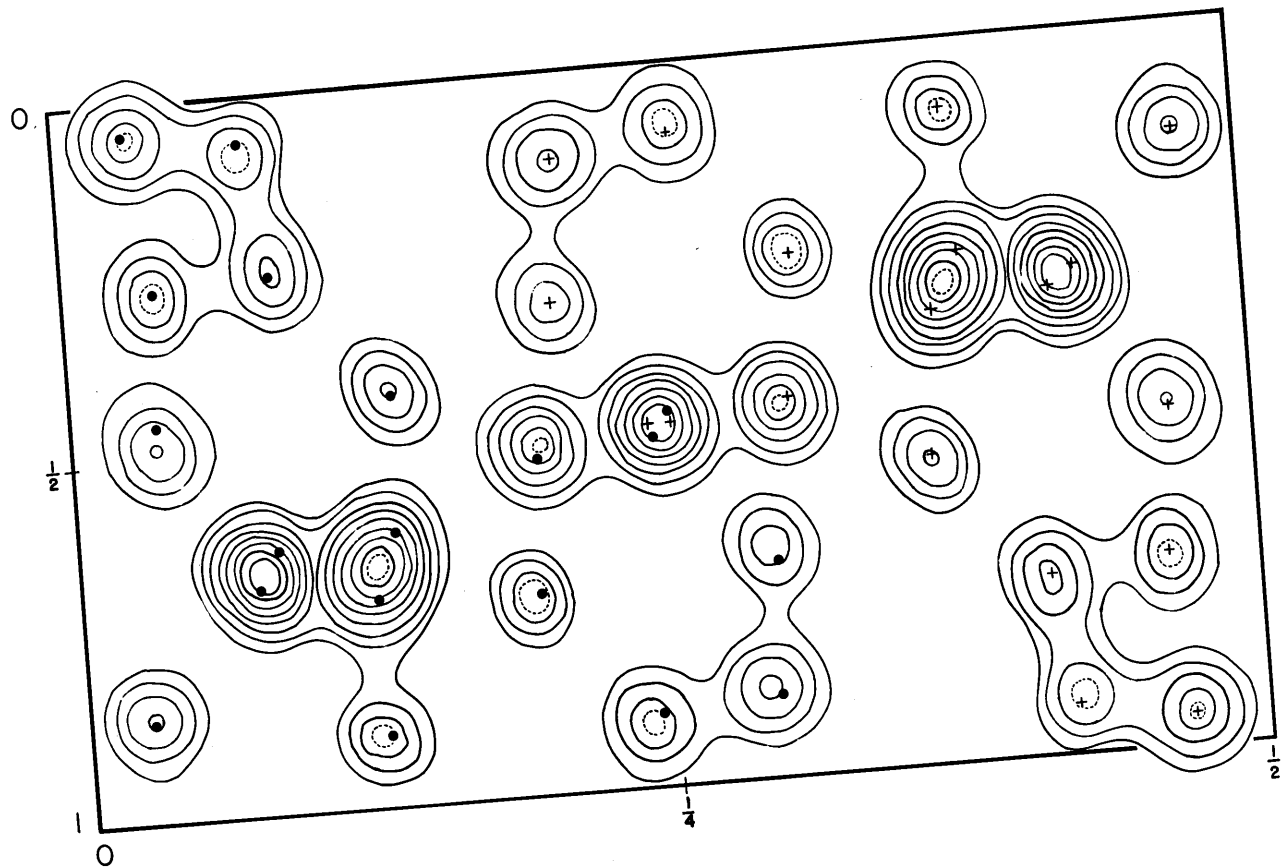


Figure 4

Fourier projection $\rho(x,z)$. Black dots (●) indicate parameters of assignment No. 1; crosses (+) represent parameters of assignment No. 2.

with $a=1.40 \text{ \AA}$, $\alpha=121^\circ$, and $b=1.46 \text{ \AA}$. (Fig. 1). The orientations of the molecules relative to each other, and the parameters of the centers of the molecules in the general positions (pqr and space group equivalents) were chosen so as to agree with the requirements of the "h=3n rule" ($p=\frac{1}{3}$; $q=0$). Parameter values for all carbon atoms were then found by matching these molecules (by trial and error), as closely as possible to the maxima of $\rho(x,y)$ and of $\rho(x,z)$. The final

choice for the parameters is recorded in Table III (Assignment No.1) and dots in Figs. 2 and 4 indicate their positions with respect to the maxima of $\rho(x,y)$ and of $\rho(x,z)$. Figs. 3 and 5 were drawn with these parameters, which were also used for the calculation of structure factors $F_{hk0}^{(1)}$ and $F_{h0\ell}^{(1)}$. These structure factors are recorded in the third columns of Tables I and II. Robertson's atomic scattering factors for hydrocarbons⁸ were used in these calculations. The agreement between $|F_{\text{calc.}}|$ and $|F_{\text{obs.}}|$ is reasonably good, but not entirely satisfactory. Attempts to orient the molecules in the general positions in a different way (abandoning the "h=3n rule") failed to give improvement.

In principle the projection $\rho(x,z)$ can be used to discard the "h=3n rule". The reasonable assumption could be made that the molecules have the symmetry $D_{2h}^{\text{-mmm}}$. The molecules in the general positions would have their centers at pqr and corresponding positions (with $p \approx \frac{1}{3}$, $q \approx 0$), and in general would have size and shape different from the molecule with center at 000. Parameters xyz could be determined (except for the small additional constant q in the parameters y) by a least-squares fit of such molecules to the maxima of $\rho(x,z)$, using the symmetry conditions as auxiliary conditions. These parameters could then be used to determine the signs of all F_{hk0} and a complete projection $\rho(x,y)$ could be constructed.

An attempt to obtain refinement along these lines was made. For simplicity, it was further assumed that the six-rings of biphenylene (Fig. 1) are regular hexagons. Although these assumptions are probably not strictly valid, they can be used as a basis for a second approximation. The two kinds of biphenylene molecules were fitted to the maxima of $\rho(x,z)$ by trial and error, rather than by a laborious least-squares treatment. The resulting parameters are recorded in Table III (Assignment No. 2), and the crosses in Fig. 4 indicate their relationship with the

Tables III

Parameters

	Assignment No. 1			Assignment No. 2		
	u	v	w	u	v	w
Molecule with center at (000):	0.029	0.011	-0.140	0.029	(-0.003)	-0.147
	0.077	0.003	-0.314	0.073	(-0.026)	-0.319
	0.127	-0.094	-0.294	0.122	(-0.119)	-0.294
	0.128	-0.179	-0.107	0.126	(-0.189)	-0.097
	0.080	-0.171	0.067	0.082	(-0.166)	0.075
Molecule with center at (pqr):	0.030	-0.074	0.047	0.033	(-0.073)	0.050
	0.363	-0.074	0.380	0.366	(-0.069)	0.370
	0.413	-0.171	0.367	0.416	(-0.161)	0.348
	0.461	-0.179	0.547	0.463	(-0.183)	0.526
	0.460	-0.094	0.734	0.460	(-0.111)	0.724
Center (pqr):	0.410	0.003	0.747	0.410	(-0.019)	0.746
	0.362	0.011	0.567	0.363	(0.003)	0.568
	0.304	-0.011	0.279	0.308	(-0.003)	0.278
	0.256	-0.003	0.099	0.261	(0.019)	0.100
	0.206	0.094	0.112	0.211	(0.111)	0.122
	0.205	0.179	0.299	0.208	(0.183)	0.320
	0.253	0.171	0.479	0.255	(0.161)	0.498
	0.303	0.074	0.466	0.305	(0.069)	0.476
Center (pqr):		0.333	0.000	0.423	0.335 ₅	(0.000)
						0.423

peaks of $\rho(x, z)$, which they approach more closely than do the parameters of assignment No. 1. It is seen that the y parameters are not in good agreement with the y parameters of assignment No. 1 corresponding to the maxima of $\rho(x, y)$. The C-C bond distances obtained for the two kinds of molecules for assignment No. 2 do not agree well with each other nor with the electron diffraction result¹. (The values are $a=1.37 \text{ \AA.}$, $b=1.58 \text{ \AA.}$ for the molecule with center at 000 , and $a=1.39 \text{ \AA.}$, $b=1.44 \text{ \AA.}$ for the molecule with center at pqr). Nevertheless the parameters obtained were used to calculate a set of structure factors $F_{h0\ell}^{(2)}$ which are recorded in the fourth column of Table II. Some improvement over the values of $F_{h0\ell}^{(1)}$ is noted. The Fourier projection shown in Fig. 4 was made using the signs of the $F_{h0\ell}^{(2)}$ (omitting a few terms with uncertain signs), since the parameters used to calculate the $F_{h0\ell}^{(2)}$ correspond more closely to the maxima of $\rho(x, z)$ than do the parameters used in the calculation of the $F_{h0\ell}^{(1)}$. In most instances the signs of $F_{h0\ell}^{(1)}$ and $F_{h0\ell}^{(2)}$ are the same. With few exceptions $|F_{h0\ell}^{(1)}| \ll |F_{h0\ell}^{(2)}|$ whenever the signs are different, so that the signs of these $F_{h0\ell}^{(2)}$ are probably correct. The remaining values $F_{h0\ell}^{(2)}$, for which the signs are less certain, appear starred in Table II, and have been omitted from the calculation of $\rho(x, z)$ of Fig. 4. There are few of them and their magnitudes are so small that their omission is not expected to change the positions of the maxima of $\rho(x, z)$ appreciably. A Fourier projection involving all the certain phase constants of the $F_{h0\ell}^{(1)}$ was carried through also, but only very slight shifts in the positions of the peaks of $\rho(x, z)$ were observed. Structure factors for reflections $(0k\ell)$ were also calculated with parameter assignment No. 1 and show qualitative agreement with intensities estimated from a Weissenberg photograph.

The improvement from $F_{h0\ell}^{(1)}$ to $F_{h0\ell}^{(2)}$ is not good enough to make parameter assignment No. 2 significant, or to suggest in which direction further improvement should be sought. The resolution of $\rho(x,z)$ is not sufficient, nor are the observed $F_{h0\ell}$ believed to be accurate enough to justify any further attempt at refinement.

Assignment No. 1 of parameters was finally adopted. It corresponds to the following orientations of the molecules at (000) and at (pqr). Let w be the direction perpendicular to u and v (Fig. 1) so that u,v,w form a right hand system. Let x and y be the directions parallel to the a and b axes of the unit cell respectively, and let z be directed normal to both, so that x,y,z form a right hand system. Then the angles between u,v,w and x,y,z are as follows:

Molecule at 000			Molecule at pqr			
u	v	w	u	v	w	
x	36.1°	90.0°	53.8°	37.6°	91.8°	127.5°
y	117.1°	50.8°	51.3°	117.1°	50.8°	128.7°
z	111.9°	140.8°	59.3°	66.1°	39.3°	60.9°

The parameters adopted are not entirely correct, since for them the "h=3n rule" holds, while experimentally there are some infractions. These may be an indication that the two molecules are not exactly of the same size and shape or that their orientations and the positions of the centers differ slightly from the ones demanded by the "h=3n rule". In addition, the general agreement between the $|F_{\text{calc}}^{(1)}|$ and the $|F_{\text{obs}}|$ is by no means perfect. However, with fifty-four parameters to dispose of, it may be considered to be reasonably satisfactory. No probable errors can be given for the adopted parameters, since the reliability of the observed $F_{h0\ell}$ is not known. It is, however, likely that most atomic positions are correct to within 0.1 Å. A few may be in error by a somewhat larger amount, as is suggested by calculations

of intermolecular distances.

Discussion.

The results of this investigation prove beyond doubt that the substance in question is dibenzcyclobutadiene.

The parameter values are, in addition, good enough to establish the packing arrangement of the molecules in the crystal. A packing drawing (Fig. 6) of the crystal was constructed in the following manner. The proper carbon atoms were provided with hydrogen atoms at C-H distances of 1.08\AA ., and in directions bisecting the corresponding C-C-C angles. Spheres with van der Waals radii⁹ of 1.85\AA . for carbon (half thickness of an aromatic molecule), and of 1.20\AA . for hydrogen were drawn about the centers of the carbon and hydrogen atoms of a molecule and intersected with each other (cf. bottom molecule in Fig. 6). The resulting van der Waals representations of the molecules, drawn in correct orientations and positions, constitute Fig. 6, which is a view of the crystal along the b axis. Two layers of molecules are drawn in Fig. 6. The complete bottom layer is shown to illustrate the interactions within one layer. The next layer is related to the bottom layer by a glide plane a, parallel to and at a distance of $\frac{1}{4}b_0$ from the first layer. It is represented by three molecules only, since these three suffice to illustrate the interactions between the two different layers. The next layer, (not shown) is a replica of the bottom layer, translated by b_0 in the direction of the b axis.

To gain an understanding of Fig. 6 comparison with Fig. 5 will prove helpful. The space group elements indicated in Fig. 5 are useful also in finding different views of the same interaction.

On the following two pages will be found

Figure 5

Two unit cells of crystal viewed along b axis are shown (parameter assignment No.1). Numbers given to three decimal places are y parameters of carbon atoms. Molecules drawn with solid lines have centers at $y=0$, those drawn with broken lines have centers at $y=\frac{1}{2}$.

Figure 6

Packing drawing of crystal, viewed along b axis. Roman numerals correspond to Roman numerals of Fig. 5.

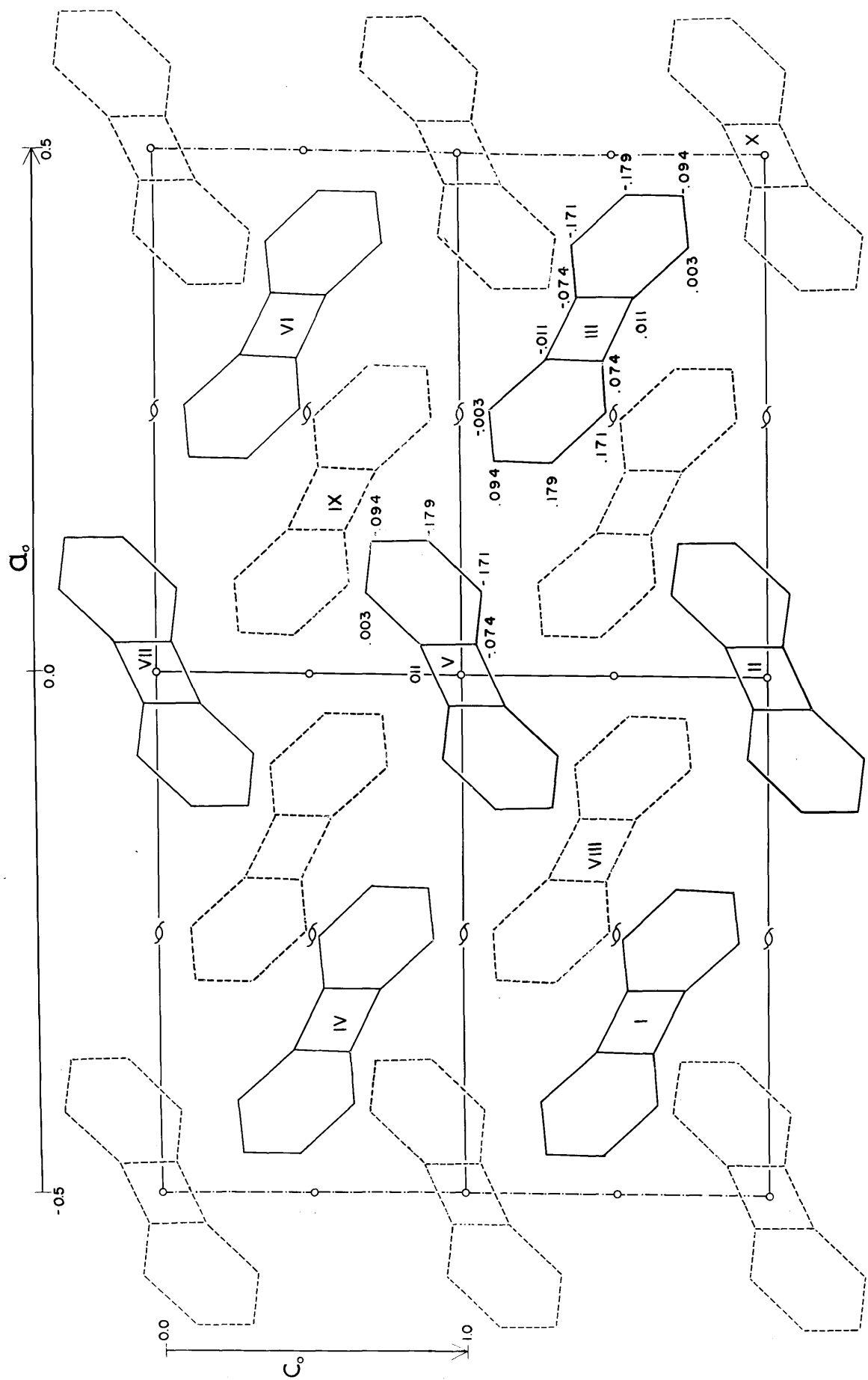


Figure 5

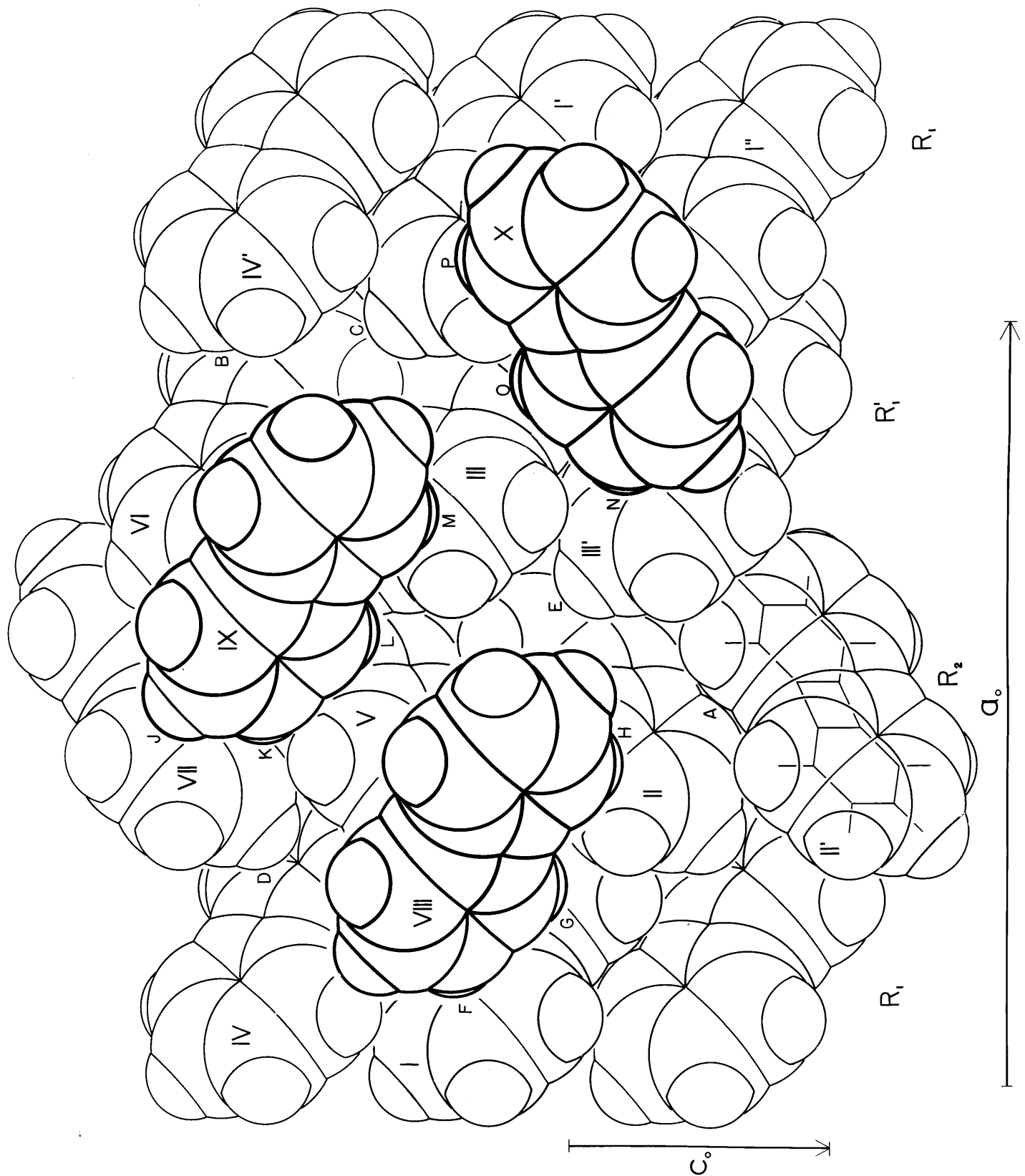


Figure 6

The following contacts are recognized in the bottom layer of Fig. 6. Molecules forming ribbons parallel to the c_0 axis interact like II and III' at A. There are three such ribbons per unit a_0 . In two of them (R_1 and R_1') the molecules are tilted in one direction from the c axis; in the third (R_2) this tilt is in the opposite direction. Ribbons of the same kind, R_1 and R_1' , interact in the following way: the benzene ring of molecule IV' partly overlaps the benzene ring of molecule VI at B, and VI and I' contact each other edge on at C. The interactions between the two different kinds of ribbons are of a different type. A hydrogen atom of VII points towards the center of the six-ring of IV (D). The same kind of contact (not shown) takes place between II' and III', while III' and II interact in an analogous manner at E, and the corresponding interaction between I and II is again not shown in Fig. 6.

The second layer again consists of ribbons of two kinds. Molecules VIII and IX belong to a type \bar{R}_1 , which is related to ribbons R_1 and R_1' by a glide plane a , while X is of a type \bar{R}_2 related in a similar manner to the ribbon R_2 . It is seen that the ribbons of the type \bar{R}_2 in the top layer (represented by molecule X) stretch across the ribbons R_1 and R_1' of the bottom layer and inversely, providing thus a very compact packing. In detail the interactions between the two layers are as follows. A hydrogen atom of molecule VIII points towards the six-ring of molecule I at F, while another hydrogen atom of VIII interacts with molecule I at G. A third hydrogen of VIII interacts with a carbon of II at H, and the hydrogen attached to this carbon of II interacts in an analogous manner (not shown here) with the carbon of VIII that carries the hydrogen first mentioned. Molecule IX lies edge on over the six-ring of VII at J and K. It makes contact with molecule V behind L, a contact of the same nature as the inter-

action at H, while another hydrogen atom interacts with molecule III at M. A hydrogen atom of molecule X points towards the six-ring of III' at N in a fashion already encountered at D, E and F. The interactions of X with III and I' at O and P respectively represent the back views of interactions already mentioned. The interaction at O corresponds to interaction H while P corresponds to L. Still another hydrogen atom of X makes contact with III' at Q.

The two crystallographically different kinds of molecules in the unit cell require discussion of the environment of representatives of each. A molecule with center at 000, as represented by X in Fig. 6, has fourteen neighbors. Four of these belong to the ribbons R_1 and R_1' of the layer below, four to analogous ribbons of the layer above, and six to the same layer (e.g. II, Fig. 6), of which two are in the same ribbon as the molecule considered. A molecule with center at pqr as represented by IX in Fig. 6 has fourteen neighbors also. Four of these belong to the layer below, while six belong to the same layer (e.g. III, Fig. 6). Since molecules IX and VIII are related by a space group center the interactions of molecule IX with its four neighbors of the layer above are analogous to the interactions of molecule VIII with the layer below. One of these four interactions, the one between VIII and VI, is weaker than the other three, since this interaction is mainly one between hydrogen atoms.

The following table gives statistics of the intermolecular distances encountered.

Distances between	molecule with center at 000 and its neigh- bors	molecule with center at pqr and its neigh- bors	
C...C	3.7-3.8 Å. 3.6-3.7 Å. 3.5-3.6 Å.	6 2 2	3 8 0
C...H	3.0-3.3 Å. 2.7-3.0 Å. 2.6-2.7 Å.	30 24 2	31 21 3
H...H	2.3-2.6 Å.	4	6

The calculated packing distances in general agree with van der Waals distances found for crystals of other aromatic hydrocarbons⁹. Some distances are somewhat short, the two worst kinds being carbon-hydrogen distances of about 2.65 Å. Both these contacts could be improved by bending the C-H bonds in question by a few degrees in the plane of the molecule. A change in the carbon parameters would, of course, change these distances also, so that no real significance can be attached to their shortness.

Of interest is the overlapping of the six-rings of molecules IV' and VI at B. The distance between the planes of the two molecules is 3.55 Å. which may be compared with the value of 3.66 Å. found for hexamethylbenzene¹⁰; the interplanar distance in the latter case is partly determined by the size of the methyl groups. The distances involved in the interactions between hydrogen atoms and benzene rings of the type D,E,F and N are quite short. For example the interaction at N involves C...H distances of 3.1, 3.0, 2.9, 2.9, 2.9, and 3.0 Å. while the distance between the centers of the six-ring and the hydrogen atom is 2.6 Å. This distance is short enough to show that the van der Waals representation of benzene rings by domes, as suggested by Mack¹¹, is inappropriate. The crater-like characterization as used in Fig. 6 represents the actual conditions much better.

The closely knit packing of the biphenylene crystal

accounts satisfactorily for the fact that no pronounced cleavages were observed. The packing is different from that characteristic of naphthalene and anthracene¹²:

I wish to express my thanks to Professor L. Pauling for suggesting this problem; to Dr. Chia-Si Lu for his collaboration in the beginning stages of this investigation, and to Dr. V. Schomaker for discussion and valuable suggestions. The tracing of the Fourier projections (Figs. 2 & 4) by Dr. Schomaker and Mr. J. Donohue, and the assistance given me in calculations and drawings by my wife, are also much appreciated. I am indebted to Dr. W.C. Lothrop for the sample of biphenylene.

Summary.

The crystal structure of biphenylene is based on a monoclinic unit cell with dimensions $a_0 = 19.60 \pm 0.03 \text{ \AA}$, $b_0 = 10.50 \pm 0.02 \text{ \AA}$, $c_0 = 5.84 \pm 0.02 \text{ \AA}$, $\beta = 91^\circ 20' \pm 20'$, containing six molecules. The probable space group is $C_{2h}^5 - P2_1/a$. The centers of two of the six molecules are space group centers. Approximate values of the fifty-four parameters for the carbon atoms are evaluated for planar molecules of dimensions suggested by an electron diffraction investigation¹. The packing of the molecules is discussed.

References Cited

1. J. Waser and V. Schomaker, J.A.C.S., 65, 1451 (1943).
2. W.C. Lothrop, J.A.C.S., 63, 1187 (1941); 64, 1698 (1942).
3. J.J. De Lange, J.M. Robertson, and I. Woodward, Proc. Roy. Soc. (London), A171, 398 (1939).
4. C.S. Lu, Rev. Sci. Inst., 14, 331 (1943).
5. G. Knott, Proc. Phys. Soc. (London), 52, 229 (1940).
6. H. Lipson and C.A. Beevers, Proc. Phys. Soc. (London), 48, 772 (1936).
7. P.A. Shaffer, Jr., Ph.D. Thesis, California Institute of Technology, 1942.
8. J.M. Robertson, Proc. Roy. Soc. (London), A150, 106, (1935).
9. L. Pauling, The Nature of the Chemical Bond, 2nd edition, Ithaca, N.Y., 1940, p.189.
10. L.O. Brockway and J.M. Robertson, J. Chem. Soc., 1939, 1324.
11. E. Mack, Jr., J.A.C.S., 54, 2141 (1932); J. Phys. Chem. 41, 221 (1937).
12. J.M. Robertson, Proc. Roy. Soc. (London), A140, 79 (1933). For packing drawings cf. R.W.G. Wyckoff, The Structure of Crystals, Supplement 1930-1934, New York, 1935, p.154-155.

ON ARSENOMETHANE

Introduction.

Arsenomethane ($(\text{AsCH}_3)_n$) was first prepared by Auger¹ by the reduction of sodium methylarsenate with hypophosphorous acid. He purified the resulting yellow oil by vacuum distillation. The product had the following properties. It was not miscible with water and was slightly soluble in alcohol, quite soluble in boiling acetic acid, and very soluble in benzene. It had a very strong, garlic-like odor. It was not attacked by alkali, but dissolved slowly in hot sulfuric acid, forming sulfur dioxide and methylarsenious oxide. Air oxidized the oil itself slowly, and the substance in benzene solution rapidly. Traces of hydrochloric acid caused rapid transformation of the yellow oil into a solid brick red to dark brown modification. The initial action of nitric acid was similar, but it was followed by rapid oxidation of the resulting mixture of the two modifications.

Dehn² reported having obtained the red modification of arsenomethane by three methods, by reduction of methylarsonic acid with zinc and hydrochloric acid, by heating dimethylarsine in a sealed glass bulb at reduced pressure, and by reacting methylarsine with methylarsenious oxide. Zappi³ obtained the red modification by reducing methylarsinedichloride with zinc and magnesium, while Paneth⁴ prepared a mixture of both modifications by the reaction of methyl radicals upon an arsenic mirror.

The following cryoscopic and ebullioscopic determinations of the molecular weight of arsenomethane have been reported. Auger¹ found the values 300-340 from freezing point lowering in benzene. The formula weight of AsCH_3 is 90. Auger neg-

lected, however, to account for the effect of the solubility of the carbon dioxide which was used to provide an inert atmosphere. Correction for this by Steinkopf, Schmidt and Smie⁵ led to $n \approx 5$, in $(\text{AsCH}_3)_n$, rather than the value $n \approx 4$ reported by Auger. These authors carried out additional molecular weight determinations in two solvents using a nitrogen atmosphere, and obtained the results listed below. They convinced themselves that the solubility of nitrogen was too small to necessitate a correction.

Solvent	g arsenomethane/g solvent	M.W.	Method
Benzene	0.0450	428	Cryoscopic
	0.0374	425	
	0.0335	436	
Nitrobenzene	0.0364	463	Ebullioscopic
	0.0295	457	
	0.0180	468	
Benzene	0.0297	440	Ebullioscopic
	0.0464	469	
	0.0386	436	
	0.0741	443	
	0.1167	461	
	0.0394	436	
	0.0822	446	
	0.1214	464	
M.W. for $(\text{AsCH}_3)_5$			450

Values connected by braces were obtained by increasing the concentration in the same solution by successively breaking small bulbs containing $(\text{AsCH}_3)_n$. The molecular weights obtained in this way indicate that $n \approx 5$. The ebullioscopic values, however, show a slight increase of the molecular weight with concentration, which was ascribed to oxidation of the arsenomethane. This explanation would seem to be based on a misconception, unless the authors tacitly assumed that oxidation is accompanied by polymerization or precipitation. It is possible that an equilibrium between different states of association manifests itself in the data, but the data are not conclusive, since the boiling point elevation in benzene may not vary linearly with the concentration. This is indicated

by a similar trend in the case of salicylic acid amylester, which was used as test substance by Steinkopf and his co-workers.

Measurements of the boiling point elevation were also made by Palmer and Scott⁶ who, using benzene and carbon disulfide as solvents and nitrogen to provide an inert atmosphere, obtained the following results on the yellow form and on a mixture of the yellow and red forms.

	g arsenomethane /cc solvent	Molecular weight
yellow form of arsenomethane in carbon disulfide	0.2177 0.0846 0.0802	483 469 469
<hr/>		
mixture of approxi- mately equal parts of red and yellow form in benzene.	0.0187 0.0070	491 461

These data indicate $n \approx 5$ but are not sufficiently accurate to show whether or not an equilibrium is at hand between different association states.

Steinkopf and Dudek⁷ reported that heating arsenomethane to 270°C. under atmospheric pressure caused decomposition into arsenic and cacodyl ((CH₃)₂As-As(CH₃)₂), which distilled at 155-164°C. Valeur and Gailliot⁸ found that the yellow form of arsenomethane has a density of 2.159 at 15°C., and a melting point of 10°C. It decomposes into arsenic, cacodyl and methylarsine when heated in a sealed tube to 200-250°C. The boiling point observed by these authors, 190°C. at 5 mm, appears very high compared to others recorded in the literature: 190°C. at 15mm¹, 193-200°C. at 15mm⁴, 190°C. at 13mm⁵ and 178°C. at 15mm⁶.

The present study includes an investigation of some of the properties of arsenomethane, particularly of the transformation between red and yellow modifications and of the

vapor density of the compound, an X-ray study of powder samples of the red modification, and electron diffraction experiments on the vapor.

Preparation and properties of arsenomethane.

The arsenomethane used in this investigation was prepared by the action of hypophosphorous acid⁶ on sodium methylarsenate, which had been prepared by refluxing an aqueous solution of sodium arsenite with methyliodide. The arsenomethane was distilled in a high vacuum and was stored in vacuum-sealed ampoules. An analysis indicated 13.22% C and 3.34% H (calculated for AsCH_3 13.35% C, 3.36% H).

The bright yellow oil remained clear during a period of six months, although a thin layer of the red modification deposited very slowly on the walls of the ampoules. The oil was observed to ignite spontaneously and burn with a pale blue flame when exposed to air over a large surface, as when spread on filter paper or asbestos.

If the yellow oil was left standing in contact with air for a period of weeks, a red solid slowly formed. Microanalysis of a sample of this material showed 9.68% C and 2.91% H, indicating oxidation by air, and X-ray powder photographs proved to be essentially identical with powder photographs of arsenious oxide. This material is therefore not a pure substance but a mixture, probably of $(\text{AsCH}_3)_n$ and As_2O_3 and other oxidation products.

Addition of traces of hydrochloric acid induced rapid transformation of the yellow oil to a solid modification of dark violet color. Microanalysis of a sample of this substance showed 13.43% C and 3.35% H, corresponding closely to AsCH_3 . Powder photographs with X-rays were taken of this AsCH_3 modification also. They will be discussed later.

Various experiments were carried out with samples of the yellow modification sealed in glass ampoules. Dipping

into liquid air or a mixture of dry ice and alcohol caused the yellow oil to solidify into a pale yellow glass. Warming to about 10°C . induced partial melting, whereupon some crystals usually appeared. The crystallization then proceeded, until, after some minutes, the whole sample had crystallized. The melting point of the crystals was 12°C . The oil could be supercooled considerably; for example, it stayed liquid for hours in a mixture of salt and ice at -10°C . the yellow crystals, kept at 4°C ., turned orange within an hour, and very dark red within a day. A liquid sample on the other hand showed no change after two weeks storage at 4°C . This behavior of the crystals seems strange and may possibly be due to a small amount of impurity and incomplete crystallization, so as to leave a solution containing the impurity in high concentration. If in this higher concentration the impurity (possibly a small amount of the red form in solution which precipitates on concentration; see below) induces the transformation, the behavior described above may result. Some support for this explanation is given by the observation that the crystals always appeared somewhat moist. On melting, the orange or dark red crystals produced a turbid mixture of yellow oil with very fine red particles in suspension, which could be filtered off. The red material so obtained yielded the same X-ray diffraction pattern as did the red modification obtained from the yellow oil with traces of HCl. When the above mentioned turbid mixture was heated for an hour or more at 100°C ., the conversion of the yellow oil to the red modification proceeded substantially, while heating of the yellow oil at 100°C . for the same or a longer time produced no change. No evident change was effected by heating the material at 100°C . in ampoules which contained, besides the clear yellow oil, some of the red modification clinging to the walls or even in the form of larger particles suspended in the liquid. It appears

that the conversion of the yellow to the red form is catalyzed by the red form and that the surface available is of importance. It was not investigated whether inert particles, such as finely ground glass, would produce the same effect.

Heating in ampoules at 180-205°C. caused the red modification or mixtures of the yellow and red modifications to revert to the yellow oil, which then remained yellow for weeks at room temperature. At 180-205°C. the yellow modification is thus the stable form, while at 100°C. and below the red modification is the more stable. No attempt was made to find a definite transition temperature, however, since it is not even certain whether or not the red modification is a uniform substance. Heating at 205-215°C. caused an irreversible change of the ampoule contents. Bubbles appeared and a precipitate formed; meanwhile, the color darkened turning first red and then black. No attempt was made to identify the decomposition products. If the yellow modification contained some of these decomposition products at room temperature, considerable change to the red form occurred within a few hours.

Vapor density determinations.

The all glass apparatus shown in Fig. 1 was used to measure the vapor density of arsenomethane in the following way. A sample, sealed into a small, thin-walled glass bulb, was inserted into the 300 ml bulb A, which was then sealed off at B. After the whole system had been evacuated, the constriction at C was sealed off and the sample bulb was broken by shaking. The bulb A was then placed in a heating bath which was brought to the desired temperatures. The manometer D, observed through the telescope E, was used as null-instrument, the pressure in the bulb being read at F after the pressure difference at D had been adjusted to zero by manipulation of

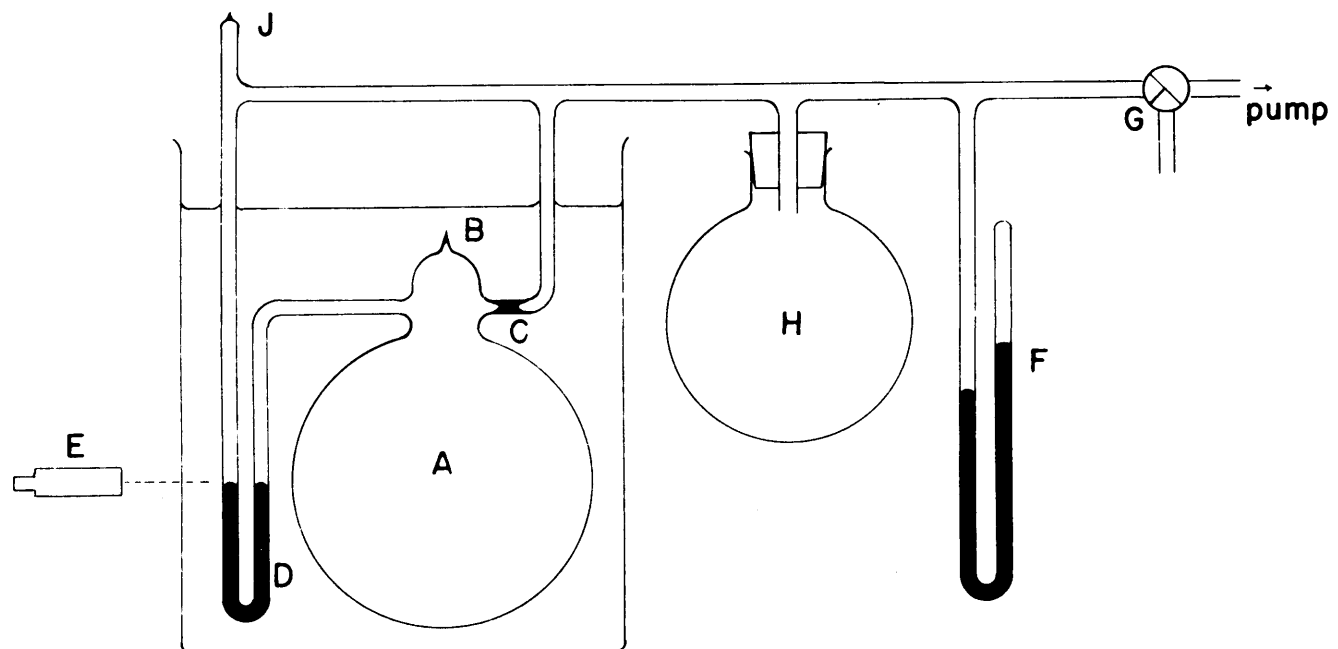


Figure 1

the stopcock G. The one-liter bulb H served to minimize any abrupt pressure changes. Mineral oil was used as heating fluid at first, but for later experiments a eutectic mixture of LiNO_3 , NaNO_3 , and KNO_3 ¹⁰ was adopted to achieve higher temperatures. The manometer D was filled at J with a low melting alloy consisting of 54 parts Bi, 28 parts Sn and 20 parts Cd. (Mercury proved to be unsatisfactory.) This alloy was not entirely satisfactory in that it tended to stick to the glass.

The working temperatures were limited by the deposition of traces of a brown mirror which began at $250-270^\circ \text{C}$. Despite the appearance of such a mirror the pressures measured at decreasing temperatures satisfactorily reproduced those obtained at increasing temperatures. After cooling the bulb to room temperature arsenomethane condensed unchanged in pale yellow droplets. The results of the two best runs are reproduced in the first three columns of Table I.

Table I

Concentration	T°K.	p mm Hg	n	p' mm Hg	n'
194 mg/l	421	(5.5)	-	(1.8)	-
	443	9.0	-	5.1	-
	463	14.0	-	9.9	-
	473	16.5	3.8	12.3	5.2
	483	17.0	3.8	12.7	5.1
	506	19.0	3.6	14.5	4.7
112 mg/l	428	(3.0)	-		
	444	5.0	-		
	452	6.5	-		
	456	8.2	-		
	463	10.0	-		
	479	11.0	3.4		
	488	11.2	3.4		
	493	11.5	3.3		
	525	14.4	2.8		
	543	15.0	2.8		

The pressures reported are averages of several readings taken during periods of about an hour. At the lower temperatures the pressures are saturation pressures, which should therefore be the same in both runs but actually differ by about 4 mm. The values p' were calculated for the runs at the higher concentration of arsenomethane by subtracting a correction corresponding to 4 mm of residual gas at 450° K. Fig. 2 shows a plot of $\log p$ versus $\frac{1}{T}$ for the pressures measured in the run with 112 mg/l and of $\log p'$ versus $\frac{1}{T}$ for the run with 194 mg/l. The straight line indicates a heat of vaporization of $\Delta H = 14.7$ kcal/mole, a boiling point at 760 mm of 640° K. (367° C.), and a value of Trouton's constant of 23 cal/deg.mole. All these values are of course only approximate.

Values for the average state of association, n in $(\text{AsCH}_3)_n$, calculated from the pressures are shown in Table I. These values provide strong indication that a temperature and concentration dependent equilibrium between different association states

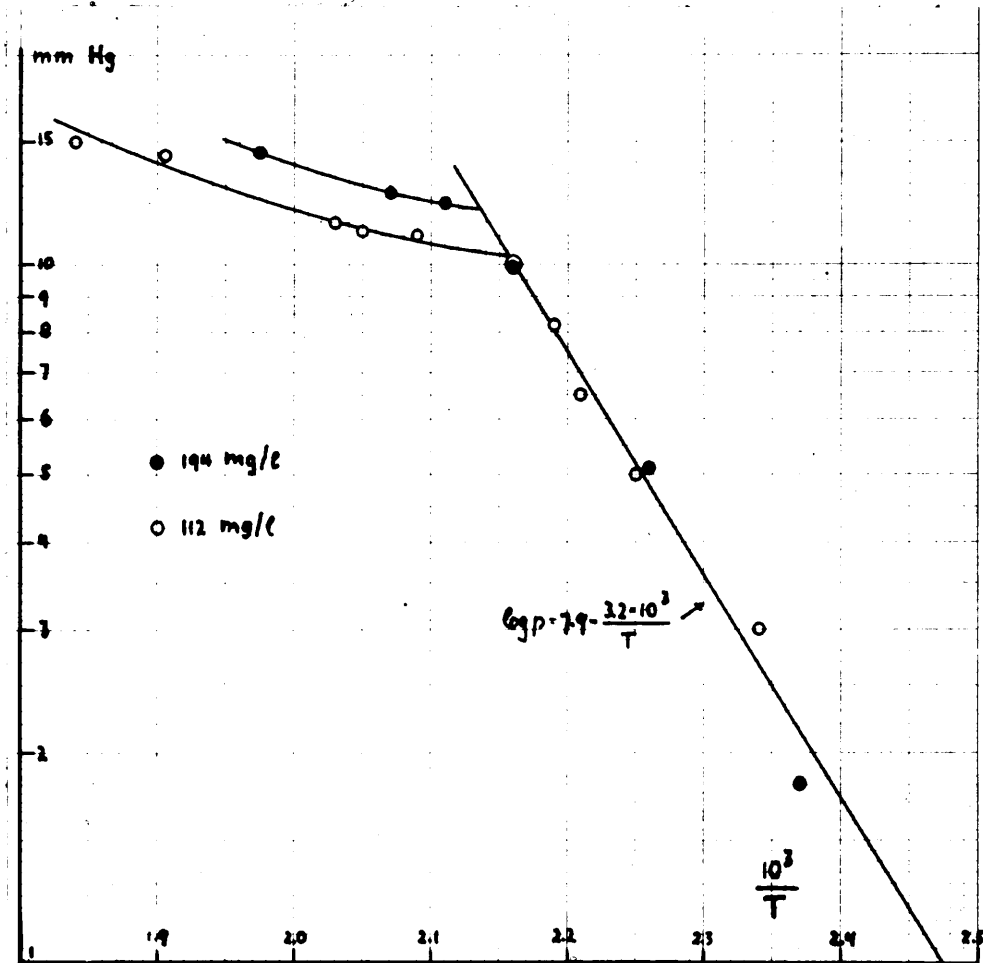


Figure 2

exists, irrespective of whether or not the above mentioned pressure correction is accepted. The establishment of such an equilibrium, possibly involving a pentamer and lower association states, is the main result of the vapor density measurements. The sources of error in the present apparatus (particularly the manometer D), causing e.g. the large discrepancy between the saturation pressures in the two runs, made it impossible to obtain any quantitative information about the equilibrium. For this reason it was not thought worthwhile to continue the measurements with this apparatus.

X-ray Diffraction Study.

Samples of the violet solid obtained by subjecting the yellow form of arsenomethane to a trace of HCl, and samples of the red modification obtained from crystals of the yellow form in the way described in a preceding section, yielded the same powder pattern with Cu K α radiation. The estimated intensities and the positions of the lines on the diffraction photographs were used in the computation of the radial distribution function

$$rD(r) = c \sum_i \frac{\sin 2\theta_i \exp(-1.5 h^2(\theta_i))}{1 + \cos^2 2\theta_i} \int_{\theta_i - \Delta}^{\theta_i + \Delta} I(\theta) d\theta \sin 2\pi h(\theta_i) r.$$

Here $h = \frac{2 \sin \theta}{\lambda}$, λ denotes the wave length, 2θ is the angle of reflection and the exponential function is a convergence factor. The integrals in the sum represent the integrated intensities of segments of equal heights of the powder lines on the film, which in the experiment had been arranged cylindrically about the powder sample.

The resulting function $rD(r)$ is represented by curve R₂ in Fig. 3. The broad feature between 1.6 and 5 Å., corresponding to interatomic distances, is unfortunately not well resolved. It however clearly contains a peak at 2.4 Å. corresponding to an As-As single bond (expected value 2.42 Å.¹¹), and another peak at 3.8 Å. corresponding, for an As...As distance, to a bond angle of about 105°. A third peak, and indeed even others, may be present between these two.

A radial distribution function for which the convergence factor was omitted was calculated also. The result showed slightly improved resolution, but also the effects of breaking off the Fourier series at a point where the coefficients were still large (cf. chapter on radial distribution method).

No detailed conclusion about the structure of the red form of arsenomethane can be drawn from this analysis of the radial distribution function. The important item, however, is

the peak at 2.4 Å. which shows clearly that whatever kinds of molecules are present in this red modification, a predominant number of them contain As-As single bonds.

Electron Diffraction Investigation.

An electron diffraction investigation on the vapor of the yellow modification was carried out with the use of the high-temperature nozzle which had to be heated to about 200°C. The diffraction pictures were made in the usual way, with an electron wave length of 0.0609 Å., at a film distance of about 10 cm, or, for a few pictures, of about 20 cm. After some of the runs the material remaining in the nozzle was investigated and found to consist of unchanged arsenomethane. The inside of the trap in the electron diffraction machine became covered after a while with what appeared to be the red modification. Both these facts indicate that the diffraction pictures obtained are characteristic of arsenomethane and not of some decomposition product like cacodyl. Moreover, all the pictures showed identical patterns, which also makes it improbable that decomposition occurred to any marked extent.

From the appearance of the rings and their measured positions the visual curve V (Fig.3) was drawn. Except for the first and second features, and in minor respects the other features out to about $q=50$, the pictures have the appearance characteristic of molecules involving one distance only. The spacing of the rings corresponds to a distance of 2.42 Å., the distance expected for the As-As single bond.

The visual curve V was used in the calculation of the radial distribution function

$$rD(r) = \int_0^{\infty} \sin(sr) I(s) \exp(-as^2) ds$$

(cf. chapter on the radial distribution method). The integral

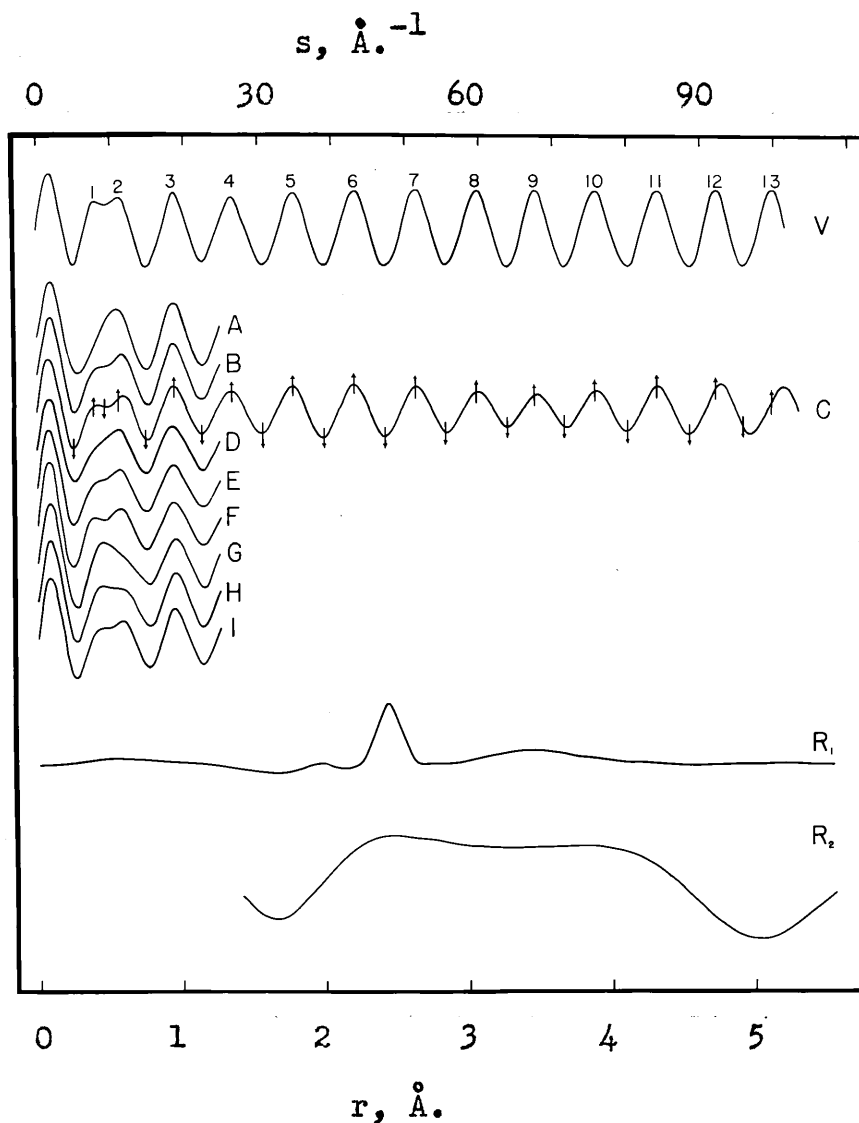


Figure 3

was approximated by the sum

$$\sum_i \sin\left(\frac{\pi}{10} q_i r\right) I'(q_i) \exp(-a' q_i^2) \Delta q ,$$

which was taken out to $q_i = 100$ in steps $\Delta q = 1$ ($q = \frac{10}{\pi} s$). The value of a' was chosen so that the exponential had the value 0.03 for the last term of the sum.

The main feature of the resulting radial distribution function (R_1 in Fig. 3) is the peak at 2.42 Å. , which corresponds to the As-As single bond. The peak at 1.98 Å. is in

exact agreement with that expected for an As-C single bond, the sum of the covalent radii being 1.98 Å.¹¹ The very broad feature with center at 3.44 Å., corresponding to an average bond angle of 90°, must represent the nonbonded As...As distances, but it must also include some of the nonbonded As...C distances. Assuming a C-H distance of 1.08 Å. and a tetrahedral configuration of the CH₃ groups, the shortest As...H distances would be expected at 2.55 Å., within the region covered by the peak at 2.42 Å. (The radial distribution curve does not go to and remain at zero for values of r smaller than 1.98 Å. because the features 1 and 2 of the visual curve V were somewhat overemphasized causing a sine wave with decreasing amplitude in $rD(r)$ with its first maximum at about 0.5 Å.).

Assuming that one kind of molecule is predominantly responsible for the electron diffraction pattern, the following speculations may be made to explain this pattern. The ratio of the area of the peak at 2.42 Å. to the area of the broad peak at 3.44 Å. is 1.2. This value is close enough to unity to suggest that each arsenic has the same number of unbonded neighbors at approximately 3.5 Å. as it has bonded neighbors at 2.42 Å. This would be the case for a five membered ring of As atoms (the most plausible example; the same would hold e.g. for a cube) but would not be true for the square, which at first sight is suggested by the observed bond angle. The only pentagon with all angles equal is, however, the planar one which has these angles equal to 108°. A pentagon with average angle of 90° will not be planar and will give rise to several diagonal distances because it cannot have all angles equal. The breadth of the peak at 3.44 Å. would require the notion of a pentagon with quite flat potential humps between the different equilibrium positions, so that this pentagon would carry out slow librations from one equilibrium position

to the others. The pentagon is quite unique in this respect inasmuch as other configurations such as tetragons, hexagons, heptagons, etc. can be constructed with equal sides and equal angles for a whole range of possible angles and not just for a certain definite angle. The breadth of the peak at 3.44 Å. therefore provides further support for the assumption of a pentagonal configuration of arsено-methane, since it can be naturally explained with this model.

A number of theoretical intensity functions

$$I'(q) = k \sum_{ij} \frac{Z_i Z_j}{r_{ij}} \sin \left(\frac{\pi}{10} qr_{ij} \right)$$

were calculated in the following way. The As-As, As-C and As...H distances were kept unvaried at 2.42, 1.98 and 2.55 Å. respectively. The same number of As-As bonds and three times as many shortest As...H distances as As-C bonds were assumed. The effective scattering power of arsenic was taken to be five times stronger than that of carbon, twenty-five times stronger than that of hydrogen. The facts that the scattering powers of these atoms vary somewhat differently with q and that the various distances actually correspond to temperature distributions of different widths were neglected. The contributions to $I'(q)$ of the nonbonded As...As and As...C distances were introduced by wide temperature distributions with positions r_0 , halfwidths w , and areas a , close to those suggested by the radial distribution function. Curves, calculated for the values of these parameters listed in Table II, are shown in Fig.3. The scale of the parameter a used in Table II is such that $a=1$ means an equal number of As-As and As...As distances. Only one of the curves (C) is shown beyond $q=25$ in Fig.3 since all the others are identical with it in this region. Curves C, F and I reproduce features 1 and 2 correctly and are in general satisfactory. Table III shows observed positions $q_{\text{obs.}}$ of the various features of the diffraction pattern, the

Table II

curve	w, A.	a	r ₀ , A.
A	0.35	0.5	3.44
B	0.35	1.0	3.44
C	0.35	1.2	3.44
D	0.52	1.0	3.44
E	0.52	1.3	3.44
F	0.52	1.7	3.44
G	0.35	1.0	3.20
H	0.35	1.0	3.32
I	0.35	1.0	3.40

Table III

max.	min.	q _{calc.}	q _{obs.}	q _{calc.} /q _{obs.}
1	1	5.1	4.9	(1.041)
		8.3	8.0	(1.037)
	2	9.7	10.0	(0.970)
		11.8	12.1	(0.975)
	3	15.2	15.4	0.987
		18.7	18.7	1.000
	4	22.5	22.5	1.000
		26.5	26.5	1.000
	5	30.6	30.8	0.994
		34.8	34.8	1.000
	6	39.0	39.2	0.995
		43.1	43.3	0.995
	7	47.5	47.5	1.000
2	8	51.7	51.6	1.002
		55.9	55.7	1.004
	9	60.0	59.8	1.003
		64.0	64.1	0.998
	10	68.2	67.7	1.007
		72.1	71.8	1.004
	11	76.1	75.9	1.003
		80.4	80.8	0.995
	12	84.5	84.4	1.001
		88.9	88.9	1.000
	13	93.1	92.4	1.007
		97.4	96.2	(1.012)
13		101.5	100.1	(1.014)
				Av. 1.000
				a.d. 0.004

values $q_{\text{calc.}}$ calculated for model C and the ratios between them.

Curve A is of special interest, representing a model which, like a tetragon, has only half as many As...As distances as As-As distances. Curve A is not satisfactory and such a model is therefore unlikely.

The calculated intensity curves thus confirm the analysis of the radial distribution curve, indicating that immediately after evaporation the arsenomethane molecule is quite possibly a pentagon with an average bond angle of 90° , librating from one equilibrium position to another. Some support to the notion of a pentagon comes from the observation^{5,6} that arsenomethane seems to exist as pentamer in solution. The establishment of the equilibrium between different states of association observed in the vapor density measurements is then presumably a slow process.

The only definite conclusions from the electron diffraction experiments are the presence in the molecule of the As-As single bond with length $2.42 \pm 0.02 \text{ \AA.}$ and of the As-C single bond with length $1.98 \pm 0.04 \text{ \AA.}$, and an As-As-As angle of about 90° .

I wish to thank Professor L. Pauling for the suggestion of the problem, and Dr. V. Schomaker for much helpful discussion, particularly in the interpretation of the electron diffraction patterns. My thanks go further to Mr. J. Renno for help in the preparation of the compound, to Dr. G. Oppenheimer for microanalyses, and to Mr. W. Shand for help with the vapor density measurements.

Summary.

A study was made of some of the properties of arsene-methane, which occurs both in a yellow liquid form and a red solid modification, particularly of the transformation between the two forms. Vapor density measurements strongly indicated the existence in the vapor of an equilibrium between different states of association. X-ray powder photographs of the red solid revealed the presence of single-bonded arsenic. An electron diffraction study of the vapor led to an As-As distance of $2.42 \pm 0.02 \text{ \AA.}$, an As-C distance of $1.98 \pm 0.04 \text{ \AA.}$, and an average angle As-As-As of 90° . A puckered five-membered ring structure is compatible with the diffraction pattern.

References cited

1. V. Auger, Compt. rend., 138, 1705 (1904).
2. W.M. Dehn, Am. chem. J., 33, 120 (1905); 35, 8 (1906); 40, 109 (1908).
3. E.V. Zappi, Bull. Soc. Chim. de France, 4 23, 322 (1918).
4. F.A. Paneth, Trans. Faraday Soc. 30, 179 (1934); J.C.S. 1935, 366.
5. W. Steinkopf, S. Schmidt and P. Smie, Ber., 59, 1463 (1926).
6. C.S. Palmer and A.B. Scott, J.A.C.S., 50, 536 (1928).
7. W. Steinkopf and H. Dudek, Ber., 61, 1906 (1928).
8. A. Valeur and P. Gailliot, Compt. rend., 185, 956 (1927).
9. A.J. Quick and R. Adams, J.A.C.S., 44, 809 (1922).
10. J. Strong, Procedures in Experimental Physics, New York, 1938, p.527.
11. L. Pauling, The Nature of the Chemical Bond, second edition, Ithaca, N.Y., 1940, p. 165.

ON THE RADIAL DISTRIBUTION METHOD
IN ELECTRON DIFFRACTION

Introduction

There are two methods which may be used to correlate experimental data from electron diffraction experiments on gas molecules with the structure of these molecules.¹ One of them, the "correlation method"^{2,3} consists in the theoretical calculation of the scattering pattern for various molecular models, and comparison of the result with the observed diffraction pattern. The other is the very elegant "radial distribution method"^{4,5,6,7} which, by a mathematical treatment of the observed scattering intensity, leads directly to a radial distribution function which represents the interatomic distance spectrum. In principle the two methods are equivalent, but in practice they do not replace each other. One of the purposes of this paper is to point out the nature of this lack of practical equivalence of the two methods, and to derive several mathematical results pertaining to it. In a first section, the difficulties in the use of the radial distribution method which arise from the absence of experimental data for scattering angles greater than a limiting angle, are discussed in terms of the Gibbs phenomenon. In later sections the elimination of these difficulties by multiplication of the observed intensity function with a suitable convergence factor is studied with the help of a general theorem, which is also used in the investigation of the effect of the multiplication of the observed intensity function by a general modification function. As a final example the relationship between the atomic scattering function and the radial distribution function is considered.

In the following paragraphs the gas molecules are assumed to consist of atoms of similar scattering power; this assumption will be discarded in the final section.

The reduced theoretical intensity function for the elastic scattering of a monochromatic, uniform beam of electrons by randomly oriented gas molecules used in this laboratory (e.g.⁸) has, for a rigid molecule made up of point atoms of scattering power Z_i , the form

$$I(s) = c \sum_{ij} \frac{Z_i Z_j}{r_{ij}} \sin s r_{ij} \quad (1)$$

where $s = \frac{4\pi}{\lambda} \sin \frac{\varphi}{2}$, φ is the angle between direct and scattered beams of wave length λ , the r_{ij} are interatomic distances, and the sum is extended over all pairs of atoms in the molecule. In this reduced intensity function, a factor of s^{-5} has been omitted from the theoretical intensity function. For a molecule giving rise to scattering function (1) there can be written the radial distribution function

$$D(r) = \sum_{ij} Z_i Z_j \delta(r - r_{ij}) = r D'_o(r) \quad *) \quad (2)$$

in which $\delta(r)$ is defined by the two conditions

$$\begin{aligned} \delta(r) &= 0 \quad \text{unless } r=0, \text{ and} \\ \int_{-\infty}^{\infty} \delta(r) dr &= 1. \end{aligned} \quad **) \quad (3)$$

$D(r)$ has infinitely narrow and infinitely high peaks for values of r which represent interatomic distances. With it the reduced intensity function can be expressed as

$$I'(s) = \frac{1}{c} \sqrt{\frac{2}{\pi}} I(s) = \sqrt{\frac{2}{\pi}} \int_0^{\infty} D(r) \sin s r dr = \sqrt{\frac{2}{\pi}} \int_0^{\infty} D'_o(r) \sin s r dr \quad (4)$$

*) $D'_o(r)$ is an odd function of r .

**) The function $\delta(r)$ is an essentially singular, improper one (cf.e.g. J. von Neumann, Mathematische Grundlagen der Quantenmechanik, Berlin 1932, p.13), which is used here formally only. Examples for δ -functions are: $\lim_{n \rightarrow \infty} n \exp(-\pi n^2 r^2)$ or $\lim_{n \rightarrow \infty} \frac{\sin nr}{\pi r}$.

from which, by Fourier inversion⁹

$$D_o(r) = \sqrt{\frac{2}{\pi}} \int_0^\infty I'(s) \sin s r ds. \quad (5)$$

Expressions (4) and (5) are formal only, but may serve as a basis for discussion.

The experimentally determined intensity function $I'(s)$ is usually better known for certain small ranges of s in which it, for example, shows more prominent features than in others. To make use of this special information the visual method is admirably suited, and can thus not be replaced by the less laborious radial distribution method which requires the knowledge of $I'(s)$ over the whole range of integration. This is one reason that the two methods cannot entirely replace each other, but are, rather, complementary in nature. The radial distribution function narrows the choice of possible models, while the visual method serves to analyse the remaining possibilities.

In principle, to evaluate the integral in (5), $I'(s)$ should be known for the whole infinite range of s , but experimentally it can be determined for a finite range only. In practice the integral may, however, be modified by a convergence factor, which makes contributions from large values of s negligible. Even when a convergence factor is used, the integration is often not extended over the whole range in which the resulting integrand has still a finite value. This gives rise to certain effects closely related to the Gibbs phenomenon, which will be discussed in the following section.

The Gibbs and related phenomena.¹⁰

The phenomenon discovered by Gibbs¹¹ and even earlier by Wilbraham¹² is briefly the following. Suppose a sectionally smooth *) periodic function $f(x)$ which has a finite

*) A sectionally continuous function with a sectionally continuous first derivative.

number of finite discontinuities (e.g. Fig. 1a) to be expanded in a Fourier series. Let $S_n(x)$ be the approximation obtained by extending the summation over the first n terms only. If the S_n are plotted for increasing values of n , a set of approximation curves is obtained which converge not to the graph obtained by plotting $f(x)$ and connecting the discontinuities by straight vertical lines (e.g. Fig. 1b), but to a graph obtained by plotting $f(x)$ and connecting the discontinuities by vertical lines which overshoot on each side by about 9% of the discontinuity. If n is finite the approximation curve $S_n(x)$ has $\frac{n}{2}$ or $\frac{n-1}{2}$ waves on each side of the discontinuity (e.g. Fig. 1d) and it is this feature which is objectionable in the case of the radial distribution curve.

It was found by Fejer¹³ that the Gibbs phenomenon does not occur (e.g. Fig. 1e) if the $S_n(x)$ are replaced by quantities $s_n(x)$ which are the arithmetic means of the first n sums $S_n(x)$ *)

$$s_n(x) = \frac{S_1(x) + S_2(x) + \dots + S_n(x)}{n} \quad (6)$$

It is interesting to investigate this behavior more closely for the case of the special function (Fig. 1a)

$$f(x) = \frac{\pi}{2} - \frac{x}{2} \quad \text{when } 0 < x < 2\pi; \quad f(0) = 0; \quad f(x+2\pi) = f(x). \quad (7)$$

Let

$$S_n(x) = \frac{a_0}{2} + \sum_{v=1}^n (a_v \cos vx + b_v \sin vx). \quad (8)$$

*) The summation method of Fejer is the application of the summation method of Cesaro¹⁴ to Fourier series.

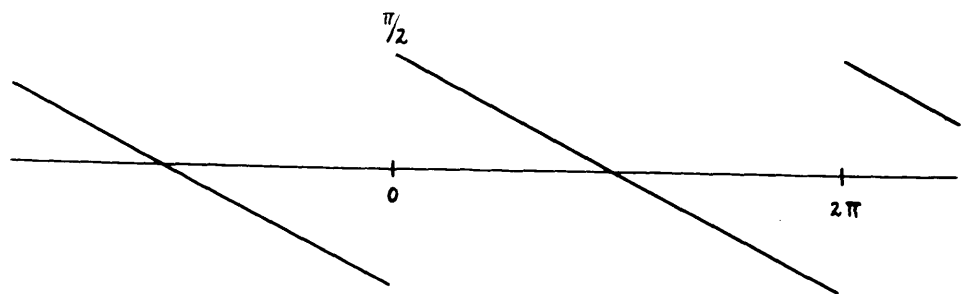


Fig. 1a

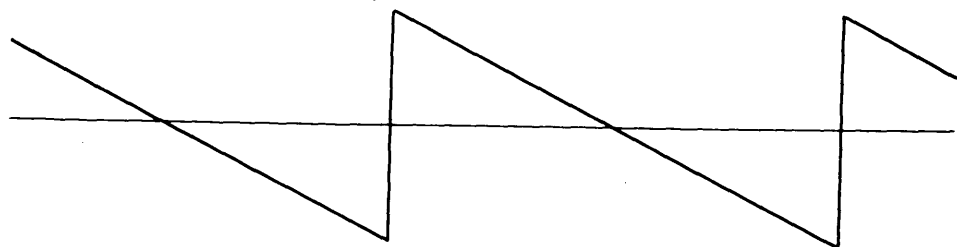


Fig. 1b

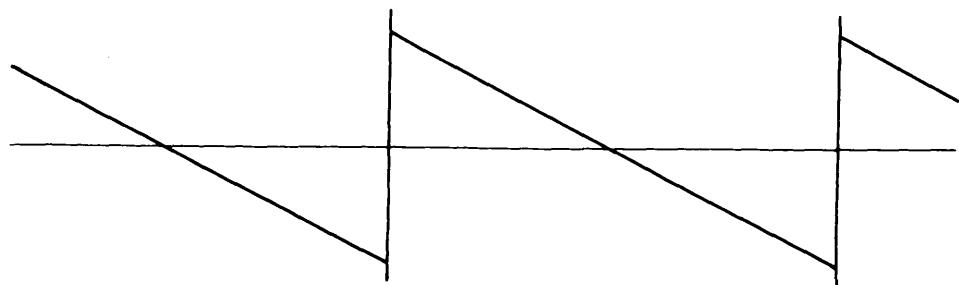


Fig. 1c

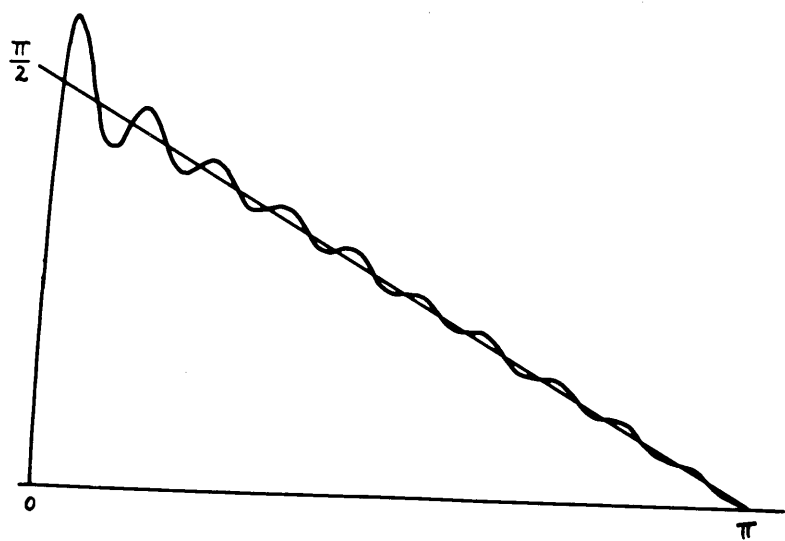


Fig. 1d

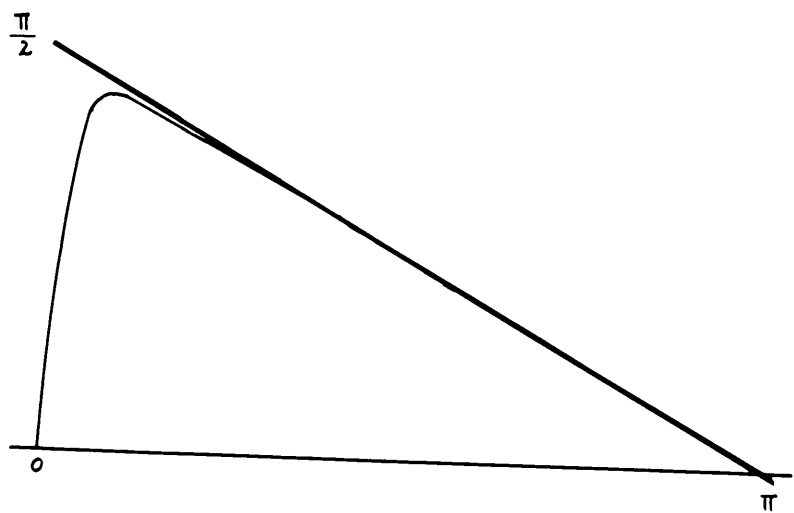


Fig. 1e

Then

$$a_v = \frac{1}{\pi} \int_0^{2\pi} f(x) \cos vx dx = 0, \quad v = 0, 1, 2, \dots$$

$$b_v = \frac{1}{\pi} \int_0^{2\pi} f(x) \sin vx dx = \frac{1}{v}, \quad v = 1, 2, 3, \dots$$

The sum thus becomes

$$S_n(x) = \sum_{v=1}^n \frac{\sin vx}{v} = \sum_{v=1}^n \int_0^x \cos vx dx = \int_0^x \sum_{v=1}^n \cos vx dx. \quad (8a)$$

Since

$$\sum_{v=1}^n \cos vx = \frac{\sin(n + \frac{1}{2})x}{2 \sin \frac{1}{2}x} - \frac{1}{2},$$

this becomes

$$S_n(x) = \frac{1}{2} \int_0^x \frac{\sin(n + \frac{1}{2})x}{\sin \frac{1}{2}x} dx - \frac{x}{2}. \quad (9)$$

The difference $R_n(x)$ between $f(x)$ and $S_n(x)$ consequently has the form

$$R_n(x) = f(x) - S_n(x) = \frac{\pi}{2} - \int_0^x \frac{\sin(n + \frac{1}{2})x}{2 \sin \frac{x}{2}} dx. \quad (10)$$

The approximation is worst for values of x for which $|R_n(x)|$ is a maximum. These values of x are given by

$$x = x_i = \frac{2i\pi}{2n+1}, \quad i = 1, 2, 3, \dots \quad (11)$$

If n increases without limit the x_i approach zero, at which value $f(x)$ is discontinuous. The crests of the waves in Fig. 1d move towards the place of discontinuity in $f(x)$. The magnitudes of the $R_n(x_i)$ do, however, not approach zero. In fact, it can be shown that the largest of them, $R_n(x_1)$, approaches in the limit the value 0.2811, which is about 9% of π , the magnitude of the discontinuity of $f(x)$ at $x=0$ (Fig. 1c).

If on the other hand, the summation method of Fejer is used, the following results are obtained. The approximation sums $s_n(x)$ (cf. (9)) are

$$s_n(x) = \frac{1}{n+1} \sum_{v=0}^n S_v(x) = \sum_{v=0}^n \frac{n-v+1}{n+1} \cdot \frac{\sin vx}{v} . \quad (12)$$

It is to be noted that (12) differs from (8a) by the inclusion of a factor $\frac{n-v+1}{n+1}$, which, as will be seen, substantially increases the convergence of the series. Introducing (9) and making use of the formula

$$\sum_{v=1}^n \sin(v + \frac{1}{2})x = \frac{\sin^2 \frac{n+1}{2}x}{\sin \frac{x}{2}} \quad (13)$$

$s_n(x)$ becomes

$$s_n(x) = \frac{1}{2(n+1)} \int_0^x \left(\frac{\sin \frac{n+1}{2}x}{\sin \frac{1}{2}x} \right)^2 dx - \frac{x}{2} . \quad (14)$$

Finally, since¹⁵

$$\frac{1}{2(n+1)} \int_0^{\pi} \left(\frac{\sin \frac{n+1}{2}x}{\sin \frac{1}{2}x} \right)^2 dx = \frac{\pi}{2}$$

the difference $r_n(x)$ between $f(x)$ and $s_n(x)$

$$r_n(x) = f(x) - s_n(x) = \frac{\pi}{2} - \frac{1}{2(n+1)} \int_0^x \left(\frac{\sin \frac{n+1}{2}x}{\sin \frac{1}{2}x} \right)^2 dx$$

assumes the form

$$r_n(x) = \frac{1}{2(n+1)} \int_x^{\pi} \left(\frac{\sin \frac{n+1}{2}x}{\sin \frac{1}{2}x} \right)^2 dx . \quad (15)$$

The discussion of this result can be limited to the interval $0 < x < \pi$, as the behavior of $r_n(x)$ everywhere else follows from symmetry and periodicity. In this interval $f(x) > 0$ and $r_n(x) > 0$, since the integrand is positive. For the same reason r_n decreases monotonically from $\frac{\pi}{2}$ to 0 as x varies from 0 to π . Thus the approximation curves $s_n(x)$ will never cross the curve of $f(x)$ as did $S_n(x)$. When $x=0$, $r_n(x) = \frac{\pi}{2}$ for all values of n ; $s_n(0)$ will thus always be equal to $0 = \lim_{x \rightarrow 0} \frac{f(x) + f(-x)}{2}$, as required by the general

theory. Further $r_n < \frac{\pi}{2(\sin^2 \frac{x}{2})(n+1)}$ in the interval considered,

which means that for any finite positive x , however small, $\lim_{n \rightarrow \infty} r_n = 0$. Thus $s_n(x)$ converges towards $f(x)$ in any interval not containing the discontinuity. There are no oscillations near the discontinuity and no Gibbs phenomenon. Fig. 1d is a plot of $s_{20}(x)$ while Fig. 1e shows $s_{20}(x)$.

It is interesting in this connection to discuss the following continuous function (Fig. 2)

$$f'(x) = \begin{cases} \frac{\pi}{2} - \frac{x}{2} & \delta \leq x \leq 2\pi - \delta \\ \frac{\pi - \delta}{2\delta} x & -\delta \leq x \leq \delta \end{cases} \quad f(x) = f(x + 2\pi) \quad (16)$$

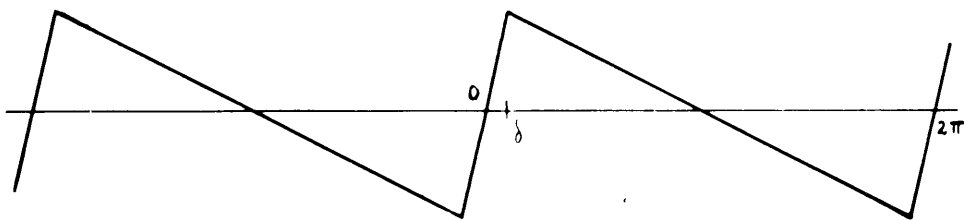


Fig. 2

$$\text{Again } a_v = 0 \text{ while } b_v = \frac{\sin \sqrt{\delta}}{\sqrt{\delta}} \quad (17)$$

so that the n -th approximation $s_n'(x)$ becomes

$$s_n'(x) = \sum_{v=1}^n \frac{\sin \sqrt{\delta}}{\sqrt{\delta}} \cdot \frac{\sin \sqrt{v}x}{\sqrt{v}} \quad (18)$$

This differs from (8a) by the inclusion of a convergence factor $\frac{\sin \sqrt{\delta}}{\sqrt{\delta}}$ and of course goes over into (8a) for $\delta \rightarrow 0$. After some transformation

s_n' becomes

$$\begin{aligned}
 s_n'(x) &= \sum_{v=1}^n \frac{1}{2v^2\delta} [\cos(x-\delta)v - \cos(x+\delta)v] = \\
 &= \frac{-1}{2\delta} \sum_{v=1}^n \int_{x-\delta}^{x+\delta} \sin vs \, ds = \frac{1}{2\delta} \sum_{v=1}^n \int_{x-\delta}^{x+\delta} \int \cos vt \, dt = \frac{1}{2\delta} \int_{x-\delta}^{x+\delta} \int \left[\sum_{v=1}^n \cos vt \right] dt \\
 &= \frac{1}{2\delta} \int_{x-\delta}^{x+\delta} \int \left(\frac{\sin(n+\frac{1}{2})t}{2 \sin \frac{1}{2}t} - \frac{1}{2} \right) dt
 \end{aligned} \tag{19}$$

$$s_n'(x) = -\frac{x}{2} + \frac{1}{2\delta} \int_{x-\delta}^{x+\delta} \int_0^s \frac{\sin(n+\frac{1}{2})t}{2 \sin \frac{t}{2}} dt$$

The difference $r_n'(x)$ between $f'(x)$ and $s_n'(x)$ is

$$r_n'(x) = f'(x) - s_n'(x) = \frac{\pi}{2} - \frac{1}{2\delta} \int_{x-\delta}^{x+\delta} \int_0^s \frac{\sin(n+\frac{1}{2})t}{2 \sin \frac{t}{2}} dt \tag{20}$$

The form of this remainder is similar to (10) obtained for the discontinuous function (7). The integral

$$\int_0^s \frac{\sin(n+\frac{1}{2})t}{2 \sin \frac{t}{2}} dt \tag{21}$$

which causes oscillations is again present but because it is averaged over the region $x-\delta \leq s \leq x+\delta$ the situation is improved. From the general theory of Fourier series¹⁶ it is known that $s_n'(x)$ converges uniformly towards $f'(x)$, so that if n becomes large enough the oscillations must die down. There is, of course, a relationship between the value of δ and the value of n beyond which oscillations become negligible. Let the assumption be made that in order to obtain a reasonable representation of $f'(x)$ the integration has to be extended over at least one maximum and minimum of (21) on each side of x . For a given δ then the relationship

$$n \gtrsim \frac{2\pi}{\delta} \tag{22}$$

has to be satisfied, because the extrema of (21) occur for the values (11) $s_i = \frac{2i\pi}{2n+1}$.

As a further example, the representation of the function (Fig.3)

$$F(x) = \begin{cases} 0 & 0 \leq x \leq x_0 - \delta \quad \text{or} \quad x_0 + \delta \leq x < \infty \\ (x - x_0 + \delta) \frac{h}{\delta} & x_0 - \delta \leq x \leq x_0 \\ -(x - x_0 - \delta) \frac{h}{\delta} & x_0 \leq x \leq x_0 + \delta \end{cases} \quad (23)$$

will be discussed. At the same time representation by a Fourier integral rather than a series will be used. Function (23) looks more like the original $D(r)$ (2) than do the functions discussed so far.

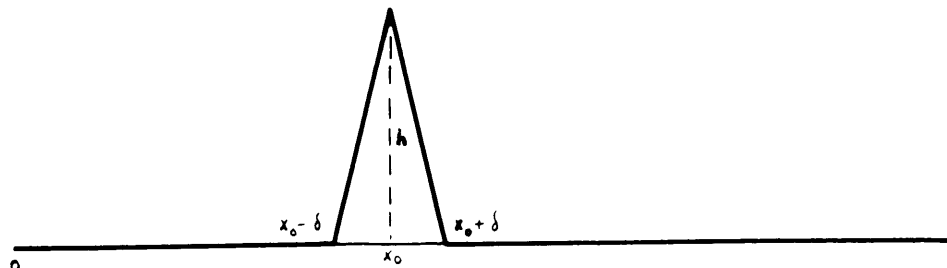


Fig. 3

The Fourier inversion¹⁷ $G(u)$ of $F(x)$ is

$$G(u) = \sqrt{\frac{2}{\pi}} \int_0^\infty F(x) \sin ux dx = \sqrt{\frac{2}{\pi} h \delta} \left(\frac{\sin \frac{u\delta}{2}}{\frac{u\delta}{2}} \right)^2 \sin ux_0. \quad (24)$$

In the limit $\delta \rightarrow 0$ where $h\delta$, the area of the triangle in Fig. 3 is kept constant, (24) becomes $G(u) = \sqrt{\frac{2}{\pi}} h\delta \sin ux_0$, corresponding to a discontinuous $F(x)$ with an infinitely high peak at $x=x_0$. By Fourier inversion of $G(u)$ the following representation of $F(x)$ is obtained

$$F(x) = \frac{2h\delta}{\pi} \int_0^\infty \left(\frac{\sin \frac{u\delta}{2}}{\frac{u\delta}{2}} \right)^2 \sin ux_0 \sin ux du. \quad (25)$$

The factor $\left[\frac{\sin \frac{u\delta}{2}}{\frac{u\delta}{2}} \right]^2$ can again be looked upon as a convergence factor in this integral.

The analog to a finite number of terms in a Fourier series is a finite upper limit in a Fourier integral.

Let therefore

$$F_T(x) = \frac{2h\delta}{\pi} \int_0^T \left(\frac{\sin \frac{u\delta}{2}}{\frac{u\delta}{2}} \right)^2 \sin ux_0 \sin ux du \quad (26)$$

which, after some transformation, becomes

$$\begin{aligned} F_T(x) &= \frac{h}{\pi\delta} \int du \left[\int dy \int \cos u z dz - \int dy \int \cos u z dz + \int dy \int \cos u z dz - \int dy \int \cos u z dz \right] \\ &= \frac{h}{\pi\delta} \left[\int dy \int dz \int \cos u z du - \int dy \int dz \int \cos u z du + \int dy \int dz \int \cos u z du - \int dy \int dz \int \cos u z du \right]. \quad (27) \end{aligned}$$

The inversion of the integration is justified by the absolute convergence of the integrals involved. In (27) occurs the integral

$$\int_0^T dz \int \cos u z du = \int_0^T \frac{\sin Tz}{T} dz = \int_0^{Ty} \frac{\sin v}{v} dv = Si(Ty) \quad (28)$$

the so-called sine integral of Ty . This integral is closely related to $\frac{1}{2} \int \frac{\sin(n+\frac{1}{2})x}{\sin \frac{1}{2}x} dx$, which was encountered before ((9), (21)). In fact, the two can be shown to be identical in the limit $T=n+\frac{1}{2} \rightarrow \infty$. Introducing (28), $F_T(x)$ becomes

$$F_T(x) = \frac{h}{\pi\delta} \left[\int_{x-x_0}^{x+x_0} Si(Ty) dy - \int_{x-x_0-\delta}^{x+x_0+\delta} Si(Ty) dy + \int_{x+x_0-\delta}^{x+x_0+\delta} Si(Ty) dy - \int_{x-x_0}^{x+x_0} Si(Ty) dy \right] \quad (29)$$

which is analogous to (19). The formula expresses an averaging over the oscillations of the sine integral which has its extrema for $y=y_1$ where $y_1 = \frac{i\pi}{T}$. If it is again assumed that the averaging is to be extended over at least one maximum and minimum, the relation

$$T \approx \frac{2\pi}{\delta} \quad (30)$$

is obtained which should hold to insure a reasonably good representation of $F(x)$ by $F_T(x)$. This relation is analogous to (22).

The artificial temperature factor.

After the discussion of the effect of a finite interval of integration on the representation of the function (23) the analogous effect of a finite integration interval in the case of the radial distribution function $D'(r)$ (2) will be briefly described.

Let

$$D'_T(r) = \sqrt{\frac{2}{\pi}} \int_0^T I'(s) \sin sr ds. \quad (31)$$

For the case of the diatomic molecule where $I'(s) = \frac{\sin sr_0}{r_0}$

$D'_T(r)$ can easily be evaluated. The result shows a main peak at $r=r_0$ with maxima and minima of decreasing magnitude on either side. In the case of a polyatomic molecule, which can be represented by a superposition of various diatomic radial distribution functions, these side peaks are objectionable in the interpretation of $D'_T(r)$. They may be eliminated by multiplying $I'(s)$ by a convergence factor. Two examples of convergence factors have been encountered so far; one is the factor $\frac{T-s}{T}$ suggested by the Fejer method of summation (which, mutatis mutandis, applies to the Fourier Integral Theorem also¹⁹); the other, the factor $\left(\frac{\sin \frac{sr}{2}}{\frac{sr}{2}}\right)^2$ encountered in formula (25), which would in the limit $T \rightarrow \infty$ give rise to a triangular shape of the peaks of $D'_T(r)$ (Fig. 3).

The convergence factor usually applied is, however, the function $\exp(-as^2)$, the so-called artificial temperature factor, which is suggested by the modification of the scattering intensity by a factor of that form due to zero-point and temperature motion of a molecule²⁰. A convergence factor of this type was perhaps first used by Weierstrass²¹ who used the factor r^{-n} ($r \leq 1$) in his discussion of Fourier series. A. Sommerfeld used the convergence factor $\exp(-as^2)$ in his doctorate thesis²², where he succeeded in obtaining with its

aid the first precise result concerning the validity of the Fourier Integral Theorem. W.L. Bragg and J. West²³ introduced the use of the artificial temperature factor in the inversion of X-ray diffraction patterns, while C. Dégard⁵ at the suggestion of Professor L. Pauling, introduced it into electron diffraction work.

The effect of the artificial temperature factor $\exp(-as^2)$ is to replace the discrete peaks of $D'(r)$ by peaks of a form closely related to Gaussian error curves $\exp(-b(r-r_0)^2)$ with $b = \frac{1}{4a}$. The consequence of extending the integration over a finite interval only, in this case, was investigated by V. Schomaker⁶ who replaced the factor $\exp(-as^2)$ by the factor $\frac{1+\cos cs}{2}$, which, for a suitable choice of c, closely approximates $\exp(-as^2)$, and the choice of which makes it possible to carry out the integration in closed form. He investigated the effect of the finite interval and the magnitude of a or c on half width and exact position of the main peaks, and the prominence of the secondary maxima.

Modification of the intensity function in general.

The general question now arises: what is the effect of any modification of the reduced intensity function (1) on the radial distribution function resulting from Fourier inversion of the modified intensity function. Such a modification may be inherent in the visual method of estimating reduced intensities, or it may have been introduced, e.g. by a convergence factor, or a factor giving special weight to particularly prominent features which are easier to observe than others. Even the effect of a finite integration interval can be reduced to this question by asking for the effect of multiplication of $I'(s)$ by a factor equal to unity in the intended range of integration and zero elsewhere.

To give an answer to this question, a few formulae from the theory of Fourier transforms have to be derived. Let $f_o(x)$ be an odd function and $g_e(x)$ an even function, and let^{9,24}

$$F_o(t) = \sqrt{\frac{2}{\pi}} \int_0^\infty f_o(x) \sin xt dx = -F_o(-t) \quad \text{be the sine transform of } f_o, \quad (32)$$

$$G_e(t) = \sqrt{\frac{2}{\pi}} \int_0^\infty g_e(x) \cos xt dx = G_e(-t) \quad \text{be the cosine transform of } g_e.$$

The transforms of $G_e(t)$ and $F_o(t)$ are in turn

$$f_o(x) = \sqrt{\frac{2}{\pi}} \int_0^\infty F_o(t) \sin xt dt, \quad g_e(x) = \sqrt{\frac{2}{\pi}} \int_0^\infty G_e(t) \cos xt dt. \quad (32a)$$

If now the sine transform of the product $f_o(x)g_e(x)$, which is an odd function of x , is formed

$$\begin{aligned} R(t) &= \sqrt{\frac{2}{\pi}} \int_0^\infty f_o(x) g_e(x) \sin xt dx = \frac{2}{\pi} \int_0^\infty f_o(x) \sin xt \int_0^\infty G_e(u) \cos xu du \\ &= \frac{1}{\pi} \int_0^\infty G_e(u) du \int_0^\infty f_o(x) \{ \sin x(t+u) + \sin x(t-u) \} dx \\ &= \frac{1}{\sqrt{2\pi}} \int_0^\infty G_e(u) \{ F_o(t+u) + F_o(t-u) \} du = \frac{1}{\sqrt{2\pi}} \int_0^\infty G_e(u) F_o(t-u) du \\ &= \frac{1}{\sqrt{2\pi}} \int_{-\infty}^0 G_e(t-u) F_o(u) du \end{aligned}$$

the result

$$R(t) = \frac{1}{\sqrt{2\pi}} \int_0^\infty G_e(u) \{ F_o(t+u) + F_o(t-u) \} du = \frac{1}{\sqrt{2\pi}} \int_0^\infty F_o(u) \{ G_e(t-u) - G_e(t+u) \} du. \quad (33)$$

is obtained. $R(t)$ is known under the name of the resultant or "Faltung" of $F_o(x)$ and $G_e(x)$.

If on the other hand $f_o(x)$ and $g_o(x)$ are two odd functions and $F_o(t)$ and $G_o(t)$ are their respective sine transforms, it can similarly be derived for the cosine transform of the product $f_o g_o$, which is an even function,

that

$$R'(t) = \frac{1}{\sqrt{2\pi}} \int_0^\infty f_0(x) g_0(x) \cos tx dx = \frac{1}{\sqrt{2\pi}} \int_0^\infty G_0(u) \{ F_0(t+u) - F_0(t-u) \} du = \frac{1}{\sqrt{2\pi}} \int_0^\infty F_0(u) \{ G_0(t+u) - G_0(t-u) \} du. \quad (34)$$

A similar formula may finally be derived for the case where f_e and g_e are even functions of x . *)

As a simple example of the result of a folding operation the resultant of two Gaussian distributions (Fig. 4)

$$G_i(r) = A_i e^{-a_i(r-r_i)^2}, \quad i = 1, 2 \quad (35)$$

will be calculated. These have maxima A_i at $r=r_i$, ($i=1, 2$) and half widths

$$w_i = \frac{0.833}{\sqrt{a_i}}, \quad i = 1, 2 \quad (36)$$

since $\exp(-0.833)^2 = \frac{1}{2}$. The resultant $G_R(r)$ of G_1 and G_2 is by (33a):

$$G_R = \frac{1}{\sqrt{2\pi}} \int_{-\infty}^{\infty} G_1(u) G_2(r-u) du = \frac{A_1 A_2}{\sqrt{2\pi}} \int_{-\infty}^{\infty} e^{-a_1(u-r_i)^2 - a_2(r-u-r_2)^2} du. \quad (37)$$

*) All these formulae are applications of the following general theorem²⁵: if $f(x)$, $F(t)$ and $g(x)$, $G(t)$ are two sets of Fourier transforms such that

$$\begin{aligned} f(x) &= \frac{1}{\sqrt{2\pi}} \int_{-\infty}^{\infty} F(t) e^{itx} dt & F(t) &= \frac{1}{\sqrt{2\pi}} \int_{-\infty}^{\infty} f(x) e^{-itx} dx \\ g(x) &= \frac{1}{\sqrt{2\pi}} \int_{-\infty}^{\infty} G(t) e^{itx} dt & G(t) &= \frac{1}{\sqrt{2\pi}} \int_{-\infty}^{\infty} g(x) e^{-itx} dx \end{aligned} \quad (32b)$$

then

$$R(t) = \frac{1}{\sqrt{2\pi}} \int_{-\infty}^{\infty} f(x) g(x) e^{-itx} dx = \frac{1}{\sqrt{2\pi}} \int_{-\infty}^{\infty} F(u) G(t-u) du \quad (33a)$$

and

$$\frac{1}{\sqrt{2\pi}} \int_{-\infty}^{\infty} R(t) e^{+itx} dt = f(x) \cdot g(x) \quad (33b)$$

In words: multiplication of two functions corresponds to forming the resultant of their Fourier transform and inversely. Formulae (33) and (34) are obtained from the general case by making use of the specified symmetries of f and g .

The exponent can be transformed to

$$-(a_1+a_2) \left[u - \frac{a_1 r_1 + a_2 (r-r_2)}{a_1+a_2} \right]^2 - \frac{a_1 a_2}{a_1+a_2} [r - (r_1+r_2)]^2 \quad (38)$$

and $G_R(r)$ becomes:

$$G_R(r) = \frac{A_1 A_2}{\sqrt{2\pi}} e^{-\frac{a_1 a_2}{a_1+a_2} [r - (r_1+r_2)]^2} \int_{-\infty}^{\infty} e^{-(a_1+a_2) \left[u - \frac{a_1 r_1 + a_2 (r-r_2)}{a_1+a_2} \right]^2} du$$

$$G_R(r) = \frac{A_1 A_2}{\sqrt{2(a_1+a_2)}} e^{-\frac{a_1 a_2}{a_1+a_2} [r - (r_1+r_2)]^2} \quad (39)$$

$G_R(r)$ is again a Gaussian distribution curve with its maximum at $r=r_1+r_2$ and proportional to the product of the magnitudes of the maxima of G_1 and G_2 . Its half width is equal to

$$w_R = 0.833 \sqrt{\frac{a_1+a_2}{a_1 a_2}} = \sqrt{w_1^2 + w_2^2} \quad (40)$$

To apply (33) or (34) to the present problem it is noted that the reduced intensity function $I'(s)$ (4) is the sine transform of $D'(r)$, and $f_O(x)$ can thus be identified with $I'(s)$. It is further noted that the actually calculated radial distribution curve, denoted by $D_O''(r)$, is the sine transform of the product of $I'(s)$ with a modification factor $M(s)$. Thus $g_e(x)$ has to be identified with $M(s)$, which is thus taken to be an even function of s . If $T(r)$ be the cosine transform of $M(s)$

$$T(r) = \sqrt{\frac{2}{\pi}} \int_0^{\infty} M(s) \cos s r ds \quad (41)$$

the formula

$$D_O''(r) = \sqrt{\frac{2}{\pi}} \int_0^{\infty} I'(s) M(s) \sin s r ds = \frac{1}{\sqrt{2\pi}} \int_0^{\infty} D_O'(u) \{ T(r-u) - T(r+u) \} du \quad *) \quad (42)$$

is obtained. $D_O''(r)$ has maxima for values of r which are equal or closely equal to the sum of the distances of the maxima of $D_O'(r)$ and $T(r)$ from the origin, provided $D_O'(r)$ and $T(r)$ are of simple shape. Multiplication of $I'(s)$

*) The term $-T(u+r)$ appears, of course, to insure the odd character of $D_O'(r)$.

with several modifying factors calls for several applications of the folding operation.

Introducing $D'(r)$ from (2), (42) becomes

$$D_o''(r) = \frac{1}{V_{2\pi}} \sum_{ij} Z_i Z_j \int_0^\infty \delta(u - r_{ij}) \frac{1}{u} \{ T(r-u) - T(r+u) \} du \quad (43)$$

$$D_o''(r) = \frac{1}{V_{2\pi}} \sum_{ij} Z_i Z_j \{ T(r - r_{ij}) - T(r + r_{ij}) \} \frac{1}{r_{ij}}.$$

This means that if a reduced intensity function which is really of the type (1) is inverted, then all peaks of $D_o''(r)$ will have the same shape (provided that the r_{ij} are large enough, so that $T(r_{ij}+r)$ and $T(r_{ij}-r)$ do not influence each other). All secondary maxima and minima have the same respective height relative to the magnitude of the corresponding main peak, and the same position with respect to it.

There is the other possibility of taking $M(s)$ to be an odd function of s and calculating the cosine transform of the product of $I'(s)$ and $M(s)$ instead of the sine transform, making use of (34). $M(s)$ should, however, be antisymmetrized only in the case that $M(0)=0$, as otherwise the discontinuity of the resulting odd function at $s=0$ is troublesome.

Examples of Modification Factors.

The following discussion will be limited to the form of $T(r)$. The function $D_o''(r)$ obtained by modifying the reduced intensity function by multiplying with the factor in question and then inverting, consists of a superposition of functions $T(r)$ moved from $r=0$ to $r=r_{ij}$, and of functions $-T(r)$ at $r=-r_{ij}$. The result will be a simple one only when $T(r)$ is of simple shape, and neighbouring peaks do not influence each other too much.

The effect of a finite integration interval may be investigated with the aid of the following $M(s)$:

$$M(s) = \begin{cases} 1 & 0 \leq |s| \leq s_m \\ 0 & s_m < |s| < \infty \end{cases} \quad (44)$$

For this choice of $M(s)$, $T(r)$ becomes

$$T(r) = \sqrt{\frac{2}{\pi}} \int_0^{s_m} \sin sr ds = \sqrt{\frac{2}{\pi}} \frac{\sin s_m r}{r}. \quad (45)$$

This function is shown in Fig. 5²⁶. The half width of its main peak at $r=0$ is

$$w = \frac{1.89}{a} \quad (46)$$

since $\frac{\sin 1.89}{1.89} = \frac{1}{2}$.

To investigate the effect of the artificial temperature factor let (Fig. 4)

$$M(s) = e^{-as^2} \quad (47)$$

for which (Fig. 4)

$$T(r) = \sqrt{\frac{2}{\pi}} \int_0^{\infty} \cos sr e^{-as^2} ds = \frac{1}{\sqrt{2a}} e^{-\frac{r^2}{4a}}. \quad (48)$$

This is a Gaussian distribution of half width

$$w = 1.666 \sqrt{a}. \quad (49)$$

The common result of both the artificial temperature factor and a finite interval of integration may be obtained by carrying out the folding operation twice, using (43), (45) and (48). It proves, however, simpler to invert directly

$$M(s) = \begin{cases} e^{-as^2} & 0 \leq |s| \leq s_m \\ 0 & s_m < |s| < \infty \end{cases} \quad (50)$$

the cosine transform of which is

$$T(r) = \sqrt{\frac{2}{\pi}} \int_0^{s_m} e^{-as^2} \cos sr ds. \quad (51)$$

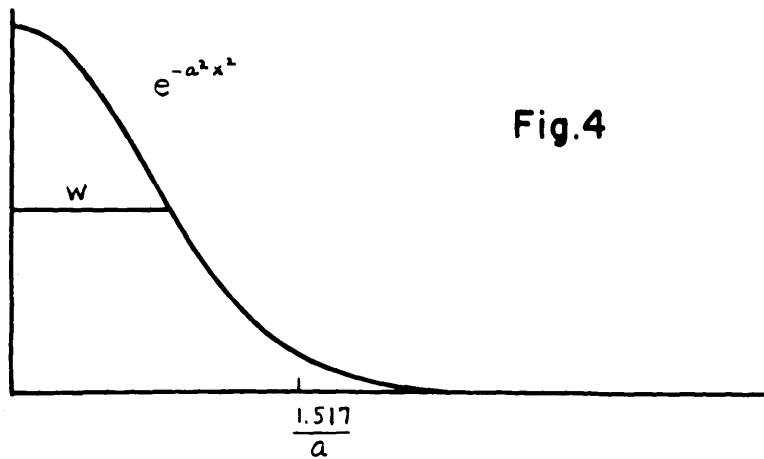


Fig.4

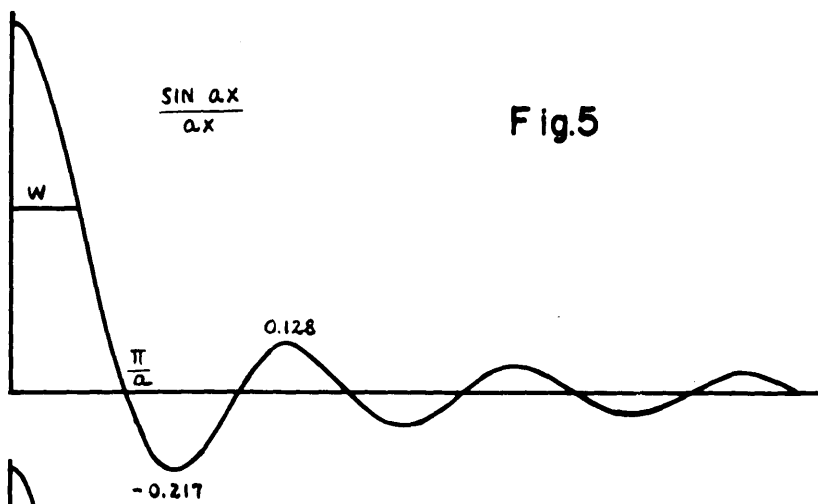


Fig.5

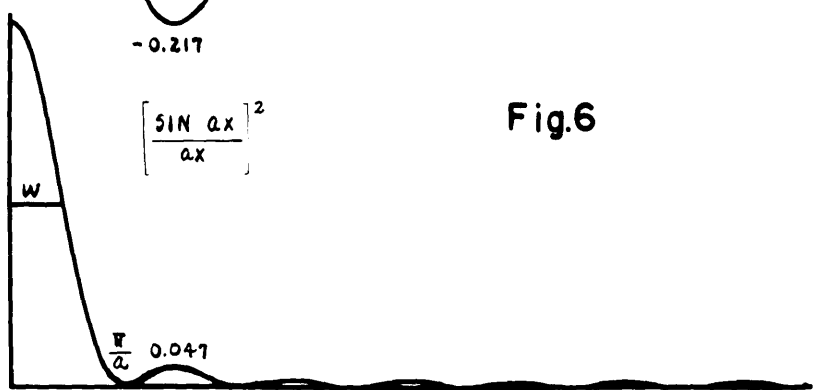


Fig.6

To approximate the integral it is convenient to replace $\exp(-as^2)$ by $\frac{1+\cos cs}{2}$ with appropriately chosen c . The resulting distribution function was discussed by V. Schomaker⁶, whose thesis should be consulted for the interesting results.

The procedure in these laboratories is to use an artificial temperature factor (47) with a value of a such that $\exp(-as_m^2)=0.10$. The main peak of the resulting transform has a half width

$$W = \frac{2.5}{s_m}. \quad (52)$$

This procedure neglects 3% of the area of $M(s)$, since

$$\frac{2}{\sqrt{\pi}} \int_{-s_m}^{\infty} \exp(-x^2) dx = 0.032 \text{ and } \exp(-(1.52)^2) = 0.10.$$

The convergence factor suggested by Fejer's theorem for Fourier series

$$M(s) = \begin{cases} \frac{s_m - |s|}{s_m} & 0 \leq |s| \leq s_m \\ 0 & s_m < |s| < \infty \end{cases} \quad (53)$$

leads to the cosine transform

$$T(r) = \sqrt{\frac{2}{\pi}} \int_0^{s_m} \frac{s_m - s}{s_m} \cos sr ds = \frac{1}{\sqrt{2\pi}} s_m \left(\frac{\sin \frac{s_m r}{2}}{\frac{s_m r}{2}} \right)^2. \quad (54)$$

This transform (Fig. 6) has the same general character as the one obtained (51) in the investigation of the joint effects of artificial temperature factor and finite integration interval. The primary peak of $T(r)$, (54), situated at $r=0$, has the half width

$$W = \frac{2.78}{s_m} \quad (55)$$

since $(\frac{\sin 1.39}{1.39})^2 = \frac{1}{2}$. The magnitude of the first secondary maximum is about 4.7% of the magnitude of the primary peak²⁶.

If sharper peaks of the radial distribution function are desired than are provided by modification of $I'(s)$ with an artificial temperature factor, the following function may be of use (Fig.6)

$$M(s) = \frac{\sin^2 as}{as^2} \quad (56)$$

Its cosine transform may be obtained by making use of (53) and (54) (cf. also (23) and (24))

$$T(r) = \sqrt{\frac{2}{\pi}} \int_0^{\infty} \frac{\sin^2 as}{as^2} \cos rs ds = \begin{cases} \sqrt{\frac{2}{\pi}} \frac{2a - |r|}{2a} & |r| \leq 2a \\ 0 & |r| > 2a \end{cases} \quad (57)$$

This transform has the shape of a triangle with its apex at $r=0$ and a base of the length $4a$. The tip of this triangle is provided by the contribution of very large s , giving rise to a very small period of the cosine in the integral for $T(r)$. If, as in practice is always the case, the integration has to be limited to a finite interval, the resulting peak will no longer have a sharp tip, but rather the maximum curvature of the cosine of the highest frequency occurring in the integral. The other feature of the peak, namely its straight-line boundaries (which may be very useful in locating its exact center), will however not be greatly disturbed as long as the integration is extended to a point where the magnitude of the modified $I'(s)$ has become a small fraction of the original $I'(s)$. This demand entails a relationship between s_m and $w = a$, the half-width of the peak. If for instance the integration be extended to the first or to the second zero of $M(s)$, the corresponding half widths w' , w'' are respectively

$$w' = \frac{3.1}{s_m} \quad w'' = \frac{6.3}{s_m} \quad . \quad (58)$$

These values do not compare very favorably with the ones resulting from the procedure used in these laboratories. They could be improved by further decreasing a , but the resulting shape of $T(r)$ would be far from triangular.

All convergence factors of the form $a(\frac{\sin as}{as})^n$ have cosine transforms which are different from zero in a finite region only (e.g. (44) and (45), (56) and (57)). For the case $n=3$

$$M(s) = a \left(\frac{\sin as}{as} \right)^3 \quad (59)$$

which looks similar to the function illustrated in Fig. 5 but has much less pronounced secondary features, the first minimum being $0.010a$. The cosine transform of (59) is (Fig. 7)

$$T(r) = a \sqrt{\frac{2}{\pi}} \int_0^\infty \left(\frac{\sin as}{as} \right)^3 \cos sr ds = \sqrt{\frac{2}{\pi}} \begin{cases} \frac{1}{4}(3 - (\frac{r}{a})^2) & |r| \leq a \\ \frac{1}{8}(9 - 6|\frac{r}{a}| + (\frac{r}{a})^2) & a < |r| \leq 3a \\ 0 & |r| > 3a \end{cases} \quad (60)$$

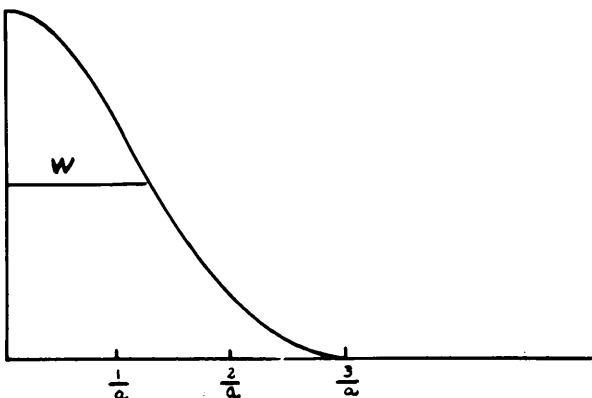


Fig. 7

and has a half width $w=1.27a$. This means that if the integration in (60) is carried only to the first zero of $M(s)$ (59) the resulting half width is

$$w = \frac{1.27 \pi}{s_m} = \frac{4.0}{s_m} . \quad (61)$$

If the integration is only extended to an upper limit s_m , such that $M(s_m)=0.10 M(0)$ and $s_m a=1.98$, the corresponding half width is

$$w = \frac{2.5}{s_m} . \quad (61a)$$

This latter procedure corresponds to the one practiced in these laboratories (cf. above) and gives rise to the same half width.

The following modification function gives rise to slightly concave peaks, provided again that the integration is extended over the whole infinite range. This function is

$$M(s) = \frac{a^2}{a^2 + s^2} \quad (62)$$

whose transform is

$$\bar{T}(r) = \sqrt{\frac{2}{\pi}} \int_0^\infty \frac{a^2}{a^2 + s^2} \cos sr ds = a \sqrt{\frac{\pi}{2}} e^{-a|r|} . \quad (63)$$

If the integration is extended over a finite range such that $M(s'_m)=0.10$ or $M(s''_m)=0.010$, the corresponding half widths w' , w'' are respectively

$$w' = \frac{2.1}{s_m} \quad w'' = \frac{6.9}{s_m} . \quad (64)$$

One of the objects of this investigation was to find, possibly, a convergence factor which would be more advantageous than the artificial temperature factor, producing a radial distribution function with the maximum resolution $w=1.89/s_m$ (46) contained in the experimental data, but with no secondary peaks. The various examples of convergence

factors (53)(56)(59)(62) indicate, however, that the artificial temperature factor is as profitable a convergence factor as can be found, and that some resolution is always lost in avoiding secondary maxima.

The following function

$$M(s) = \begin{cases} 1 + \alpha \cos^2 \left(\frac{s-s_0}{2\sigma} \pi \right) & s_0 - \sigma \leq |s| \leq s_0 + \sigma \\ 1 & \text{otherwise} \end{cases} \quad (65)$$

continuously boosts the features of $I'(s)$ in an interval of the width 2σ around $s=s_0$ by a maximal amount of $\frac{\alpha}{100}\%$. The corresponding cosine transform is the sum of the δ -function $\delta(0)$ and of $T'(r)$:

$$T'(r) = \frac{\alpha}{2} \sqrt{\frac{2}{\pi}} \int_{s_0-\sigma}^{s_0+\sigma} (1 + \cos \left(\frac{s-s_0}{\sigma} \pi \right)) \cos sr ds \quad (66)$$

$$T'(r) = \frac{\alpha \sqrt{2} \pi^{3/2} \cos s_0 r \sin \sigma r}{r (\pi^2 - r^2 \sigma^2)}.$$

$T'(r)$ has in general a main peak at $r=0$, two side features at $r=\pm \frac{\pi}{\sigma}$, minima or maxima depending on the sign of $\cos \frac{s_0}{\sigma} \pi$, and many secondary features. The resulting $D''_0(r)$ has superimposed on the peaks of $D'_0(r)$ (which is reproduced by $\delta(0)$), the pattern of $T'(r)$. The effects of a convergence factor and finite integration interval complicate the result further, so that it appears hardly feasible to investigate with the aid of (65) what the effect would be of a specially characteristic feature of $I'(s)$ on the radial distribution function.

The elastic scattering intensity function of fast electrons by gas molecules contains a factor s^{-5} . For this reason the intensities and positions of the features close to the center of an electron diffraction picture cannot be estimated very reliably. One is tempted to exclude these features from the construction of a radial distribution function by multiplying $I'(s)$ by a function like

$$M(s) = s^2 e^{-as^2} \quad (67)$$

whose cosine transform is

$$T(r) = \sqrt{\frac{2}{\pi}} \int_0^\infty s^2 e^{-as^2} \cos sr ds = \frac{2a - r^2}{4\sqrt{2} a^{5/2}} e^{-\frac{r^2}{4a}} \quad (68)$$

This transform has three extrema, one maximum at $r=0$ and two equally shaped minima at $r=\pm\sqrt{6a}$, 44.6% the size of the maximum. The peak has a half width

$$w = 0.87\sqrt{a} \quad (69)$$

since $(2-(0.87)^2)\exp(-(\frac{0.87}{2})^2) = 1$, and $T(r)$ becomes 0 for $r=\pm\sqrt{2a}$. $T(r)$ has thus a simple shape, but unfortunately the two deep minima impair the usefulness of (67) in electron diffraction work. The effect of a finite integration interval which has been described previously also adds complications.

A modification function of the same type is

$$M(s) = \begin{cases} \cos^2 \left(\frac{s_m - 2s}{2s_m} \pi \right) & 0 \leq |s| \leq s_m \\ 0 & \text{otherwise} \end{cases} \quad (70)$$

with the transform

$$T(r) = \sqrt{\frac{2}{\pi}} \int_0^{s_m} \left(\cos \left(\frac{s_m - 2s}{s_m} \pi \right) + 1 \right) \cos sr ds = (2\pi)^{3/2} \frac{\sin s_m}{r(4\pi^2 - s_m^2 r^2)} \quad (71)$$

This has a primary maximum at $r=0$, two minima at $r=\pm\frac{2\pi}{s_m}$, half the size of the maximum, and secondary features of rapidly decreasing amplitude. It is seen that $M(s)$ (70) also does not lend itself to application to the construction of a radial distribution function.

The atomic scattering factor.

Expression (1) for $I(s)$ contains the assumption that the differences between the $\frac{Z-F}{Z}$ of different atoms may be neglected. In the following this assumption is no longer made.

$$M(s) = s^2 e^{-as^2} \quad (67)$$

whose cosine transform is

$$T(r) = \sqrt{\frac{2}{\pi}} \int_0^\infty s^2 e^{-as^2} \cos sr ds = \frac{2a - r^2}{4\sqrt{2} a^{5/2}} e^{-\frac{r^2}{4a}}. \quad (68)$$

This transform has three extrema, one maximum at $r=0$ and two equally shaped minima at $r=\pm\sqrt{6a}$, 44.6% the size of the maximum. The peak has a half width

$$w = 0.87\sqrt{a} \quad (69)$$

since $(2-(0.87)^2)\exp(-(\frac{0.87}{2})^2) = 1$, and $T(r)$ becomes 0 for $r=\pm\sqrt{2a}$. $T(r)$ has thus a simple shape, but unfortunately the two deep minima impair the usefulness of (67) in electron diffraction work. The effect of a finite integration interval which has been described previously also adds complications.

A modification function of the same type is

$$M(s) = \begin{cases} \cos^2 \left(\frac{s_m - 2s}{2s_m} \pi \right) & 0 \leq |s| \leq s_m \\ 0 & \text{otherwise} \end{cases} \quad (70)$$

with the transform

$$T(r) = \sqrt{\frac{2}{\pi}} \int_0^{s_m} \left(\cos \left(\frac{s_m - 2s}{s_m} \pi \right) + 1 \right) \cos sr ds = (2\pi)^{3/2} \frac{\sin s_m}{r(4\pi^2 - s_m^2 r^2)} \quad (71)$$

This has a primary maximum at $r=0$, two minima at $r=\pm\frac{2\pi}{s_m}$, half the size of the maximum, and secondary features of rapidly decreasing amplitude. It is seen that $M(s)$ (70) also does not lend itself to application to the construction of a radial distribution function.

The atomic scattering factor.

Expression (1) for $I(s)$ contains the assumption that the differences between the $\frac{Z-F}{Z}$ of different atoms may be neglected. In the following this assumption is no longer made.

The molecular scattering intensity of a rigid molecule is given by the expression¹

$$\bar{I}(s) = c \sum_{ij} \sum' \frac{f^i(s) f^j(s)}{r_{kk}^{ij} s} \sin r_{kk}^{ij} s = c \sqrt{\frac{2}{\pi}} s^h \bar{I}(s) \quad (72)$$

where the indices refer to the k -th atom of the kind i and the ℓ -th atom of the kind j . The prime on the second sum means that terms where $k=\ell$ and $i=j$ simultaneously shall be omitted. In the reduced intensity function $\bar{I}(s)$ there has been omitted a factor s^h , where h is an odd (to make $\bar{I}(s)$ odd) integer, arbitrary for the moment. The atomic scattering factors $f^i(s)$ can be expressed as follows¹

$$f^i(s) = k \int_0^\infty \frac{\sin sr}{sr} V^i(r) r^2 dr = k' \frac{Z^i \cdot F^i(s)}{s^2} \quad (73)$$

where V^i is the potential due to the atomic field of an atom of the kind i , r is the distance from the center, Z^i is the nuclear charge and $F^i(s)$ the atomic scattering factor for X-rays of the atom under consideration. Let

$$\bar{D}_0^{ij}(r) = r \bar{D}_0^{ij}(r) = \sum_{kk} \delta(r - r_{kk}^{ij}) \quad (74)$$

where $k \neq \ell$ if $i=j$, and let

$$S^{ij}(r) = \sqrt{\frac{2}{\pi}} \int_0^\infty \frac{f^i(s) f^j(s)}{s^{h+1}} \cos sr ds. \quad (75)$$

Then

$$\bar{I}(s) = \sqrt{\frac{2}{\pi}} \sum_{ij} \frac{f^i(s) f^j(s)}{s^{h+1}} \int_0^\infty \bar{D}_0^{ij}(r) \sin sr dr = \sum_{ij} \frac{f^i(s) f^j(s)}{s^{h+1}} \bar{I}^{ij}(s) \quad (76)$$

where

$$\bar{I}^{ij}(s) = \sqrt{\frac{2}{\pi}} \int_0^\infty \bar{D}_0^{ij}(r) \sin sr dr.$$

The sine transform of $I^{ij}(s)$ is

$$\bar{D}_0^{ij}(r) = \sqrt{\frac{2}{\pi}} \int_0^\infty I^{ij}(s) \sin sr ds. \quad (77)$$

Inverting $\bar{I}(s)$ the radial distribution function $\bar{D}_0(r)$ is obtained

$$\bar{D}_0(r) = \sqrt{\frac{2}{\pi}} \int_0^\infty \bar{I}(s) \sin sr ds \quad (78)$$

which may be transformed into

$$\begin{aligned}
 \bar{D}_0(r) &= \sqrt{\frac{2}{\pi}} \sum_{ij} \int_0^\infty \frac{f^i(s) f^j(s)}{s^{h+1}} I^{ij}(s) \sin sr ds \\
 &= \sum_{ij} \frac{1}{\sqrt{2\pi}} \int_0^\infty \bar{D}_0^{ij}(u) [S^{ij}(r-u) - S^{ij}(r+u)] du \\
 \bar{D}_0(r) &= \frac{1}{\sqrt{2\pi}} \sum_{ij} \sum_{ke} \frac{1}{r^{ij}_{ke}} [S^{ij}(r-r_{ke}^{ij}) - S^{ij}(r+r_{ke}^{ij})]. \tag{79}
 \end{aligned}$$

The function $\bar{D}_0(r)$ is thus a superposition of peaks of shape (75) characteristic of the pair of atoms ij represented by the peak.

For the case that $h=-3$, corresponding to inversion of $s^3 I(s)$, this shape of the peaks can be interpreted in terms of the electric potentials in the atoms i and j . Here $S^{ij}(s)$ becomes

$$S^{ij}(r) = \sqrt{\frac{2}{\pi}} \int_0^\infty s^2 f^i(s) f^j(s) \cos sr ds. \tag{80}$$

But $sf(s) = k \int_0^\infty \sin sr (r V(r)) dr$,

$$(81)$$

the sine transform of which is

$$r V(r) = k \cdot \frac{2}{\pi} \int_0^\infty \sin sr (s f(s)) ds = C(r). \tag{82}$$

The right hand side of this equation represents the charge $C(r)$ which would have to be concentrated at the center of the atom to produce the potential $V(r)$ at r ,

$$C(r) = [eZ - \int_0^r u(r) dr - r \int_r^\infty \frac{u(r)}{r} dr], \tag{83}$$

where $u(r)$ is the amount of negative charge in a shell of thickness dr at r .

Application of (34) gives

$$S^{ij}(r) = k' \int_0^\infty C(u) \{C^j(r+u) - C^j(r-u)\} du = \int_{-\infty}^\infty k' C(u) C^j(u-r) du, \tag{84}$$

the resultant of folding $C^i(r)$ into $C^j(r)$. *) The structure of (84) is that of a one dimensional radial distribution function, with C^i and C^j centered at the origin.

The case $h=-5$, the inversion of $s^5 I(s)$, has been treated by Debye and Pirenne²⁷, who started with the formula for the scattering amplitude of a molecule

$$f(s) = \frac{k''}{s^2} \int \rho(r) e^{i(n - n_0 \cdot \underline{r})} dV \quad (85)$$

where ρ is the charge density in the molecule, n and n_0 are unit vectors in the direction of incident and scattered beams, \underline{r} the radius vector of the volume element dV , and averaging over all orientations of the molecule has yet to be carried out. This equation can be derived from the usual one¹, involving the potential $V(r)$, by assuming that the charges of the nucleus are smeared out over a finite region. Debye and Pirenne obtained for the intensity $i(s)$ scattered by randomly oriented molecules the expression

$$i(s) = \frac{c}{s^4} \int_0^\infty d(r) \frac{\sin sr}{sr} 4\pi r^2 dr. \quad (86)$$

Here

$$rd(r) = \frac{1}{2\pi^2 c} \int_0^\infty s^5 i(s) \sin sr ds \quad (87)$$

is a radial distribution function defined by

$$d(r) = \frac{1}{4\pi} \int \rho(r_1) dV_1 \int \rho(r_2) d\Omega_2 \quad (88)$$

where $r = |\underline{r}_1 - \underline{r}_2|$ and the integrations have to be carried out as follows. Place a sphere of radius r in the molecule and determine on its surface the average of the charge density $\frac{1}{4\pi} \int \rho(r_2) d\Omega_2$, where $d\Omega_2$ is the diffe-

*) $C(r)$ is formally an odd function of r as may be seen e.g. from (82). The difficulty that $C(0)=Z \neq 0$ which arises from the fact that $V(r)$ has a singularity at the origin is not serious, as in actual molecules the nuclear charge is always smeared out over a finite region.

rential of the solid angle. Multiply the result with $\rho(r)$, the charge at the center of the sphere, and integrate, moving the sphere through the whole molecule.

The function $d(r)$ can be expressed as the sum

$$d(r) = \sum_{ij} d_{ij}(r) \quad (89)$$

over the contributions d_{ij} of the various pairs of atoms i and j in the molecule. The atomic terms d_{ii} arise from the fact that $i(s)$ (86) includes both atomic and molecular scattering. Since the experimental intensities obtained in the visual method contain only molecular scattering³ the atomic terms in $d(r)$ should be omitted. If the charge distributions of the atoms have spherical symmetry the functions $d_{ij}(r)$ may be expressed by the formula

$$d_{ij}(r) = \pi \int_0^\infty w^2 \left\{ \int_0^\pi \rho_i(\sqrt{r_{ij}^2 + w^2 - 2r_{ij}w \cos \beta}) d\cos \beta \right\} \left\{ \int_0^\pi \rho_j(\sqrt{r^2 + w^2 - 2rw \cos \alpha}) d\cos \alpha \right\} dw \quad (90)$$

where the various symbols are explained by Fig. 8.

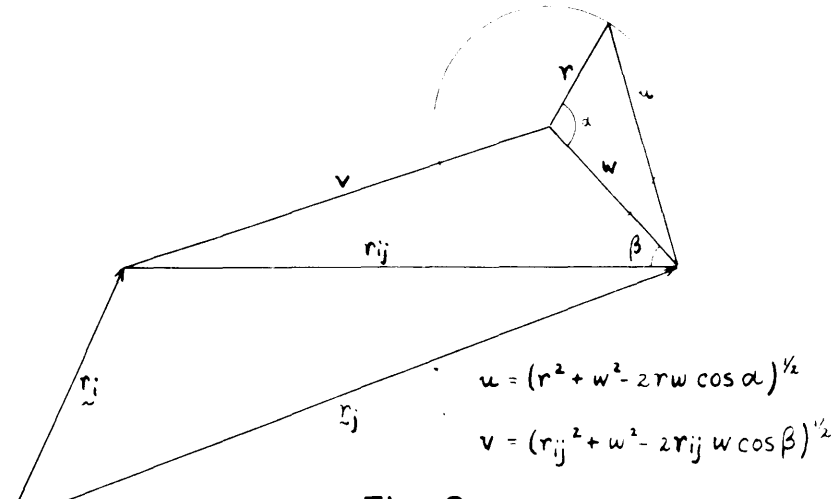


Fig. 8

It is seen that (90) is much more complicated than (84) and that (90) could not have been obtained by using the folding theorem, which corresponds to a one dimensional distribution function, while (88) is a three dimensional distribution function.

Starting with (85) the inversion of $s^7 I(s)$ could be interpreted by the folding theorem in terms of $r\rho(r)$. But all these interpretations have no application to the actual practice of inverting a certain reduced visual intensity function, since at the present it is impossible to obtain accurate experimental knowledge of the molecular scattering intensity. Indeed, the method used in these laboratories is to represent the observed scattering by a function of the type (1) involving sine terms with constant coefficients. Interpretation of such an intensity function in terms of the actual charge distribution in the molecule is, however, not possible.

All formulae derived in previous sections still apply since (78) has the same form as (5) except that instead of using (2) in (42), (79) should be used.

Summary.

The Gibbs and related phenomena, which cause undesirable secondary features in the radial distribution function are discussed and illustrated by several simple examples. The effect of convergence factors and Fejer's method of summation are described. The "Folding" theorem for Fourier transforms is derived and applied to the general discussion of the effects of modifications of the reduced intensity function on the corresponding radial distribution function. Various special types of modifications are investigated. A discussion of the effect of the atomic scattering factors of different atoms is given.

References cited

1. L.O. Brockway, Rev. Mod. Phys. 8, 231 (1936).
2. R. Wierl, Ann. der Phys. ser. 5, 8, 251 (1931).
3. L. Pauling and L.O. Brockway, J. Chem. Phys. 2, 867 (1934).
4. L. Pauling and L.O. Brockway, J.A.C.S. 57, 2684 (1935).
5. C. Dégard, Thesis, University of Liège, 1937.
6. V. Schomaker, Thesis, California Institute of Technology, 1938.
7. J. Walter and J.Y. Beach, J. Chem. Phys. 8, 601 (1940).
8. R. Spurr and V. Schomaker, J.A.C.S. 64, 2693 (1942).
9. R. Courant and D. Hilbert, Methoden der Mathematischen Physik, 2. Aufl. Berlin 1931, vol. 1, p.65.
10. M. Bôcher, Annals of Math. 2nd series, 7, 81 (1906).
11. J.W. Gibbs, Nature, 59, 606 (1899).
12. H. Wilbraham, Camb. and Dublin Math. Journal 3, 198 (1848).
13. L. Fejer, Math. Ann. 58, 51 (1904); 64, 284 (1907).
14. E.T. Whittaker and G.N. Watson, A course of Modern Analysis, Amer. ed., New York 1943, p.155.
15. reference 14, p.171.
16. reference 14, p.179.
17. reference 9, p.68.
18. R. Courant, Differential and Integral Calculus, London, 1934, vol. 1, p.450.
19. reference 9, p.86.
20. R.W. James, Phys. Zeit. 33, 737 (1932).
21. reference 10, p. 103 footnote
22. A. Sommerfeld, Über die willkürlichen Funktionen in der Mathematischen Physik, Königsberg, 1891.

23. W.L. Bragg and J. West, Phil. Mag. 7th series, 10, 323 (1930).
24. D.L. Titchmarsh, Introduction to the Theory of Fourier Integrals, Oxford 1937, p.3-4.
25. reference 24, p.51, 59.
26. E. Jahnke and F. Emde, Tables of Functions, New York 1943, Addenda p.30, 32.
27. P. Debye and M.S. Pirenne, Ann. der Phys. ser. 5, 25, 617 (1938).

Note: On April 13, 1944, after this paper had been completed, the Library of the California Institute of Technology received volume 9 (1942) of the Dutch journal "Physica". On page 461 of this journal appears the article "Diffraction effects in Fourier series, and their elimination in X-ray structure investigations" by L.L. van Reijen, in which the effects of breaking off a Fourier series in crystal structure work are discussed in a manner similar to that used in the present study.

SUMMARY

An introduction illustrates with examples how, in the past, diffraction methods have supplemented classical chemical methods in determining the topological configuration of atoms in molecules, and the spatial arrangement of groups attached to a carbon atom.

An experimental part records the results of an electron diffraction investigation and a crystal structure determination of biphenylene and an account of various investigations on arsenomethane, including an electron diffraction investigation of its vapor. Biphenylene is dibenzcyclobutadiene, as seemed probable from its synthesis. Interatomic distances are reported and the packing of the molecules in the crystal is discussed. Evidence is presented that an equilibrium between different states of association exists in the vapor of arsenomethane, but that immediately after evaporation the molecule is probably a pentamer. Detailed individual summaries will be found on pages 27, 50, and 68.

A theoretical part deals with conversion and certain other problems arising in the radial distribution method in electron diffraction. A more detailed summary will be found on page 100.

ACKNOWLEDGEMENT

I am grateful to Professor L. Pauling for much advice, encouragement and discussion, without which the present investigations could not have been undertaken. Dr. V. Schomaker's continued interest in my research problems, and his many helpful discussions and suggestions have been of great value. His efforts in teaching me English style and in reading over the draft of this thesis are much appreciated. I also wish to thank Professor L. Zechmeister, Professor E.H. Swift, Professor J.H. Sturdivant, Dr. R.B. Corey and Dr. C.S. Lu for friendly advice and interest.

PROPOSITIONS

- 1) The folding theorem of Fourier transforms is very useful in the discussion of radial distribution functions.
- 2) The expression for the atomic scattering factor for electrons¹

$$f(\vartheta, \varphi) = - \frac{2\pi me}{h^2} \int \exp(ik(n_0 - n_r)) \phi(r) dv,$$

where $\phi(r)$ is the electrostatic potential function, can be transformed with the potential equation into

$$f(\vartheta, \varphi) = \frac{8\pi^2 me^2}{h^2 s^2} (Z - F(\vartheta, \varphi)),$$

where $F(\vartheta, \varphi) = + \int \rho(r) \exp(ik(n_0 - n_r)) dv$

is the atomic scattering factor for X-rays and where no averaging over all orientations in space has been carried out.

- 3) Inclusion of the scattering of hydrogen atoms in the calculation of X-ray structure factors for crystals of long-chain hydrocarbons would doubtless have improved the agreement between the observed and calculated scattering amplitudes reported by Bunn².

- 4a) In a paper by Clark and Yohe³ on an X-ray examination of crystals of phenylaminoacetic acid the heretofore unchallenged statement was made that certain space groups demand the presence of asymmetric molecules. This is not true since a given molecule in a crystal can have higher symmetry than is required by the space group. It will have an asymmetric environment in these space groups, but that need not have appreciable effect on the molecule's own symmetry.

If in addition a crystal with the specific space group C_{2v}^5 -Pca, chosen by Clark and Yohe for d- and l-phenylaminoacetic acid, contained enantiomeric molecules, it would have to contain both the d- and the l-form in equal number, since the space group has glide planes. If Clark and Yohe really investigated crystals of d- and of l-phenylaminoacetic acid, as they claimed, their space group would appear to be ruled out on the basis of all present knowledge on optical activity.

- 4b) From X-ray data and with a detailed theory of development of crystal faces, etch figures or similar properties it should

be possible, in favorable cases, to decide which of two enantiomorphic structures belongs to a given optically active substance. This seems of importance since doubt has been expressed⁵ as to the validity of structure assignments made on the basis of present theories of optical activity.

5) The reason given by Sauter⁶ for contesting the reality of certain maxima of the charge density shown by X-ray investigations to exist in certain regions of the lattices of magnesium⁷ and ruthenium⁸ crystals, is not valid. It is, however, not contended that these maxima are necessarily real.

6) If in the first order Schrödinger perturbation theory a degeneracy is not removed great care should be taken in the choice of the combinations of the first order wave functions used in the calculation of the second order correction of the energy (e.g.).

7) One reason for the statement made by Glockler and Evans¹⁰ that their approximate quantum mechanical solution of the one-dimensional double minimum problem is not valid for $q \neq 1$, is that the solution does not, in that region, satisfy a theorem by Sturm and Liouville which applies to exact solutions.

8) Two equivalent, cylindrical bonds of "strengths" 1,528 and forming a bond angle of 60° may be constructed by sp-hybridization.

9) The chromatographic adsorption method could be applied to measure the rate of dissociation of hexaarylethanes.¹¹

10) Of all n-gons ($n \geq 4$) the pentagon is the only one for which the following is true: the construction of an equilateral, equiangular pentagon is possible for only two values of the angle. For all other n-gons (excepting the trivial case of the triangle) there is a whole range of angles for which an analogous construction is possible. The pentagon under consideration is planar, the possible angles are 108° and 36° .

X₁) A basic knowledge of statistics should be required of any candidate for the degree of Doctor of Philosophy.

X₂) There should be a ruling that Candidacy Examinations are to be announced at least four weeks in advance so as to permit adequate preparation.

References cited

1. L.O. Brockway, Rev. Mod. Phys., 8, 231 (1936).
2. C.W. Bunn, Trans. Faraday Soc., 35, 482 (1939).
3. G.L. Clark and G.R. Yohe, J.A.C.S., 51, 2796 (1929).
4. L. Pauling and R.G. Dickinson, J.A.C.S., 53, 3820 (1931).
5. E. Hückel, Z. Elektrochemie, 50, 13 (1944).
6. F. Sauter, Naturwissenschaft., 31, 302 (1943).
7. R. Brill, H.G. Grimm, C. Hermann and C. Peters, Ann. Physik (5) 34, 393 (1939); C. Peters, Z. Elektrochemie, 46, 436 (1940).
8. G.W. Brindley and P. Ridley, Nature, 140, 461 (1937).
9. L. Pauling and E.B. Wilson, Introduction to quantum mechanics, New York 1935, p.178.
10. G. Glockler and G.E. Evans, J.C.P., 10, 607 (1942).
11. L. Zechmeister and J.T. Maynard (unpublished investigation).